Comparison of rat and porcine jejunum as *in vitro* models for P-glycoprotein mediated efflux using the Sweetana-Grass diffusion method

H.J. OOSTHUIZEN

Dissertation submitted for the degree Magister in Scientiae in Pharmaceutics at the Potchefstroom campus of the North-West University

Supervisor: Dr. M.M. Malan

Co-supervisor: Prof. J.H. Hamman

November 2010

Acknowledgements

To perform any research, the expertise, assistance, and inspiration of people around you are of extreme importance. Although words are not enough to express my gratitude towards those who made this study possible, I would like to try.

First and foremost I would like to thank my heavenly Lord and Saviour for giving me more love and grace than I deserve. I thank Him for giving me the talent and opportunity to be able to complete this study.

To my parents Tienie and Doreen Oosthuizen, thank you for all your love, advice, financial support and encouragement. Thank you for giving me the opportunity to study at a university and undertake post-graduate study. Thank you for everything I am, I love you very much.

To my supervisor Dr. Maides Malan who helped me in such an incredible way. *Tannie* Maides, I thank you for all your hard work during this study, but most of all I thank you for the manner in which you guided me: always friendly, supportive, reliable, patient and especially for always having time for me. It was an immense privilege to be taught by you.

I also want to specially thank my co-supervisor Prof. Sias Hamman for helping me to complete this study. Thank you that I was always a priority to you. You gave me enormous insight into this study and I appreciate that I could benefit from your knowledge.

To Prof. Jan du Preez and Francois Viljoen in the Analytical Technology Laboratory, thank you for your guidance and helping with the validation of my analytical method.

Thank you to Cor Bester, Antoinette Fick and Petri Bronkhorst in the Animal Research Centre for their friendly help with the rats.

To Mrs. Anina Oosthuizen for helping me in some of my experiments, I appreciate it very much.

Thank you to Mrs. Wilma Breytenbach from Statistical Consultation Services for the planning, help and advice with the statistical analysis of the data.

To everybody in the Department of Pharmaceutics who was always friendly, supportive and willing to help with any problem. I am very thankful that I could work amongst you.

Thank you to my friend Amé Snyman for her willingness to do the daunting task of proofreading of the dissertation. I value it very much.

To my special colleague friends, Alta, De Wet and Sarel, and my brother, Derick, thank you for all your help, caring, support and willingness to listen. I am very grateful to have you in my life. Also to all my other friends and fellow *Patriane*, thank you for being my family and friends away from home, you made the years fly by and ensured that I enjoyed every moment of it.

I also want to thank the North-West University, for the financial support during the course of this study.

Table of contents

Abstract

Absorption of drug substances across the intestinal epithelium is a complex and dynamic process. Counter transport proteins are responsible for the efflux of specific drug molecules after they have been absorbed. One of the key counter transport efflux proteins, which is of importance in this study, is P-glycoprotein. The efflux pump P-glycoprotein plays a major role in altering the pharmacokinetics of a wide variety of drugs limiting their absorption and therefore also bioavailability. Many flavonoids have been shown to interact with P-glycoprotein mediated efflux *in vitro* studies. Numerous *in vitro* methods have been used to study drug absorption across the intestinal membranes, but it is often not possible to use only one *in vitro* model to accurately predict permeability characteristics.

The purpose of this study was to determine the effect of four selected hydroxy- and methoxy-flavonoids on the *in vitro* transport of Rhodamine 123, a known P-gp substrate, across excised rat and pig intestinal tissue using the Sweetana-Grass diffusion apparatus. The results were further used to determine if the two different animal tissue models corresponded with regard to the flavonoids' effects on P-glycoprotein related efflux. Two control groups were included in the experimental design. In the negative control group, the transport of Rhodamine 123 was tested alone and no modulator was added. In the positive control group, the transport of Rhodamine 123 was determined in the presence of Verapamil, which is a known P-glycoprotein inhibitor. The experiments with the flavonoids Morin, Galangin, 6-Methoxyflavone and 7-Methoxyflavone were done in triplicate to determine repeatability of the results. The transport of Rhodamine 123 was evaluated in both the apical to basolateral (absorptive) and basolateral to apical (secretory) directions. The relative transport of Rhodamine 123, the apparent permeability coefficient (P_{app}) values and flux (J) values in both directions as well as the efflux ratio (ER) and net flux (J_{net}) were calculated. The concentration Rhodamine 123 present in the acceptor chamber was determined by means of a validated HPLC method. Statistical analysis was used to compare the results of the test groups with the control groups in order to indicate significant differences.

It has been found that Morin, Galangin and 6-Methoxyflavone have a significant inhibitory effect on the Rhodamine 123 efflux (probably P-glycoprotein related) in both the rat and pig intestinal tissue models with p-values smaller than 0.05. On the other hand, 7-Methoxyflavone showed a significant effect on the efflux of Rhodamine 123 in the pig intestinal tissue model ($p < 0.05$) but not in the rat intestinal tissue model ($p > 0.05$). These flavonoids may increase the

bioavailability of drugs that are substrates for P-glycoprotein and thereby cause clinically significant pharmacokinetic interactions, however, this should be confirmed with *in vivo* studies. On the other hand, these flavonoids may be used for drug absorption enhancement when applied under controlled circumstances.

With regard to the different animal tissue models used it can be concluded that data obtained from the rat intestinal tissue model cannot be compared and extrapolated to data obtained from the pig intestinal tissue model. It is recommended that the *in vitro* results be correlated to *in vivo* findings to identify the most suitable model.

Keywords: P-glycoprotein, rhodamine 123, Sweetana-Grass diffusion cells, flavonoids, *in vitro* models

Uittreksel

Die absorpsie van geneesmiddels en ander verwante stowwe deur intestinale epiteel is ‘n komplekse en dinamiese proses. Sekere transportproteïene werk hierdie proses teen en veroorsaak effluks van spesifieke geneesmiddels nadat hulle geabsorbeer is. Een van die sleutel transportproteïene wat hierdie effluks veroorsaak en van belang is vir hierdie studie, is P-glikoproteïen (P-gp). Hierdie effluksspomp speel ‘n baie belangrike rol in die verandering van die farmakokinetiese eienskappe van ‘n wye verskeidenheid geneesmiddels deur die beperking van absorpsie en dus ook hul biobeskikbaarheid. Baie flavonoïede toon ‘n interaksie met P-gp geïnduseerde effluks in *in vitro* studies. Verskeie *in vitro* modelle is al gebruik om geneesmiddelabsorpsie oor die intestinale membrane te bestudeer, maar dit is nie raadsaam om van slegs een *in vitro* model gebruik te maak tydens die bestudering van deurlaatbaarheidseienskappe nie.

Die doel van hierdie studie was om die effek van vier hidroksie- en metoksieflavonoïede op die *in vitro* transport van Rhodamien 123, ‘n bekende P-gp substraat, oor rot en vark intestinale weefsel met behulp van die Sweetana-Grass diffusie-apparaat vas te stel. Die resultate is gebruik om vas te stel of die twee verskillende dierweefselmodelle ooreenkomste toon ten opsigte van die flavonoïede se effek op P-gp geïnduseerde effluks. Twee kontrole groepe is in die beplanning van die eksperimente ingesluit. Die negatiewe kontrole is gebruik om die transport van Rhodamien 123 in die afwesigheid van flavonoïede te toets. Die positiewe kontrole is gebruik om die transport van Rhodamien 123 in die teenwoordigheid van ‘n bekende P-gp inhibeerder, Verapamiel, vas te stel. Eksperimente met die flavonoïede Morin, Galangin, 6-Metoksieflavoon en 7-Metoksieflavoon is in drievoud gedoen om die herhaalbaarheid van die resultate te bevestig. Transport van Rhodamien 123 in die apikale na basolaterale (absorpsie) sowel as in die basolaterale na apikale (sekresie) rigting is vasgestel. Die relatiewe transport van Rhodamien 123, die deurlaatbaarheidskoëffisiënt (P_{app}), fluks (J), effluks ratio (ER) en netto fluks (J_{net}) is bereken. Die konsentrasie Rhodamien 123 teenwoordig in die ontvangersel is deur middel van ‘n gevalideerde HPLC-metode bepaal. Resultate van die eksperimentele groepe is statisties met die kontrole groepe vergelyk om beduidende verskille aan te dui.

Morin, Galangin en 6-Metoksieflavoon het ‘n betekenisvolle inhiberende effek op die effluks van Rhodamien 123 (waarskynlik P-gp verwant) op beide die rot en vark intestinale weefselmodelle getoon ($p < 0.05$). 7-Metoksieflavoon het ‘n betekenisvolle effek op die effluks van Rhodamien 123 in die intestinale weefselmodel van die vark getoon ($p < 0.05$), maar nie in dié van die rot nie ($p > 0.05$). Uit die resultate van hierdie studie is dit duidelik dat Morin, Galangin en 6-Metoksieflavoon die biobeskikbaarheid van geneesmiddels, wat substrate van P-gp is, verhoog en sodoende ook klinies betekenisvolle farmakokinetiese veranderinge bewerkstellig, maar dit moet met *in vivo* studies bevestig word. Verder kan hierdie flavone ook gebruik word om die absorpsie van geneesmiddels te verbeter wanneer dit onder gekontroleerde omstandighede toegedien word.

Met betrekking tot die twee dierweefselmodelle wat gebruik is, kan die gevolgtrekking gemaak word dat data wat met die rot intestinale weefselmodel verkry is, nie met data wat vanaf die vark intestinale weefselmodel verkry is, vergelyk kan word nie. Derhalwe word voorgestel dat hierdie *in vitro* resultate met *in vivo* toetse vergelyk moet word om die beste model te vind.

Sleutelwoorde: P-glikoproteïen, rhodamien 123, Sweetana-Grass diffusie-apparaat, flavonoïede, *in vitro* modelle

List of tables

List of figures

List of abbreviations

ABC	Adenosine triphosphate-binding cassette
ADMET	Absorption, distribution, metabolism, elimination, toxicity
ANOVA	One-way analyses of variance
AOTP2B1	Organic anion transporting polypeptide 2B1
AP-BL	Apical to basolateral
ATP	Adenosine triphosphate
ATPase	Adenosine triphosphatase
BCRP	Breast cancer resistant protein
BL-AP	Basolateral to apical
ER	Efflux ratio
GI	Gastrointestinal
HPLC	High pressure liquid chromatograph
ISBT	Ileal sodium dependent bile acid transporter
J	Flux
J_{net}	Net flux
MDR	Multidrug resistance
MRP	Multidrug resistance-associated protein
MRP1	Multidrug resistance protein 1
MRP2	Multidrug resistance protein 2
MRP3	Multidrug resistance protein 3
NBD	Nucleotide-binding domains
NBD1	Nucleotide-binding domain 1
NBD2	Nucleotide-binding domain 2
OSTα	Organic solute transporter α

OSTβ	Organic solute transporter β
PAMPA	Parallel artificial membrane permeability assays
P_{app}	Apparent permeability
PEPT1	Oligopeptide transporter 1
P-gp	P-glycoprotein
SAR	Structural activity relationship
SD	Standard deviation
TMD's	Transmembrane domains

Chapter 1

Introduction and aim of the study

1.1 Background

Although oral drug absorption includes several different processes, drug permeability through the intestinal membrane is one of the most important factors in defining oral drug absorption (Yamashita *et al*., 2000:195). The first major obstacle to overcome during the drug absorption process is the intestinal epithelium (Chan *et al*., 2004:25). In addition to metabolism, intestinal efflux is a limiting factor to the absorption of a variety of structural unrelated compounds. The intestinal efflux component is responsible for an active secretion from the epithelial cells to the luminal side, or in some cases, to the serosal side (Deferme *et al.,* 2008:187).

P-glycoprotein (P-gp) is the most extensive studied active membrane transporter that has been known to have an impact on the absorption, distribution, metabolism, elimination and toxicity of drug molecules (Balimane *et al*., 2006:2). P-gp is localized at the apical surface of epithelial cells in the intestine and acts as a biological barrier by extruding toxic substances and xenobiotics out of the cell (Deferme *et al*., 2008:187). P-gp is therefore ideally positioned to limit or prevent the absorption of compounds into the blood, by driving these compounds from inside the epithelial cell back into the intestinal lumen (Chan *et al.*, 2004:34). In fact, P-gp is considered to be a major determinant of disposition of a wide array of drugs in humans (Balimane *et al*., 2006:1). Multidrug resistance (MDR) refers to the ability of cells, exposed to a single drug, to develop resistance to a broad range of structurally and functionally unrelated drugs due to enhanced outward transport (efflux) of these drugs mediated by a membrane glycoprotein “drug transport pump” (Hunter & Hirst, 1997:132).

The most conspicuous feature of the transport activity of P-gp is the diversity of its substrates. An enormous number of unrelated neutral or cationic lipophilic organic compounds are transported by P-gp. A similarly diverse array of compounds, known as “chemosensitisers”, “resistance modulators” or “reversing agents”, inhibit transport by P-gp. Many, but not all of these latter compounds are themselves transported by P-gp (Shapiro & Ling, 1998:228).

A number of drugs have been identified which are able to reverse the effects of P-gp, multidrug resistance protein (MRP1) and their associated proteins on MDR (Hunter & Hirst, 1997:129; Choi *et al.*, 2004:672). Deliberate inhibition of intestinal P-gp can lead to substantial improvement in the bioavailability of some drugs given orally (Evans, 2000:134). Flavonoids which are present in the diet are capable of interfering with drug metabolism *in vitro* and it is known that different flavonoids are able to inhibit the action of P-gp (Choi *et al*., 2004:678; Van Huyssteen, 2005:42; Dodd, 2005:58). The effects produced by some flavonoids are found to be comparable to those of well-known P-gp inhibitors verapamil and cyclosporine (Bansal *et al.*, 2009:46). According to Bansal *et al.* (2009:46) flavonoids form the third generation, non-pharmaceutical category of P-gp inhibitors.

Because whole animal studies cannot be used as a screening tool to determine the extent of intestinal absorption that takes place, a number of *in silico*, *in situ* and *in vitro* experimental methods has been developed in order to estimate intestinal drug permeability and absorption, each with its advantages and disadvantages (Le Ferrec *et al*., 2001:651; Deferme *et al.,* 2008:182).

The successful application of *in vitro* models of intestinal drug absorption depends on the extent to which the model comprises the relevant characteristics of the *in vivo* biological barrier. Despite the obvious difficulties associated with trying to reproduce all the characteristics of the intestinal mucosa *in vitro*, various systems have been developed which mimic, to varying degrees, the relevant barrier properties of the intestinal mucosa (Hidalgo, 2001:389). Currently, a variety of experimental methods are available when evaluating intestinal permeability. A few commonly used *in vitro* models include artificial lipid membranes such as parallel artificial membrane permeability assays (PAMPA), cell culture based systems such as Caco-2 cells, tissue based Ussing chambers as well as the Sweetana-Grass diffusion technique. *In situ* models include intestinal single-pass perfusion experiments while *in vivo* methods utilise whole animals where blood plasma is analysed for drug concentration after administration of a single dose (Balimane *et al*., 2006:2). The models used are supposed to simulate human intestinal absorption.

The Sweetana-Grass apparatus (Grass & Sweetana, 1988:372) is a model where excised animal intestinal tissues are used to determine permeability. The Sweetana-Grass diffusion apparatus is similar to the well-known Ussing type diffusion chambers. In both these systems substances can be exposed at either the mucosal side (apical) or the serosal side (basolateral),

which makes it an attractive *in vitro* model to study drug transport in both directions across intestinal tissue (Le Ferrec *et al*., 2001:654). There is, however, no perfect absorption model and the importance of combining different absorption models is stressed by Deferme *et al.* (2008:187) in order to mimic drug absorption in the *in vivo* situation.

Recent advances in our understanding of these active processes such as epithelial transporters are of great importance. Preclinical drug development is changing rapidly and the role of *in vitro* and *ex vivo* approaches in this process are becoming increasingly more important. It is clear that the results from such *in vitro* tests are especially important during the early pre-clinical drug development process (Pelkonen *et al.*, 2001:621).

1.2 Research problem

There is a global rise in the use of natural and herbal products in conjunction with allopathic medicines, while most patients do not inform their health care providers of the use of these natural products (Ingersoll, 2005:434). Simultaneous intake of herbs and drugs may lead to pharmacokinetic interactions that may change the bioavailability of the drug, which is specifically important for drugs with narrow therapeutic indices. Many plants contain a complex mixture of phytochemicals (e.g. some medicinal plants contain flavonoids), which may impact on the absorption of co-administered drugs. It is therefore important to identify potential pharmacokinetic interactions between phytochemicals such as flavones and drugs, to make informed decisions regarding patient safety (Tarirai *et al.,* 2010:3).

1.3 Aim of this study

The aim of this study was to determine the effect of four selected hydroxy- and methoxy-flavonoids on the *in vitro* transport of Rhodamine 123, a known P-gp substrate, across stripped excised rat and pig intestinal tissue using the Sweetana-Grass diffusion technique. It was further important to determine whether the transport results obtained with the two different animal tissue models corresponded to each other with regard to possible P-gp inhibition.

The results of these transport studies would be valuable in the extrapolation of findings in rat models, a well described model compared to those of pig models.

1.4 Structure of dissertation

In this dissertation, the introductory chapter is followed by a review of the relevant literature (Chapter 2). In Chapter 3 the experimental procedure and statistical methods are described. Chapter 4 displays the results with discussions and possible explanations, while Chapter 5 gives the final conclusions and future recommendations.

Chapter 2

Drug delivery and the role of P-glycoprotein influencing bioavailability

2.1 Introduction

Oral administration is the most popular and commonly used route for drug administration since dosing is convenient, non-invasive and many drugs are well absorbed by the gastrointestinal tract (Pelkonen *et al.,* 2001:621; Chan et al., 2004:27). Therefore, absorption of drugs via the oral route is a subject of intense and continuous investigation in the pharmaceutical industry since bioavailability implies that the drug should reach the systemic circulation after oral administration (Pang, 2003:1507). For the drugs to fulfil their purpose they must be absorbed from the gastrointestinal tract and enter the systemic circulation in adequate quantities (Pelkonen *et al.,* 2001:621). Several factors, which include the physicochemical properties of the drug and the physiological factors at the region of absorption, influence the rate and extent of a substance's absorption after oral administration. Physiochemical properties of a substance such as lipophilicity, ionization state and molecular size are possibly the most important factors that influence bioavailability and are completely independent of the animal species. Perhaps the most enigmatic properties that affect absorption, and also those that causes the greatest interspecies differences, are the anatomy and physiology of the gastrointestinal tract (DeSesso & Jacobson, 2001:209).

Although oral drug absorption includes several different processes, drug permeability through the intestinal membrane is one of the most important factors in defining oral drug absorption (Balimane *et al*., 2000:301). Permeation is essentially a two-way process. In the intestines the flow of the substances from the lumen into the bloodstream (absorption) and the flow from the bloodstream into the lumen (exorption or efflux) occur simultaneously. The primary physiological function of the gastrointestinal tract is absorption. The net result of permeation is usually absorption, but exorption cannot be neglected (Csáky, 1984:52).

The small intestine is the principle site of absorption of any ingested compound (Chan *et al*., 2004:27). The rate of permeation across any biological membrane depends on the structure of the membranes as well as the physicochemical properties of the substance (Csáky, 1984:52).

The transport of drug substances across the intestinal membrane is a complex and dynamic process (Balimane *et al.*, 2000:301). In order to understand the absorption and efflux of drugs that may take place, the anatomy and physiology of the small intestine, different absorption mechanisms as well as the mechanisms of the efflux of drugs will be discussed. Different models that may be used to determine intestinal permeability will also be discussed in this chapter.

2.2 Anatomy and physiology of the small intestine

The gastrointestinal (GI) tract of humans has many morphological similarities with most animal species used in drug absorption studies, especially at the level of microscopic evaluation (DeSesso & Jacobson, 2001:210). The small intestine is the major site for the absorption of nutrients, water and electrolytes (DeSesso & Jacobson, 2001:216) and approximately 90% of all absorption in the GI tract takes place in the small intestinal region. The small intestine is divided in three unequally sized regions called the duodenum, jejunum and ileum (Balimane *et al.*, 2000:301-302).

The mucosa in the absorbing region of the GI tract exhibits a variety of modifications that increase the surface area including folds (plicia), depressions (crypts) and finger-like projections (villi). A cross-section of the small intestines of humans (A) and rats (B) that illustrate luminal surface modifications is shown in Figure 2.1 (DeSesso & Jacobson, 2001:213). Macroscopic valve like folds, called circular folds, encircling the inside of the intestinal lumen are estimated to increase the surface area of the small intestine three-fold. Millions of finger-like projections called villi increase the surface area 30-fold and the numerous projections from the luminal surface of the epithelial cell, called microvilli or brush border, increase it by 600-fold. Thus, such unique structures lead to a tremendous increase in the surface area available for absorption in the small intestines (Balimane *et al.*, 2000:301-302). This increased surface area of the mucosa is conducive to transfer substances from the lumen to the vascular system (DeSesso & Jacobson, 2001:213).

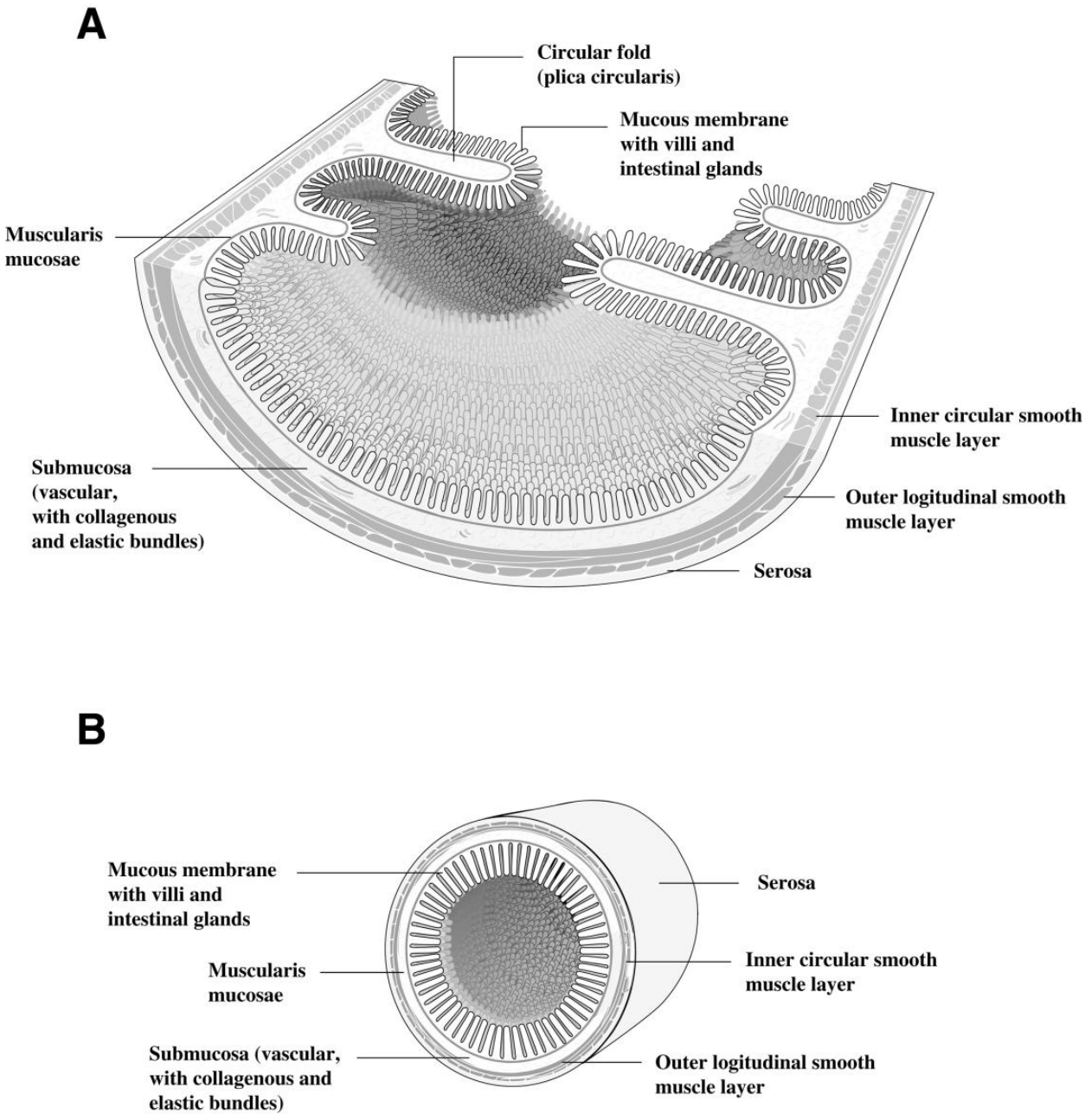

Figure 2.1: Cross-section of the proximal human small intestine of humans (A) and rats (B) (DeSesso & Jacobson, 2001:215)

A diagram of the structure of an intestinal villus is shown in Figure 2.2. The luminal surface of the entire GI tract, including the villus, is lined with a single layer of epithelial cells. The brush border on the surface of the villus is also visible in Figure 2.2.

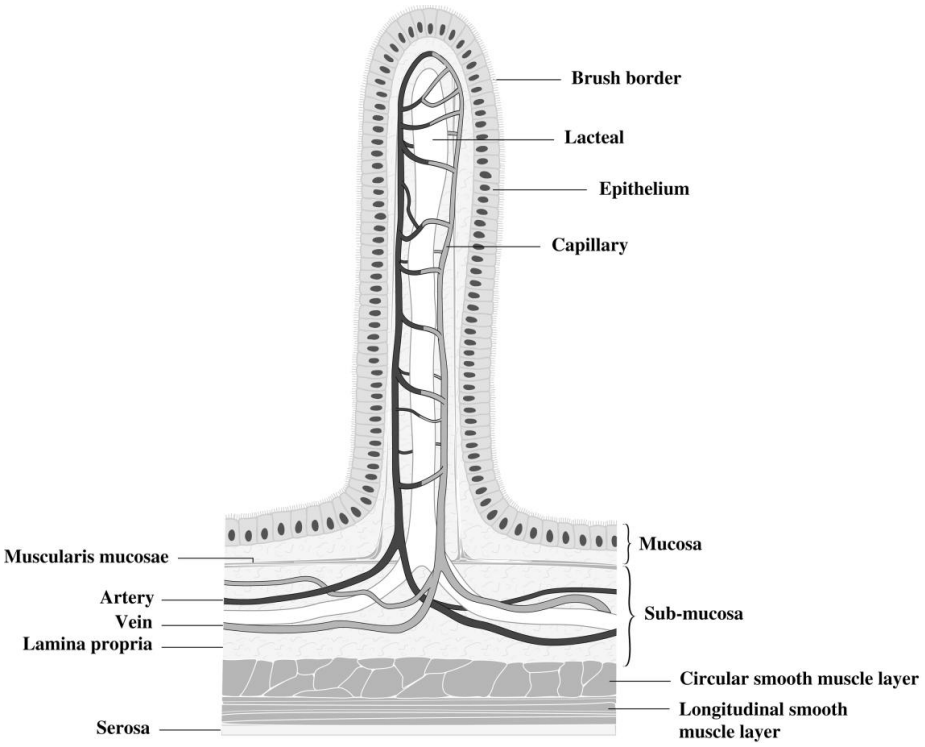

Figure 2.2: Diagram of the structure of an intestinal villus (DeSesso & Jacobson, 2001:216)

The deep structure of the villus is characterised by a large, blind-ending lymphatic vessel, the lacteal, which is responsible for the absorption of higher molecular weight substances, including fats. A small plexus of blood capillaries surrounds the lacteal. In addition to the vascular structures, the villus contains loose connective tissue and small amounts of smooth muscle (*muscularis mucosae*) which wiggles the villus back and forth in the liquid adjacent to the intestinal wall, thereby increasing the efficacy of absorption (DeSesso & Jacobson, 2001:216; Daugherty & Mrsny, 1999:144-145).

Although the epithelium of the absorbing areas of the GI tract is not composed of a uniform population of cells, there is one cell type that is important in the absorption of materials from the lumen and it is the predominant cell involved in all absorbing regions. This cell type is referred to as an enterocyte. A diagram of a typical intestinal epithelial cell or an enterocyte is shown in Figure 2.3.

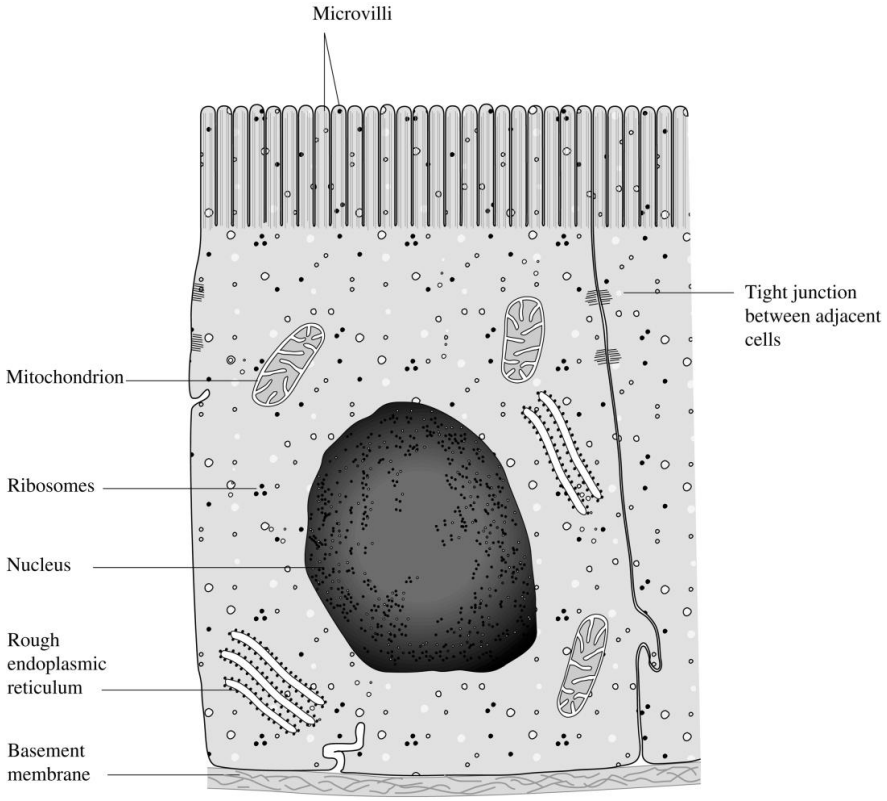

Figure 2.3: Diagram of a typical intestinal enterocyte (DeSesso & Jacobson, 2001:213)

Enterocytes are high cuboidal to low columnar epithelial cells that are bound firmly to their adjacent cells by tight junctions and embedded on a basement membrane. Their apical cell membranes possess numerous microvilli (approximately 3000-7000 per cell) which also greatly increase the surface area available for absorption. The presence of microvilli on the enterocyte creates the appearance of a brush border that is seen with a light microscope. The absorptive epithelia rest on the basement membrane and possess a carbohydrate-rich glycocalyx coat on the surface of the microvilli. Nearly all substances taken up from the intestinal lumen must cross the enterocyte cytoplasm. Lipids and fats are absorbed at the base of the microvilli, crossing the cytoplasm and exit the cell at its side, beneath the tight junctions. Amino acids, triglycerides and carbohydrates are absorbed along the length of the microvilli, passes through the entire cytoplasm and exit the cell at its base (DeSesso & Jacobson, 2001:214).

2.2.1 Structural differences between human, rat and pig small intestine

While the gross organisation of the individual segments of the GI tract of all the mammals are essentially similar, there are wide differences in the dimensions of some GI structures, as well as in the lengths and absorptive surface areas of the various sub-divisions. In addition, the environmental conditions such as the pH and fluidity of the chyme, number and type of bacterial flora as well as the transit time within the lumen of the various sub-divisions differ greatly among species. The differences, and the comparison of such to the human condition, must be taken into account when selecting an animal for drug disposition studies. Regardless of its function, every region in the GI tract is lined by a mucous membrane composed of epithelial cells joint by tight junctions and underlain by a basement of loose and connective tissue (*lamina propria*), which is richly vascularised in those areas where absorption is involved (DeSesso & Williams, 2008:356).

The physicochemical properties of drugs and chemicals are relatively constant in different test systems, whereas factors such as the absorptive surfaces and luminal milieus are to a great extent influenced by the gastrointestinal anatomy and physiology of the species under consideration (DeSesso & Williams, 2008:353).

Despite the fact that the human small intestine is only about five times the length of the rat small intestines, its surface area is 200 times that of the rat. A Comparison of the anatomical lengths of the GI tract and its major subdivisions in humans, rats and pigs are given in Table 2.1.

The length of the human GI tract is only about five times the length of the rat intestinal tract, despite the much larger body size of the human (70 kg) compared with the rat (0,25 kg). In rats, about 90% of the total small intestine is comprised of jejunum while in humans only 38% of the total small intestine is comprised of jejunum. In humans three types of anatomical modifications (i.e. Kerckring's folds, villi and microvilli) increase the surface area of the small intestines, but in rats Kerckring's folds are absent. The Kerckring's folds increase the surface area in human small intestines by the factor 3, while the villi present in humans and rats increase the surface area by a factor 5 and 10 respectively. Human and rat enterocytes possess thousands of microvilli which increase the surface area of the rat and human small intestine with a factor 20. In both humans and rats, these anatomic modifications increase the surface area to a greater extent in the duodenum and upper jejunum than in the ileum. For both humans and rats, the majority of surface area is found in the jejunum (DeSesso & Jacobson, 2001:217). Because of the differences in size between rats and humans, absolute surface areas are not directly

comparable, and a more meaningful comparison is obtained when data are normalised for body size. The comparison reveals that the relative surface area of the human small intestine is more than three times that of the rat. As the amount of substance that crosses the enteric mucosa is determined by its flux (amount of mass per unit surface per unit time), the impact of the increase relative enteric surface area in humans on the comparative absorption of substances is two-fold. Firstly substances that are equally well absorbed in both rats and humans are likely to be absorbed more quickly in humans and secondly substances that are poorly or incompletely absorbed by both species are likely to be absorbed to a greater extent by humans (DeSesso & Jacobson, 2001:217).

With regard to interspecies differences in terms of secretions into the GI tract, it is important to note the anatomical differences that exist between humans, rats and pigs. The small intestine receives secretions from several organs, including the pancreas (high in volume and rich in digestive enzymes and bicarbonate), liver (bile), and enteric glands (located in the wall of the small intestine, their secretions are rich in bicarbonate that neutralises the acid from the stomach). The volume of these secretions in primates, dogs and pigs are more than double the secretions from the salivary glands and stomach and serve to make the chyme watery with a lower pH and a negligible bacterial content. In rats the chyme remains rather pasty with a higher pH and contains many bacteria (DeSesso & Williams, 2008:355-367). Further the rat lacks a gallbladder, which causes the bile not to be concentrated. In rats, bile enters the duodenum continuously as it is made in rather copious amounts when compared to the concentrated bile in humans, which is released only when chyme is present (DeSesso & Jacobson, 2001:222).

Possibly the most important aspect that may influence the rate and extent of absorption between species relates to the alterations in the anatomical structure of the epithelial layer that increase the surface area available for absorption (DeSesso & Williams, 2008:355). In Table 2.1 and Table 2.2 the differences regarding surface area can be seen.

Table 2.1: Comparison of lengths of the gastrointestinal tract and its major subdivisions in humans, rats and pigs (DeSesso & Jacobson, 2001:214; DeSesso & Williams, 2008:360)

Region of GI tract	Human			Rat			Pig		
	Length (cm)	% of total	% of region	Length (cm)	% of total	% of region	Length (cm)	% of total	% of region
Duodenum	25		4	9,5-10		8	-		-
Jejunum	260		38	90-135		90	-		-
Ileum	395		58	2,5-3,5		2	-		-
Total small intestine	680	81		125	83		1500-2000	70-85	
Total intestinal tract	835			150			2350		

Table 2.2: Total small intestinal surface areas in rats and pigs (DeSesso & Williams, 2008:362)

	Rat	Pig
Body weight (kg)	0,3	47
Smooth luminal surface area (m^2)	0,016	1,4
Fold-increase factors:		
Plicae	1	1
Villi	5	6
Microvilli	20	20-25
Combined multiplication factor	100	120
Estimated total surface area (m^2)	1,6	168-210

2.3 Intestinal absorption

For the GI tract epithelial cell membrane to fulfil its role of absorption, it depends upon specific membrane transport systems and intracellular metabolising enzymes. The extent to which a compound is absorbed across the intestinal epithelium is a critical factor in determining its overall bioavailability (Chan *et al.*, 2004:26).

Drug absorption across the intestinal membrane is a complex multi-path process as illustrated schematically in Figure 2.4. Passive diffusion as an absorption mechanism occurs most commonly through the cell membrane of the enterocytes (transcellular route) or via the tight junctions between the cells (paracellular route). On the other hand, carrier-mediated absorption occurs via an active (or secondary active process) or facilitated diffusion process. Various efflux transporters such as P-glycoprotein (P-gp), breast cancer resistant protein (BCRP) and multidrug resistance protein 2 (MRP2) can limit absorption of substances that are substrates. Intestinal enzymes could be involved in metabolising drugs to alternate moieties, which might even be better absorbed than the parent molecule. Finally receptor-mediated endocytosis could play a role in the absorption process (Balimane *et al.,* 2006:2). There are thus two major transport mechanisms of drug transport across the gastrointestinal epithelium, namely the transcellular pathways and paracellular pathways (Aulton, 2007:279).

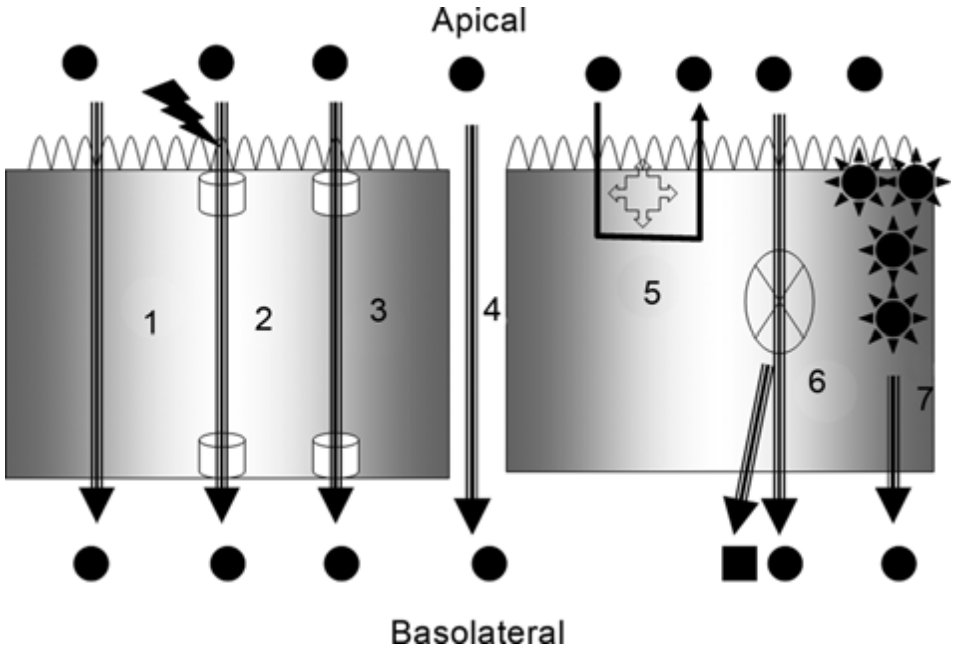

Figure 2.4: Different pathways for intestinal absorption: (1) passive diffusion, (2) active transport, (3) facilitated diffusion, (4) paracellular transport, (5) absorption limited by P-gp and/or other efflux transporters, (6) intestinal first-pass metabolism, and (7) vesicular transport or receptor-mediated endocytosis (Balimane *et al.,* 2006:2)

Because of the multivariate processes involved in intestinal absorption of drugs, it is often difficult to use a single *in vitro* model to accurately predict the *in vivo* permeability characteristics of compounds (Balimane *et al.,* 2006:2).

2.3.1 Transcellular pathway

The transcellular pathway is the transport that occurs across the epithelial cells and is further divided into simple passive diffusion, carrier-mediated transport (active transport and facilitated diffusion) and vesicular transport (Shargel & Yu, 1999:101-102; Aulton, 2007:279).

2.3.1.1 Passive diffusion

Passive diffusion is the common route of transport for rather small lipophilic molecules and thus many drugs. This is the route by which molecules spontaneously diffuse from an area of high concentration in the lumen to an area of lower concentration in the blood (Aulton, 2007:279). The driving force for passive diffusion is the concentration gradient due to the higher drug concentration on the mucosal side compared to the concentration in the blood. Passive diffusion of drugs across the gastrointestinal-blood barrier can be described mathematically by Fick's Law of diffusion (equation 2.1).

$$\frac{dQ}{dt} = \frac{DAK}{h}(C_{GI} - C_p) \qquad 2.1$$

Where:

dQ/dt = rate of diffusion; *D* = diffusion coefficient; *K* = lipid water partition coefficient of drug in the biologic membrane that controls drug permeation; *A* = surface area of the membrane; *h* = membrane thickness; and $C_{GI} - C_p$ = difference between the concentrations of drug in the GI tract and in the plasma (Shargel & Yu, 1999:102).

This transport route is passive because the membrane does not play any active role in the process and no external energy is expended (Shargel & Yu, 1999:102). The rate of transport is determined by the physicochemical properties of the active ingredient, the nature of the membrane and the concentration gradient of the active ingredient across the membrane (Aulton, 2007:279). Molecules have a tendency to move randomly in all directions in solution because they have kinetic energy and regularly collide with each other. As molecules diffuse over the membrane from a high concentration to a lower concentration and *vice versa* (small arrows in Figure 2.5), the net result would be the transfer of molecules to the other side (large

arrow in Figure 2.5). This resultant movement is called the net flux (J) and represents the rate of transfer (Shargel & Yu, 1999:102).

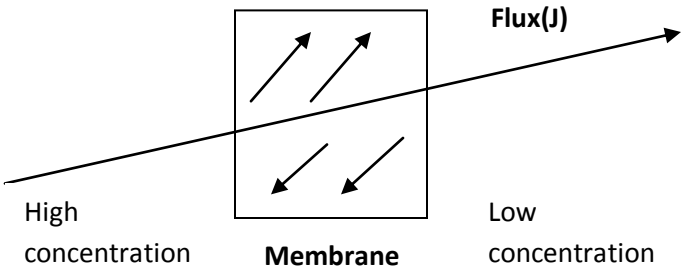

Figure 2.5: Passive diffusion of molecules (Shargel & Yu, 1999:102)

For the process of diffusion to initiate, it involves the partitioning of the drug between the aqueous fluids within the GI tract and the lipoidal-like membrane of the epithelium. The drug in solution in the membrane then diffuses across the epithelial cells on the inside surface of the GI tract to blood in the capillary network in the *lamina propria*. When the drug reaches the blood, it will be rapidly distributed to maintain a much lower concentration than that at the absorption site (Aulton, 2007:279-280). The passive diffusion process is driven solely by the concentration gradient of the diffusible species of the drug that exists across the gastrointestinal-blood barrier (Aulton, 2007:281).

2.3.1.2 Carrier-mediated transport

Although the majority of drugs are absorbed across cells by means of passive diffusion, certain compounds and many nutrients are absorbed transcellularly by a carrier-mediated transport system of which there are two main types, namely active transport and facilitated transport.

2.3.1.2.1 Active Transport

In contrast with passive diffusion, active transport involves the active participation of the apical cell membrane of the columnar absorption cells in the absorption process. A carrier or membrane transporter is responsible for binding to a drug molecule and transporting it across the membrane (Aulton, 2007:281). Active transport can take place against a concentration gradient, from regions of low concentration of a drug to regions with high concentrations. For this reason energy is needed for the transport to take place. Additionally, active transport is a specialised process that requires a carrier that binds to the substance to form a complex that shuttles the substance across the membrane and dissociates from the substance at the other

side of the membrane. The carrier returns to its initial position at the apical side of the epithelia to await the arrival of another molecule or ion. The carrier molecule may be highly selective for the substance and therefore substances with a similar structure usually compete for binding sites on the carrier. For this reason, when compared to passive transport as can be seen in Figure 2.6, the rates of absorption increases with the concentration of the substance until the carrier molecules are completely saturated. At higher drug concentrations, the rate of drug absorption remains constant. During passive transport the rate of absorption increases in a linear relationship to the concentration of the particular substance (Shargel & Yu, 1999:105-106).

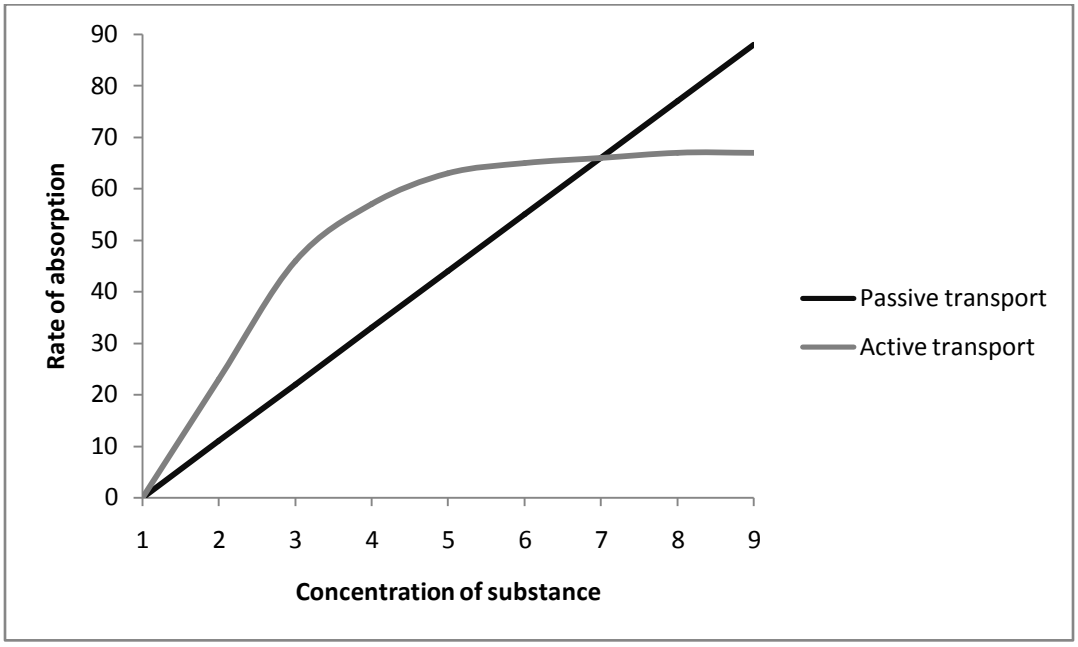

Figure 2.6: Relationship between rate of absorption and concentration of substance for active and passive transport (Aulton, 2007:282)

2.3.1.2.2 Facilitated transport

Facilitated transport is a carrier-mediated transport system that differs from active transport in that the drug moves only along a concentration gradient. Movement is thus from a region of high drug concentration to a region of low drug concentration. For this reason, facilitated transport does not require an energy input but a concentration gradient. This process is also saturable and is subject to inhibition by competitive inhibitors. In terms of drug absorption, facilitated transport seems to play a very minor role (Shargel & Yu, 1999:106).

2.3.1.3 Vesicular transport

Vesicular transport is the method of transport where the cell engulfs particles or dissolved materials. This includes pinocytosis, phagocytosis and (receptor mediated) endocytosis, all processes that enable the cell membrane to absorb substances, especially macromolecules (Shargel & Yu, 1999:107).

2.3.2 Paracellular pathway

The paracellular pathway differs from all the other absorption pathways in the sense that substances do not move across the cells but through the aqueous intercellular spaces between the cells which are joined together by tight junctions at their apical sides. These intracellular spaces occupy only about 0,01% of the total surface area of the epithelium. The paracellular pathway becomes less important as you move down the length of the GI tract, because of the decreasing number and size of the pores between the epithelia cells. This route is especially important for the transport of ions such as calcium and for the transport of sugars, amino acids and peptides at concentrations above the capacity of their carriers, and also for small hydrophilic and charged substances that do not distribute into the cell membranes (Aulton, 2007:283).

2.4 Membrane transporters

Membrane transporters are responsible for two important permeation mechanisms, namely active uptake (absorption) and efflux (exsorption). Carrier mediated transport can contribute significantly to the pharmacokinetic characteristics of a compound (Kerns & Di, 2008:103; Daugherty & Mrsny 1999:149). There are counter transport efflux proteins that expel specific drugs after they have been absorbed. One of the key counter transport efflux proteins, and which is also of importance in this study, is P-glycoprotein (Aulton, 2007:283; Varma *et al.*, 2006:367).

Transporters, in general, can affect the absorption, distribution, metabolism, elimination, toxicity (ADMET) characteristics of substances. Transport occurs when a drug contains a chemical group similar to the natural substrate of a transporter, or if it has structural elements that facilitate binding to a transporter with wide substrate specificity, for example P-gp (Kerns & Di, 2008:104; Bohets *et al.*, 2001:378-379). Transporters can affect ADMET in the following ways:

- Uptake transporters enhance the absorption of some molecules in the intestine,
- Efflux transporters oppose the absorption of some molecules in the intestine,
- Transporters assist the uptake of some molecules into hepatocytes to enhance metabolic and biliary clearance,
- Efflux transporters oppose the distribution of some drugs from the bloodstream into certain organs such as the brain,
- Uptake transporters enhance the distribution of some drugs into some organs,
- Elimination of many drugs and metabolites is enhanced by active secretion in the nephrons of the kidney and
- Co-administered drugs can compete for a transporter for which they both have affinity, resulting in drug-drug interactions and modification of the pharmacokinetics of one of the compounds (Kerns & Di, 2008:104).

Different transporters that have been identified in intestinal epithelial cells are shown in Figure 2.7.

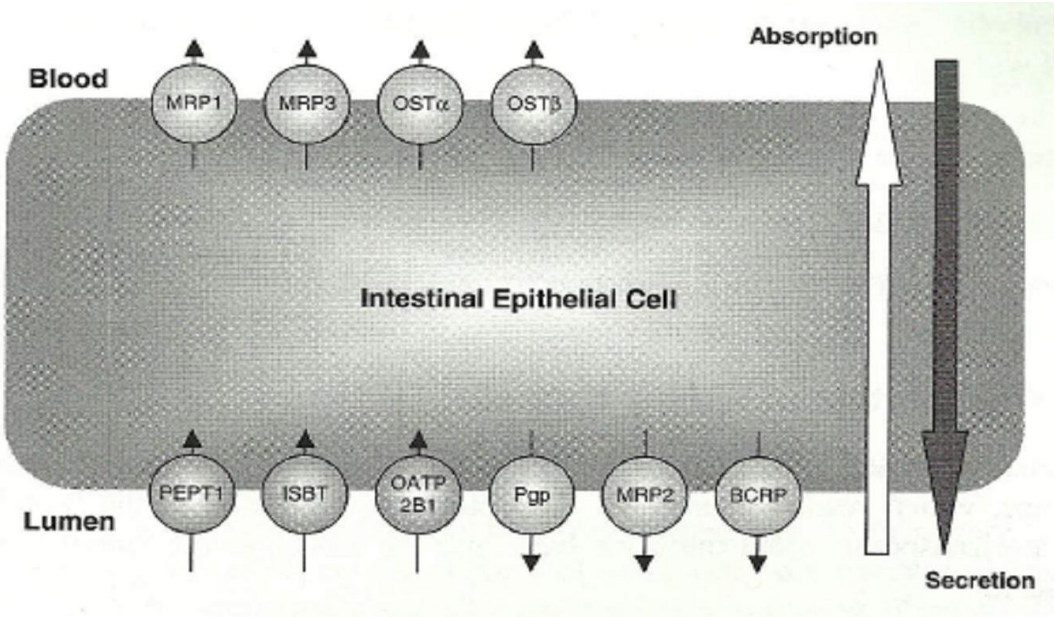

Figure 2.7: Transporters that have been identified in intestinal epithelium cells (Kerns & Di, 2008:109)

In the intestinal epithelial cells, transporters are involved in the absorptive uptake as well as the efflux of drugs. Absorptive uptake occurs from the gastric lumen through epithelial cells and into blood. Transporters that are responsible for this process include the oligopeptide transporter

(PEPT1), ileal sodium dependent bile acid transporter (ISBT), organic anion transporting polypeptide (OATP2B1), multidrug resistance proteins (MRP1, MRP3) and organic solute transporters (OSTα, OSTβ). Efflux is the movement of substances from the epithelial cell membrane back into the gastric lumen and transporters that are responsible for this process includes P-glycoprotein (P-gp), multidrug resistance proteins (MRP2) and breast cancer resistance protein (BCRP) (Kerns & Di, 2008:108).

2.5 Efflux of substances from the intestine

Drugs that cross the apical membrane may be substrates for apical efflux transporters, which extrude compounds back into the lumen. These apical efflux transporters are principally adenosine triphosphate-binding cassette (ABC) proteins such as P-glycoprotein (P-gp), multidrug resistance (MDR) and multidrug resistance-associated protein (MRP). These proteins are ideally situated to act as the first line of defence by limiting the absorption of potentially harmful foreign substances. Compounds that are already present in the blood may also undergo active blood-to-lumen secretion facilitated by these transporters (Chan *et al.*, 2004:26).

2.5.1 ABC transporters

ABC transporters are present in all species, from microbes to man. They play a wide variety of physiological roles and are of great medical and economic importance. In microorganisms, ABC transporters are central to antibiotic and antifungal resistance and in humans many are associated with genetic diseases such as cystic fibrosis, Tangier disease, obstetric cholestases, and drug resistance of cancers. Although each ABC transporter is relatively specific for its own substrate, it is significant that there is an ABC transporter for almost every type of molecule that must cross a cellular membrane (Higgins, 2001:205-206).

One form of drug resistance is multi-drug resistance (MDR), which is defined as the ability of cells exposed to a single drug to develop resistance to a broad range of structurally and functionally unrelated drugs due to enhanced outward transport (efflux) of these drugs mediated by a membrane transporter molecule (Hunter & Hirst, 1997:132).

2.5.2 P-glycoprotein

P-gp is an adenosine triphosphate (ATP) driven efflux pump capable of transporting a wide variety of structural diverse compounds from the cell into the extracellular space (Hochman *et*

al., 2002:18). In 1976, Juliano and Ling found a membrane glycoprotein that appeared to be unique in the sense that it displayed altered drug permeability in mutant cells. They named it P-glycoprotein (P-gp) where the "P" stands for permeability (Juliano & Ling, 1976:152). P-gp is a phospho-glycoprotein that belongs to the ABC transporter family (Berggren, 2006:14). P-gp was the first member of what is now a large and diverse super family comprising of around fifty human ATP-binding cassette (ABC) proteins that perform numerous and diverse functions. Because drug transport is important, the glycoprotein P-gp can have a major impact on drug disposition and drug resistance to especially chemotherapy and physiological homeostasis. These drug efflux proteins primarily comprise the MDR and MRP-type transporters (Chan *et al.*, 2004:25). P-gp is one of the most widely studied transporters that have been indisputably known to impact the ADMET characteristics of drug molecules. A ubiquitous transporter is present on the apical surface of enterocytes, the canalicular membrane of hepatocytes, and on the apical surface of kidney, placenta, and endothelial cells of brain membrane. Because of its strategic location, it is widely known that P-gp is a major determinant in disposition of a wide collection of drugs in humans (Balimane *et al.*, 2006:2). P-gp thus lowers bioavailability of drugs by preventing complete absorption of the drugs by means of efflux (Choi, 2005:1). The arsenal of ABC transporters that mediate drug efflux is supported by drug metabolising enzymes, which modify drugs to yield metabolites that are themselves substrates for these transporters. Thus, a synergistic relationship exists within excretory tissues to protect the body against invasion by foreign compounds (Chan *et al.*, 2004:26).

2.5.2.1 Structure of P-glycoprotein

P-glycoprotein is the most typical efflux pump in the cell membrane that is responsible for transporting various xenobiotics out of the cell by using ATP. P-gp is a 170 000 g/mol protein with 1280 amino acids (Kerns & Di, 2008:111), 12 hydrophobic transmembrane domains (TMD's) as well as 2 nucleotide-binding domains (NBD). It consists of two homologous halves. Each half contains a highly hydrophobic domain with 6 transmembrane α-helices involved in drug efflux and a hydrophilic domain located at the cytoplasmic face of the membrane, nucleotide binding domain 1 (NBD1) or NBD2, containing an ATP-binding site with characteristic Walker motifs A and B and the S signature of the ABC transporters as illustrated in Figure 2.7 (Choi, 2005:2). One NBD connects two TMD's with a hydrophilic NBD loop. TMD's form channels for substrate drugs, determine the characteristics of substrate and efflux substrate drugs whereas NBD's are located in the interior of cytoplasm and participate in ATP binding and hydrolysis (Choi, 2005:4-5). Studies reveal that the drug-binding site is formed by the TMD's of

both halves of P-gp and substrates gain entry to these sites from within the membrane. The NBD's of ABC proteins are highly conserved (Sharom, 2006:982).

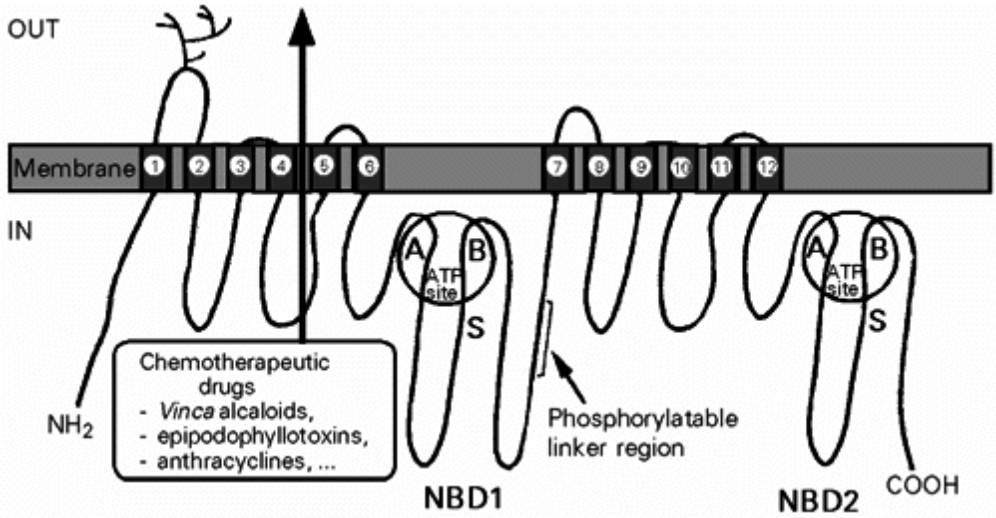

Figure 2.8: Schematic structural organisation of P-glycoprotein (Choi, 2005:2)

When one of the two NBD's of P-gp is inactivated, not only drug transport, but also ATP hydrolysis of normal NBD is inhibited. This result indicates that two NBD's would function cooperatively and they could not hydrolyse ATP independently. Structural changes of NBD's are brought about when a drug binds to TMD so that the distance between NBD's is changed to affect the activity of ATPase. The interactions of NBD's are not simple due to the fact that they function differently for every transport. Although the exact site and number of P-gp binding with drugs have not been determined, the important binding sites such as TMD 4, 5, 6, 10, 11 and 12 have been determined (Choi, 2005:5; Ambudkar *et al.*, 2006:396).

2.5.2.2 Efflux mechanisms

The three prevalent models of how P-gp transports substrates out of the cell suggest two possible sites for substrate interactions as illustrated in Figure 2.9. In the "classical pump" or "pore" model, drugs associate with P-gp in the cytosolic compartment and are transported out of the cell through a protein channel. According to the "pore model", there is a major reorganisation of the transmembrane domains throughout the entire depth of the membrane on binding of nucleotide. This restructuring opens the central "pore" along its length in a manner that allows access of the hydrophobic drug or substance directly from the lipid layer to the central pore of the transporter (Bansal *et al*., 2009:51). In the "flippase" model, drugs that are embedded in the inner leaflet of the plasma membrane bind to P-gp within the plane of the

membrane and are translocated to the extracellular (outer) leaflet of the bilayer from which they passively diffuse into the extracellular fluid (Hochman *et al.*, 2002:261). Thus, drugs approaching the extracellular side of the plasma membrane will rapidly partition into the outer leaflet, then "flip-flop" into the inner leaflet, a process that is known to be slow for many P-gp substrates (Sharom, 2008:114). P-gp intercepts lipophilic drugs as they move through the lipid membrane and flip the drug from the inner leaflet to the outer leaflet and to the extracellular medium (Bansal *et al*., 2009:52). The third model is known as the "hydrophobic vacuum cleaner" model that combines features of the other two models (Hochman *et al.*, 2002:261). Drugs that enter cells from the extracellular side are intercepted at the plasma membrane and are transported to the exterior without entering the cytosol (Sharom, 2008:114; Bansal *et al*., 2009:52). The binding process comprises two steps, namely partitioning of drug from water into membrane, and subsequently transfer of drug from the lipid to the binding pocket of the protein (Sharom, 2008:114). Experimental data most strongly supports the hydrophobic vacuum cleaner model (Hochman *et al.*, 2002:261).

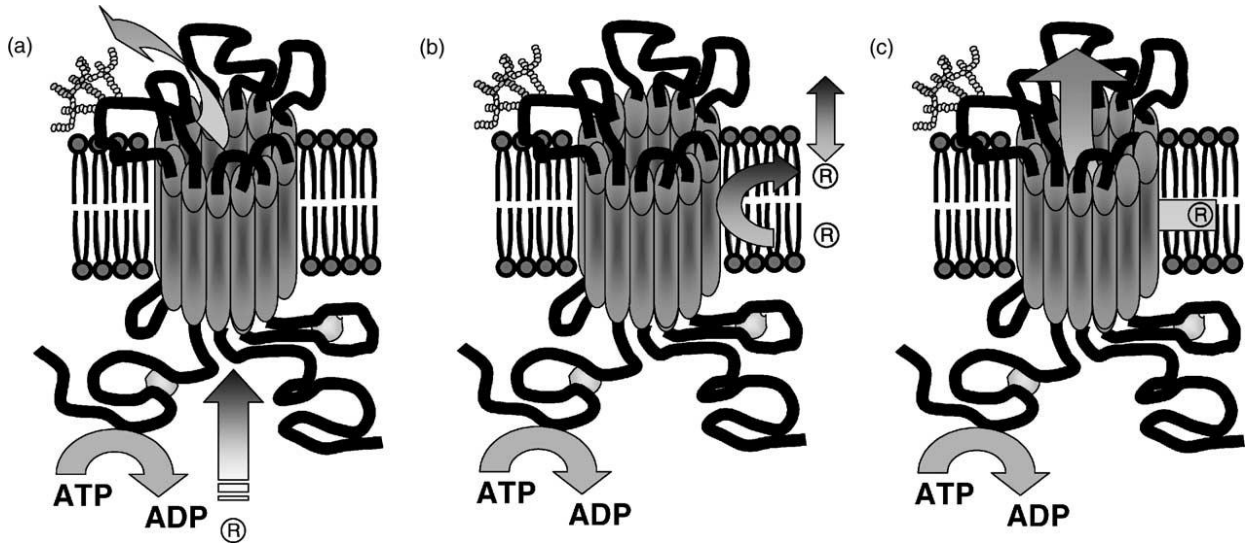

Figure 2.9: Proposed models to explain the mechanism of drug efflux by P-gp. (a) Pore model, (b) flippase model and (c) hydrophobic vacuum cleaner model (Varma *et al.*, 2003:348)

It is clear that these mechanisms are more elaborate than conventional models for enzyme substrate interactions because of the complexities of P-gp substrate interactions, such as the involvement of membrane partitioning and potential multiple drug interaction sites (Hochman *et al.*, 2002:262).

2.5.2.3 Mechanism of P-gp inhibition

P-gp can be inhibited by more than one mechanism. In general a drug molecule attaches to the binding domain of P-gp, which appears to be within the bilayer membrane. Then two ATPs bound to the ATP binding region, become hydrolysed and induce a conformation change to open a pathway for the drug molecule to pass through to the extracellular fluid (Kerns & Di, 2008:111).

There could be a blockade of the drug binding site either competitively, non-competitively or allosterically by interference with the ATP hydrolysis process, alteration in integrity of cell membrane lipids or decrease in P-gp expression as illustrated in Figure 2.10. Drugs such as Cyclosporine A inhibit transport function by interfering with both substrate recognition and ATP hydrolysis. Others, like Flupentixol, prevent substrate translocation and dissociation due to allosterical changes produced in the drug transporter. Compounds inhibiting ATP hydrolysis could serve as better inhibitors, since they are unlikely to be transported by P-gp, and these kinds of agents require a low dose which is achievable at the target site. Not one of the inhibitors known until now have been found to interact with the nucleotide binding sites to interfere with the P-gp ATPase catalytic cycle (Bansal, 2009:55).

Flavonoids are used during this study and according to Bansal *et al*. (2009:56) one potential mechanism for the flavonoid inhibition of P-gp mediated efflux may be the inhibition of P-gp ATPase by interacting directly with the adjacent ATP-binding site. Flavonoids have also been shown to directly interact with the purified recombinant C-terminal nucleotide-binding domain from mouse P-gp (NBD2) and this binding domain may overlap with the ATP binding site and adjacent steroid binding site. Different flavonoids may also interact with P-gp differently.

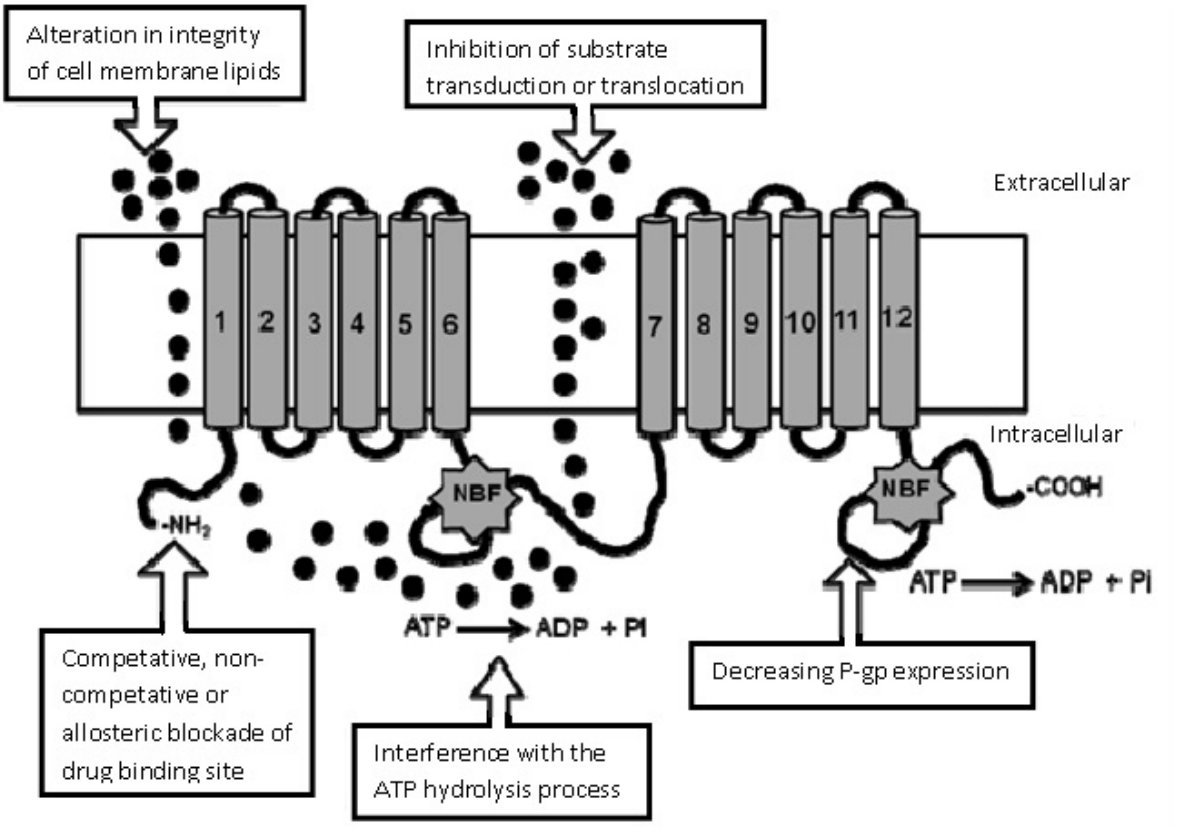

Figure 2.10: Potential mechanisms of P-gp inhibition (Bansal, 2009:62)

2.5.2.4 P-glycoprotein substrates and inhibitors

P-gp transports a wide range of structurally dissimilar compounds, many of which are clinically important (Sharom, 2008:106). Studies done by Scala *et al*. (1997:1024) defined compounds as P-gp substrates if cytotoxicity was increased more than four times by die addition of Cyclosporine, and as P-gp inhibitors or antagonists if inhibition of efflux increased Rhodamine 123 concentration more than four times. P-gp substrates are transported but do not block the transport of other substrates (Scala *et al*., 1997:1024). P-gp substrates are given in Table 2.3.

Certain rules based on chemical structure and referred to as the “rule of 4” have been created for the initial assessment of a compound for being a P-gp efflux substrate. A compound is more likely to be a P-gp substrate if its structure has an equal amount or more than 8 nitrogen and oxygen atoms combined (N + O ≥ 8), has a molecular weight higher than 400 g/mole and if it is acidic with a pK_a value higher than 4. A compound is also more likely not to be a P-gp substrate if it’s structure has an equal amount or less than 4 nitrogen and oxygen atoms combined (N + O

≤ 4), a molecular weight lower than 400 g/mole and is alkaline with a pK_a lower than 8 (Kerns & Di, 2008:112). However, P-gp substrates and inhibitors show considerable diversity and the structural requirements for interaction with P-gp are not yet well resolved. Thus far, simple structural predictions to identify compounds that interact with P-gp are not very effective (Hochman *et al.*, 2002:267).

Table 2.3: P-glycoprotein substrates (Balayssac *et al.*, 2005:321)

Analgesics	**Beta blockers**
▪ Asimadoline	▪ Talinolol
▪ Morphine	**Calcium channel blockers**
Antibiotics	▪ Verapamil
▪ Erythromycin	**Cardiac glycosides**
▪ Valinomycin	▪ Digoxin
▪ Gramicidin D	**Corticosteroids**
▪ Rifampicin	▪ Dexamethasone
▪ Grepafloxacin	▪ Hydrocortisone
Anticancer drugs	▪ Corticosterone
▪ Vinca alkaloids (vinblastine, vincristine, vindesine, vinorelbine)	▪ Triamcinolone
▪ Anthracyclines (doxorubicin, daunorubicin, epirubicin, idarubicin)	▪ Aldosterone
▪ Taxanes (paclitaxel, docetaxel)	**Curare**
▪ Epipodophyllotoxins (etoposide, teniposide)	▪ Vecuronium
▪ Anthracenes (bisanthrene, mitoxanthrone)	**Diagnostic dyes**
▪ Others (Actinomycin D, mitomycin C, dactinomycin, topotecan, irinotecan,m tamoxifen, methotrexate, trimetrexate, amsacrine, imitinib)	▪ Rhodamine 123
Antidepressants	▪ Hoechst 33342
▪ Venlafaxine	**HIV protease inhibitors**
▪ Paroxetine	▪ Saquinavir
	▪ Ritonavir
	▪ Nelfinavir
	▪ Indinavir
	▪ Lopinavir
	▪ Amprenavir
	H1-receptor antagonists
	▪ Fexofenadine

Antidiarrheal agents	**H2-receptor antagonists**
▪ Loperamide	▪ Cimetidine
▪ Antiemetics	**Immunosuppressive agents**
▪ Domperidone	▪ Cyclosporine A
▪ Ondansetron	▪ Tacrolimus
Antiepileptics	▪ FK506
▪ Carbamazepine	**Proton pump inhibitors**
▪ Phenobarbital	▪ Omeprazole
▪ Phenytoin	▪ Lansoprazole
▪ Lamotrigine	▪ Pantoprazole
▪ Felbamate	**Pesticides, anthelmintics, acaricides**
Antifungus	▪ Ivermectin
▪ Itraconazole	▪ Abamectin
Anti-gout agents	**Statin**
▪ Colchicine	▪ Lovastatin

From Table 2.3 it is clear that P-gp is a huge stumbling-block in the management of drug treatment of certain diseases. Therefore, it is of interest to discover new compounds to inhibit this efflux transporter in order to improve the bioavailability of drugs that are affected by efflux.
A few of these substrates were identified to inhibit P-gp, setting off an opportunity in MDR reversal. Improved clinical efficacy of various drugs observed by P-gp inhibition, especially drugs subjected to MDR, lead to the design and development of modulators, which specifically block P-gp efflux. P-gp inhibitors are gaining recognition to improve bioavailability by inhibiting P-gp. Some classical drugs are able to down-modulate P-gp activity and examples are given in Tabel 2.4.

Table 2.4: P-glycoprotein inhibitors (Balayssac *et al.*, 2005:321)

Antiarythmics drugs ▪ Amiodarone ▪ Quinidine ▪ Verapamil **Anticancer drugs** ▪ Actinomycine D ▪ Doxorubicin ▪ Vinblastine **Antibiotics** ▪ Clarithromycin ▪ Erythromycin **Antidepressants** ▪ Paroxetine ▪ Sertraline ▪ Desmethylsertraline	**Proton pump inhibitors** ▪ Esomeprazole ▪ Lansoprazole ▪ Omeprazole ▪ Pantoprazole **Others** ▪ Cyclosporin A ▪ Colchicine ▪ Fenofibrate ▪ Propafenone ▪ Reserpine ▪ Trifluoperazine ▪ Progesterone ▪ Ritonavir

The mechanism of P-gp modulation may be different in different classes of compounds. Two different types of interaction exist, namely a direct interaction of one or more of the binding sites on P-gp that block transport of substrates (e.g. Verapamil and Cyclosporine A) as competitive or non-competitive inhibitors and secondly an inhibition of ATP binding (e.g. Vanadate), ATP hydrolysis (e.g. Cyclosporine A) or coupling of ATP hydrolysis to the translocation of the substrate. But the mechanisms of P-gp inhibition are rather complicated and depend on both substrates and inhibitors and do not always follow simple kinetics (Balayssac *et al.*, 2005:321).

2.6 Flavonoids as inhibitors of transport proteins

Flavonoids consist of a large group of polyphenolic anti-oxidants found in fruits, vegetables and plant-derived beverages such as tea and red wine as well as in dietary supplements. In foods, flavonoids are often present as β-glycosides of aglycones and in methoxylated forms. Upon ingestion, flavonoid glycosides are deglycosylated and the aglycones are metabolised into glucuronide-, sulphate- and methoxylated conjugates. Flavonoids and flavonoid-rich extracts have been implicated as beneficial agents in a multitude of disease states, including cancer, cardiovascular diseases, neurodegenerative disorders and osteoporosis (Brand *et al.*,

2006:512). It has become clear that flavonoids or their metabolites are important modulators or substrates of intestinal membrane bound transporter proteins including P-gp. Their properties to modulate ABC transport proteins and MDR make them interesting therapeutic candidates (Brand *et al.*, 2006:512).

2.6.1 Structure and mechanisms behind flavonoid mediated P-gp inhibition

Flavonoids possess a chromane ring skeleton with an additional aromatic ring attached at position 2, 3 or 4. Based on different substitution and the oxidation status of ring C, flavonoids can be classified into several subclasses including flavones, flavonols, flavonones, flavanols, isoflavones and chalcones of which examples are given in Table 2.5 (Bansal *et al*., 2009:54).
The concentration required for flavonoids to produce a significant modulation of P-gp activity seem to be, in general, 10 µM or higher, which appears to be achievable in the intestine after ingestion of food and dietary supplementation. Although flavonoid glycosides may not potently interact with P-gp, their corresponding aglycones released from these glycosides in the intestine could be present in high enough concentrations to inhibit intestinal P-gp, resulting in drug interactions. However, the main metabolites of flavonoids may not interact with P-gp because these metabolites are organic anions. Thus, systemic inhibition of P-gp by flavonoids or their metabolites may be insignificant after regular supplementation. Interaction could occur after administration of an extremely high dose, especially by intravenous injection (Bansal *et al*., 2009:54).

Table 2.5: Classes of flavonoids, their basic chemical structures and examples (Bansal *et al*., 2009:59).

Class of Flavonoid	Structure	Examples
Chalcones	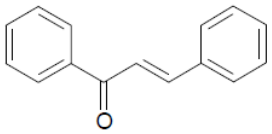	Phloretin
Flavan-3-ols	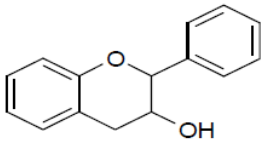	Acacetin, catechin, epi-catechin, epi-gallocatechin
Flavanones	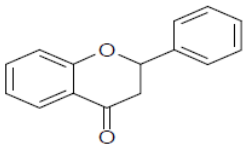	Naringenin, naringin, hesperitin, eriodictoyl, hesperidin, pinocembrin, likvirtin
Flavones	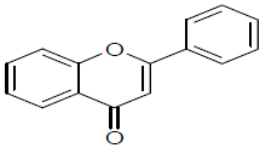	Apigenin, Luteolin, nobiletin, rpoifolin, tangeretin, flavone, baicalein, chrysin, techtochrysin, diosmetin, diosmin
Flavonols	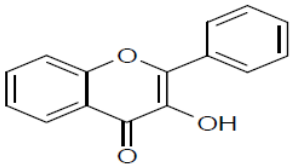	Isoquercetrin, kaemferol, morin, rutin, myricetin, quercetin, quercetrin, myricitrin, spiraeocide, galangin, robinin, kaempferide, fisetin, rhamnetin
Isoflavones	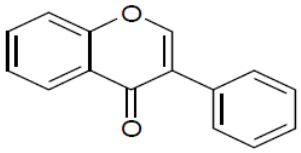	Genistein, daidzin
Flavanolols	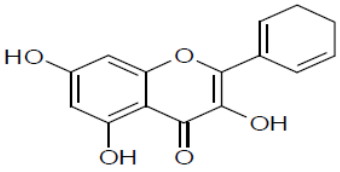	Silibinin, silymarin, taxifolin, pinocembrin

The underlying mechanisms by which herbal constituents, particularly flavonoids, alter P-gp mediated cellular efflux are elucidated by examining passive permeability, P-gp expression, P-gp ATPase activity and studying direct binding using the photo affinity labels such as azidopine. Some flavonoids and P-gp modulators have been shown to be able to change membrane lipid packing order and thus change membrane fluidity or permeability. It is thus

possible that the observed effects of the flavonoids on drug accumulation could be due to their non-specific interaction with the cell membrane resulting in increased passive membrane permeability. Alternatively a flavonoid-induced decrease in P-gp expression in P-gp positive cells could be another possibility. P-gp has been demonstrated to be an ATP dependent carrier and many P-gp substrates and modulators have been shown to interact with P-gp ATPase activity causing both stimulation and inhibition. For example, the P-gp inhibitor Verapamil has been reported to be one of the best stimulators of P-gp ATPase. Thus, one potential mechanism responsible for the flavonoid inhibition of P-gp mediated efflux may be the inhibition of P-gp ATPase by interacting directly with the vicinal ATP-binding site (Bansal *et al*., 2009:56).

In addition, flavonoids have also been shown to directly interact with the purified recombinant C-terminal nucleotide-binding domain from mouse P-gp, and this binding domain may overlap with the ATP binding site and vicinal steroid binding site. Various flavonoids may also interact with P-gp differently, since opposite effects on P-gp ATPase activity have been observed for different flavonoids (Bansal *et al*., 2009:56).

2.6.2 Structural activity relationship for flavonoid - P-gp interaction

The structural activity relationship (SAR) for flavonoid-P-gp interaction has been extensively studied by evaluating the binding affinity of different flavonoids with mouse NBD2. Although most of the compounds inhibit P-gp function by blocking drug binding sites, the presence of multiple binding sites complicate understanding as well as hinder developing a true, conclusive structural activity relationship for substrates or inhibitors. In general, the presence of the 5-hydroxyl group, the 3-hydroxyl group and the 2, 3-double bond appears to be important for potent flavonoid – nucleotide-binding domain interaction. In addition, isoflavonoids with ring B branched at position 3 instead of 2 have lower P-gp interaction activity (Bansal *et al*., 2009:56).

Isoflavones have been described as inactive on P-gp mediated MDR. Chalcones, flavones and flavonols have been demonstrated to possess MDR reversing activity through high affinity binding with P-gp because of a hydroxyl group on position 5 (position 6 in chalcones). The hydroxyl loses its acidic properties because of the chelating effect induced by the adjacent carbonyl group and therefore does not affect the activity which can be decreased by the presence of acidic groups. Hydroxylation on position 7 (position 4 in chalcones) was deleterious for activity, probably due to the acidic group influence, whereas methoxylation was slightly beneficial. The 2, 3 double bond (the α, β-double bond in chalcones) and the carbonyl group are also essential for MDR modulation (Bansal *et al*., 2009:58).

The chemical structures of the flavones that will be investigated in this study are given in Figure 2.11.

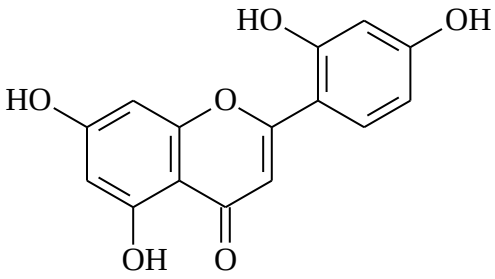

Morin

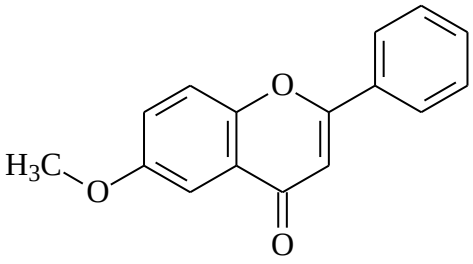

6-Methoxyflavone

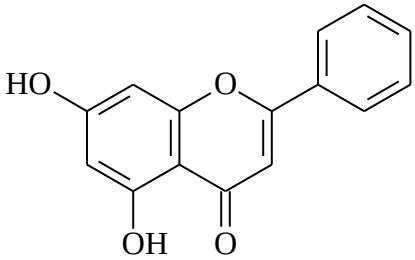

Galangin

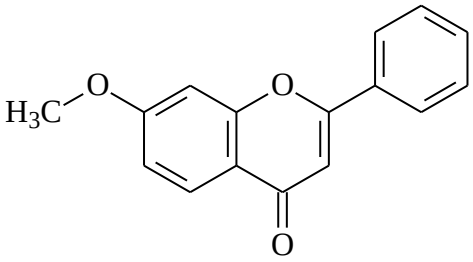

7-Methoxyflavone

Figure 2.11: Chemical structures of the flavones used in this study

The co-administration of food extracts that contain flavonoids, with drugs known to be P-gp substrates might be a useful, safe and convenient way to enhance the intestinal absorption of these drugs (Bansal *et al*., 2009:63).

2.7 *In vitro* models used for the evaluation of intestinal permeability and absorption

Transport of drug substances across the intestinal membrane is a complex and dynamic process. It includes the passage of compounds across the intestinal epithelium by means of various functional pathways in parallel. Passive transport occurs through the cell membrane of enterocytes (transcellular) or via the tight junctions between the enterocytes (paracellular). Various influx and efflux mechanisms (via carriers) are also functional. Because of the multivariate processes involved in drug absorption from the intestine, it is often difficult to use just one *in vitro* model to accurately predict the *in vivo* permeability characteristics (Balimane *et al.*, 2000:301).

Although physicochemical parameters can be used to predict the permeability characteristics of compounds, they are often limited in scope and do not take into account drug-membrane interactions or other important physiological factors that can completely override the physicochemical properties (Balimane *et al.*, 2000:302).

Numerous *in vitro* methods have been used in the drug selection process for assessing the intestinal absorption potential of drug candidates. *In vitro* techniques for the assessment of permeability are less labour and cost-intensive compared to *in vivo* animal studies. One universal issue with all the *in vitro* systems is that the effect of physiological factors such as gastric emptying rate, gastrointestinal transit rate and gastrointestinal pH cannot be incorporated in the data interpretation (Balimane *et al.*, 2000:305).

Each *in vitro* method has its distinct advantages and drawbacks. Based on the specific goal, one or more of these methods can be used as a screening tool for selecting compounds during the drug discovery process. The successful application of *in vitro* models to predict drug absorption across the intestinal mucosa depends on how closely the *in vitro* model mimics the characteristics of the *in vivo* intestinal epithelium. Although, it is very difficult to develop a single *in vitro* system that can simulate all the conditions existing in the human intestine, various *in vitro* systems are used routinely as decision making tools in early drug discovery (Balimane *et al.*, 2000:305).

2.7.1 Animal tissue based models

It is extremely difficult to obtain viable human tissues for permeability studies on a regular basis. Since animal intestinal tissues are also composed of essentially the same kind of epithelial cells, permeability screening for drug discovery purposes is routinely carried out using various animal species. Excised animal tissue models have been used since the 1950's to explore the mechanism of absorption of nutrients from the GI tract (Balimane *et al.*, 2000:305).

2.7.1.1 Everted gut technique

During this method, the intestinal sac is everted to expose the mucosal surface. It is then incubated in mucosal fluids and oxygenated to keep the tissue viable. The drug to be tested is then introduced into mucosal fluid and the absorption mechanism studied and compared. The transport of the drug across the mucosal membrane into the serosa (absorption) as well as the movement of drug from the serosal to the mucosal side (secretion) can be studied. This technique, when coupled to dissolution studies, allows for systematic evaluation of the potential absorbability of drug in its initial stages of development (D'Souza, 2008:1). A diagram of the everted gut procedure is given in Figure 2.12.

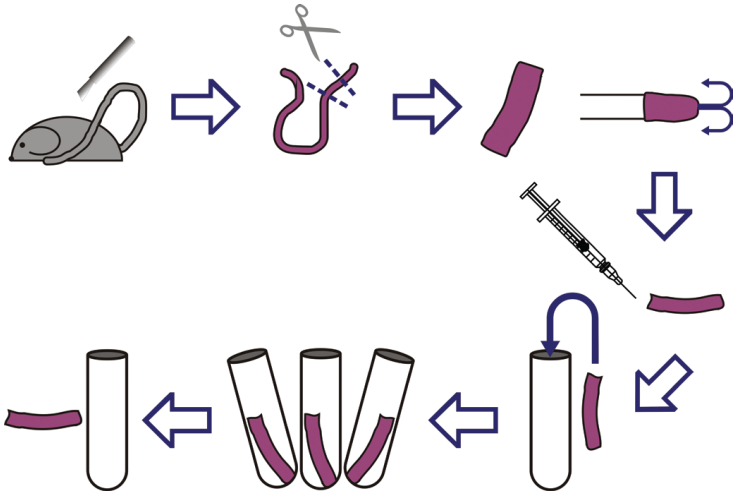

Figure 2.12: Diagram of the everted gut procedure (Carvalho *et al.*, 2010:8).

This model is ideal for studying the absorption mechanism of drugs since both the passive and active transport can be studied. This model may also be used to evaluate the role of efflux transporters in the intestinal absorption of drugs by comparing the transport kinetics of drug in the absence and presence of P-gp inhibitors or substrates (Balimane *et al.*, 2000:305).

The everted gut model has an additional analytical advantage over other *in vitro* models because the sample volume on the serosal side is relatively small and drugs accumulate faster. Some of the disadvantages include the lack of active blood and nerve supply that can lead to a rapid loss of availability. In addition, everting the intestinal tissue can lead to morphological damage causing misleading results (Balimane *et al.*, 2000:305). Another disadvantage is the presence of the *muscularis mucosa*, which is usually not removed from everted sac preparations. Therefore, this model does not reflect the actual intestinal barrier, because compounds under investigation pass from the lumen into the *lamina propria* (where blood and lymph vessels are found) and across the *muscularis mucosa* (Le Ferrec *et al.*, 2001:654).

2.7.1.2 Ussing chamber

The Ussing chamber was named after its inventor, Hans Ussing, and the first application of this technique was for studies of ion transport across frog skin. Later the Ussing chamber was utilised for the measurements of drug tissue permeability to predict intestinal drug absorption by Sweetana & Grass (Berggren, 2006:18) (see section 3.2). This method involves the isolation of intestinal tissues, cutting it into strips of appropriate size, clamping it on a suitable device and then the rate of drug transport across the tissue is measured (Balimane *et al.*, 2000:305).

When evaluating efflux with this technique, the ratio of the permeability from the basolateral (or serosal) to apical (or mucosal) chamber half is compared with the permeability in the reverse direction (Berggren, 2006:18). Thus the permeability is measured based on the appearance of drug in the serosal side rather than the disappearance of drug in the mucosal side (Balimane *et al.*, 2000:305).

The most important advantage of the Ussing chamber, compared to cell culture models, is that excised tissues is used, which ensures that the appropriate membrane characteristics for drug transport are investigated. This technique is also well suited to study the differences of drug transport in different parts of intestine (Berggren, 2006:18).

Tissue samples used for Ussing chamber investigations are most often taken from common laboratory animals such as rats, which make the model rather simple to use. However, using animal tissue causes problems in the interpretation of permeability data owing to interspecies differences, especially as there could be differences in the expression levels of enzymes and transporters and also physiological differences. The desired material for drug permeability

studies would be human intestinal samples, but generally the access to such material is sparse (Berggren, 2006:18-19).

The disadvantages of this technique include the lack of blood and nerve supply, rapid loss of viability of the tissue during the experiments and the changes of morphology and functionality of transporter proteins during the process of surgery and mounting of the tissue (Balimane *et al.*, 2000:305-306).

2.7.2 Membrane based models

2.7.2.1 Parallel artificial membrane permeability (PAMPA) method

The model consists of a hydrophobic filter material coated with a mixture of lecithin and phospholipids dissolved in an inert organic solvent such as dodecane, creating an artificial lipid membrane barrier that mimics the intestinal epithelium. The use of 96-well microtiter plates coupled with rapid analysis using a spectrophotometric plate reader makes this system a very attractive model for screening a large number of compounds (Balimane *et al.*, 2006:3). The fluxes measured relate to human absorption values with a hyperbolic curve, resembling very much the relationship obtained in Caco-2 screening (Deferme *et al.*, 2008:189).

However, difficulties are experienced with polar compounds that are transported via the paracellular pathway and with actively transported compounds. Another disadvantage is the strong dependency of membrane permeability on pH, especially with compounds having pK_a values near the pH of the incubation buffer used (Deferme *et al.*, 2008:189).

2.7.3. Cell-based *in vitro* models

A variety of cell monolayer models that mimic *in vivo* intestinal epithelium in humans have been developed and enjoy widespread popularity. Unlike enterocytes, human immortalised (tumor) cells grow rapidly into confluent monolayers that exhibit several characteristics of differentiated epithelial cells. Therefore, the cell culture model provides an ideal system for the rapid assessment of the intestinal permeability of drug candidates (Balimane & Chong, 2005:337).

2.7.3.1 Caco-2 cells

The Caco-2 cell model has been most extensively characterised and is a useful cell model in the field of drug permeability and absorption (Balimane *et al.*, 2000:306; Balimane & Chong, 2005:337). Caco-2 cells, a human colon adenocarcinoma, undergo spontaneous enterocytic

differentiation in culture. When they reach confluency on a semi-permeable porous filter, the cell polarity and tight junctions are well established. However, it is very difficult to compare the absolute permeability coefficient value of individual compounds reported in the literature, particularly with compounds that primarily permeate via the paracellular route (Balimane *et al.*, 2000:306). A schematic presentation of a culture of Caco-2 cells in a monolayer on a transport filter in a two-chamber well is given in Figure 2.13.

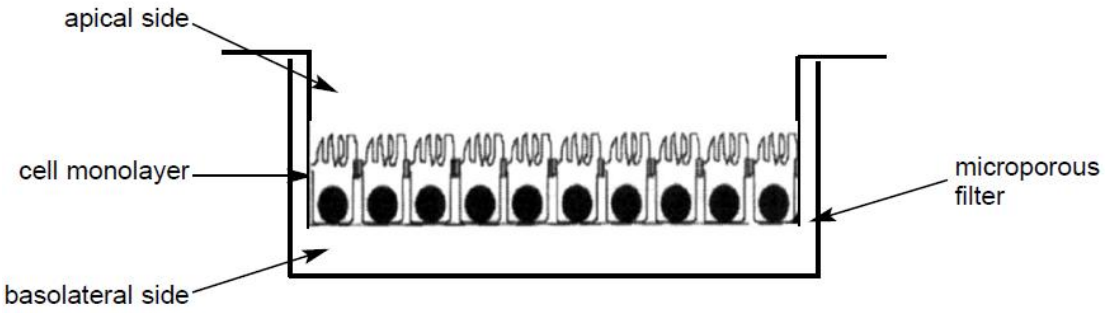

Figure 2.13: A schematic presentation of a culture of Caco-2 cells (Le Ferrec *et al.*, 2001:658).

Despite the widespread use and acceptability of the Caco-2 cell model, this model has several shortcomings that render it less than optimal as a one-stop cell-based permeability screening tool (Balimane & Chong, 2005:342). These limitations include the following:

- Caco-2 cell model measures passive drug transport (both transcellular and paracellular),
- low molecular weight hydrophilic compounds showed poor permeability in this cell model despite adequate absorption in humans,
- the use of organic cosolvents is limited. The integrity of tight junctions is easily compromised by commonly used organic solvents, even at a minute concentration,
- a significant physical loss due to nonspecific drug binding to plastic devices may lead to underestimation of permeability and
- the preparation of a fully functional cell monolayer generally requires a 3-week cell culture period with eight to nine laborious cell feedings (Balimane *et al.*, 2000:306-307).

Another potential issue with cell-based models is that the integrity of tight junctions in the Caco-2 cell monolayers can be compromised when incubated with test compounds and the extent of damage is typically concentration dependent. The permeability across the compromised

monolayer is often much higher compared with the intact monolayers and the permeability becomes artificially high in both directions. In that case, the efflux ratio often becomes unity and the test compound is classified as a non-substrate, even if it is a true substrate. It appears that the basolateral membrane of Caco-2 cell monolayers is more sensitive than the apical membrane (the cell damage occurs more frequently in the basolateral to apical direction, than the apical to basolateral direction). When this occurs, basolateral to apical permeability is significantly higher than apical to basolateral permeability and the test compound is classified as a P-gp substrate even if it is a non-substrate (Balimane *et al.*, 2006:10).

Despite these limitations, the Caco-2 cell model is the most widely used intestinal culture model and it is providing valuable information to the decision making process in early drug discovery (Balimane *et al.*, 2000:306-307). Caution must however be exercised in interpreting the results obtained by cell-based permeability models (Balimane & Chong, 2005:342).

2.8 Conclusion

One of the most important challenges facing the pharmaceutical industry today is to develop high-throughput, cost effective and predictive permeability/absorption screening models that can be used during the lead optimization process early in drug discovery. As discussed, Caco-2 cells and PAMPA are valuable research tools that are currently used in screening compounds for absorption and P-gp interaction potential. Despite the popularity and acceptability of PAMPA and Caco-2 cell models, it is important to recognise the associated limitations associated with these models to fully realise their potential. It is also important to realise that simplistic *in vitro* models such as PAMPA and Caco-2 cells are inadequate to represent the complicated absorption mechanism in the human intestinal tract (Balimane *et al.*, 2006:11).

Since these models cannot give quantitative predictions of drug absorption in humans, another possibility is to use excised animal tissue models such as the everted gut technique, Ussing chambers and the Sweetana-Grass diffusion techniques. Drug absorption in humans can be extrapolated reasonably well from animal data, when information on first-pass metabolism is also available (Le Ferrec *et al.,* 2001:17).

Transport of drug substances includes the passage of compounds across intestinal epithelial cells by various functional pathways in parallel. Passive transport occurs through the cell membrane of enterocytes (transcellular) or via the tight junctions between the enterocytes (paracellular). Various influx and efflux mechanisms (via carriers) are also functional. Because

of the multivariate processes involved in drug absorption in the intestine, it is often difficult to use just one *in vitro* model to accurately predict the *in vivo* permeability characteristics (Balimane *et al.*, 2000:301).

For the purpose of this study four hydroxy- and methoxy- flavonoids were selected to determine the *in vitro* transport of Rhodamine 123, a known P-gp substrate, across excised rat and pig jejunum segments using the Sweetana-Grass diffusion apparatus.

Chapter 3

Experimental procedure

3.1 Introduction

The transport of drug substances across the intestinal membrane is a complex and dynamic process. It includes the passage of compounds across various functional pathways in parallel. Passive transport occurs through the cell membrane of the enterocytes (transcellular) or via tight junctions between the enterocytes (paracellular). Various active influx and efflux mechanisms (via carriers) are also functional in the gastrointestinal epithelium. Because of the multivariate process involved in drug absorption from the intestine, it is often difficult to use just one *in vitro* model to accurately predict the *in vivo* permeability characteristics (Balimane *et al*., 2000:301). Various *in vitro* methods or techniques are available to determine intestinal permeability in order to predict the *in vivo* intestinal drug absorption potential (Hidalgo, 2001:385).

For the purpose of this study Sweetana-Grass side-by-side diffusion cells were used to evaluate the effect of different compounds on the transport of Rhodamine 123 through the epithelial barriers present in the excised intestinal mucosa of two different animal models (Grass & Sweetana, 1988:372). Excised intestinal jejunum segments from rats and pigs were used to perform the transport studies. The purpose of this study was to compare the results from both research animals in order to determine whether findings obtained from the permeation studies done on excised pig jejunum intestinal tissue correspond with the results obtained from the excised rat jejunum intestinal tissue.

3.2 Diffusion apparatus

Sweetana and Grass developed and patented an apparatus, which was derived from the Ussing chamber, for the measurement of tissue permeability. This diffusion cell apparatus incorporates the attributes of using a single material and laminar flow across the tissue surface. In addition, the design allows optimization of surface area to volume for a variety of tissues. This diffusion apparatus is applicable for the evaluation of transport of compounds across mucosal/epithelial

barriers such as excised gastrointestinal tissue (Grass & Sweetana, 1988:372). An illustration of the apparatus is given in Figure 3.1.

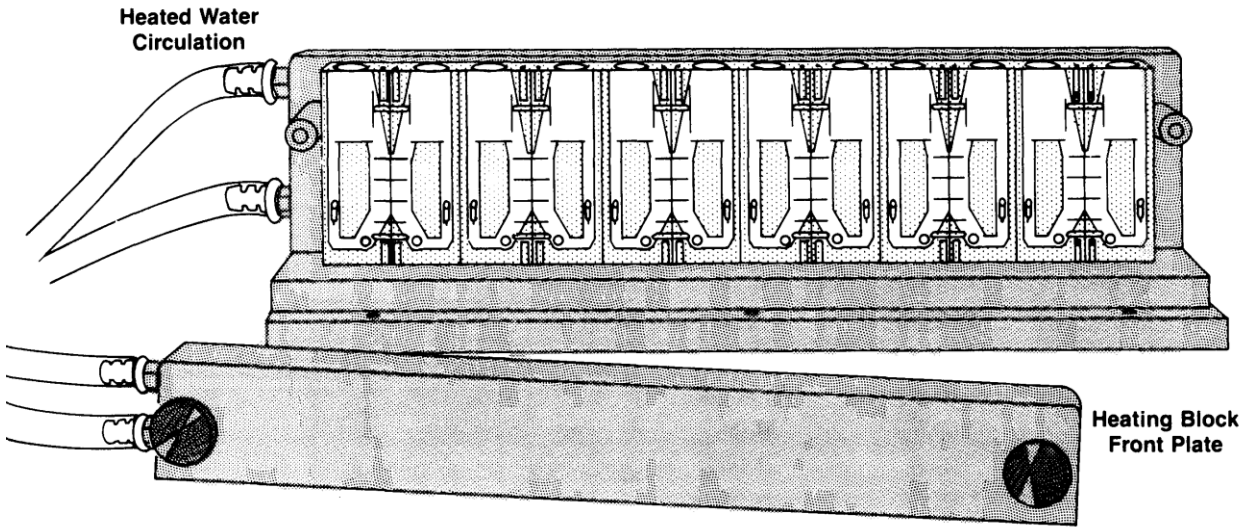

Figure 3.1: Diffusion chamber system used for transport studies (Grass & Sweetana, 1988:374)

This apparatus consists of six cell blocks where each cell block includes two half-cells clamped side-by-side together, which holds the tissue membrane in between. A circulation path by means of gas flow is provided in each half-cell block for agitation of the fluid to prevent stagnant layer formation and for maximum exposure of the fluid to both sides of the membrane. The cell blocks are placed linearly in a base unit including a front and back plate which are heated to maintain the cell blocks at a desired temperature (Sweetana *et al.,* 1993:1). A NaviCyte Snapwell vertical diffusion chamber system (Costar catalogue no. 3436) was used for the transport studies in this research project.

3.3 Materials

Krebs-Ringer bicarbonate-buffer (product no. K4002), Rhodamine 123 (product no. R8004), Morin (product no. M4008), Galangin (product no. 28,220-0), 6-Methoxyflavone (product no. 419737) and 7-Methoxyflavone (product no. 41,974-5) were purchased from Sigma-Aldrich, Kempton Park, RSA. Verapamil was a gift from Novartis SA. The buffer and Rhodamine 123 solutions were prepared daily and refrigerated until needed. The flavones were dissolved in 700µl ethanol after which it was made up to volume with Krebs-Ringer bicarbonate buffer.

According to Bansal *et al.*, (2009:46) flavonoids form the third generation, non-pharmaceutical category of P-gp inhibitors. The effects produced by some of these components are found to be

comparable to those of well-known P-gp inhibitors Verapamil and Cyclosporine. The flavonoids Morin, Galangin, 6-Methoxyflavone and 7-Methoxyflavone used in this study were selected on availability as pure compounds to serve as model compounds.

3.4 Tissue preparation

Excised intestinal segments (jejunum) of rats and pigs were used to perform the Rhodamine 123 transport studies in the diffusion apparatus. Jejunum pieces were used because permeability decreases in order of jejunum > ileum > colon (Artursson *et al.,* 1993:1123).

3.4.1 Rat intestinal tissue preparation

Non-fasted adult Sprague-Dawley rats (350-370 g) were obtained from the Animal Research Centre (North-West University). The North-West University Ethics Committee approved the project under protocol number NWU-0018-09-A5. Non-fasted rats were randomly selected and anaesthetised by the inhalation of halothane. An incision was made in the thorax, urging the lungs to collapse. An incision was further made in the abdomen to expose the small intestine. Starting 10 cm from the pylorus sphincter, a 20-30 cm piece of jejunum was excised and rinsed with ice-cold Krebs-Ringer bicarbonate buffer and pulled onto a glass rod (Figure 3.2: slides 1 & 2).

Slide 1 **Slide 2**

Figure 3.2: Photos demonstrating the washing of the excised rat jejunum and the handling of the tissue to pull it onto the glass rod

One hand was used to lift and hold the one end of the rod. The jejunum was then gently scoured long the mesenteric border with the back of a scalpel (Figure 3.3: slide 3). Using the index finger along the length of the jejunum, the serosa and muscle layer were gently pushed back and peeled off (Figure 3.3: slides 4 & 5). The jejunum was kept moist with cold Krebs-Ringer bicarbonate buffer at all times and kept in an ice bath. The jejunum was cut above and along the mesenteric border with a scalpel blade and washed off the glass rod with a buffer-filled syringe onto a strip of filter paper (Figure 3.3: slide 6).

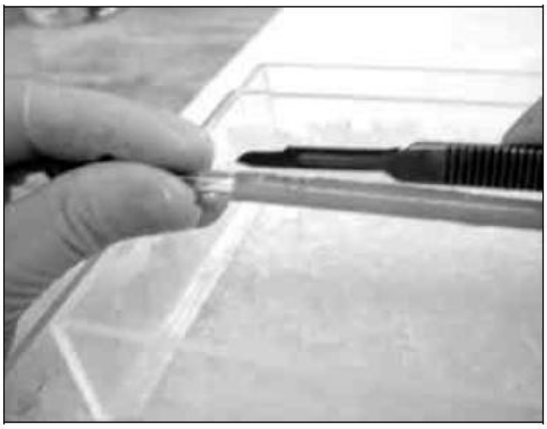

Slide 3

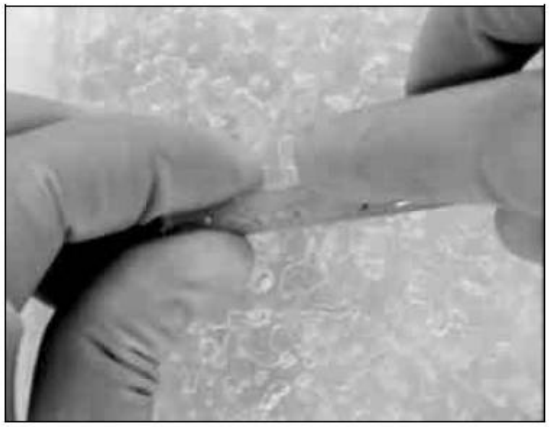

Slide 4

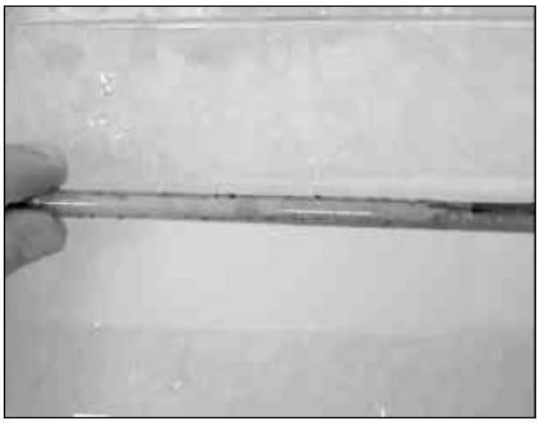

Slide 5

Slide 6

Figure 3.3: Photos demonstrating removal of the serosal layer from the rat jejunum with blunt dissection

The jejunum and filter paper was then cut simultaneously into lengths of approximately 3 cm (Figure 3.4: slide 7). The segments were kept moist with ice cold Krebs-Ringer bicarbonate buffer and were kept on ice during the procedure. Segments containing Peyer`s patches were identified visually and avoided (Figure 3.4: slide 8), as these lymph like tissues would cause greater variation in the rates of transport because of altered morphology and thickness of the epithelial layer.

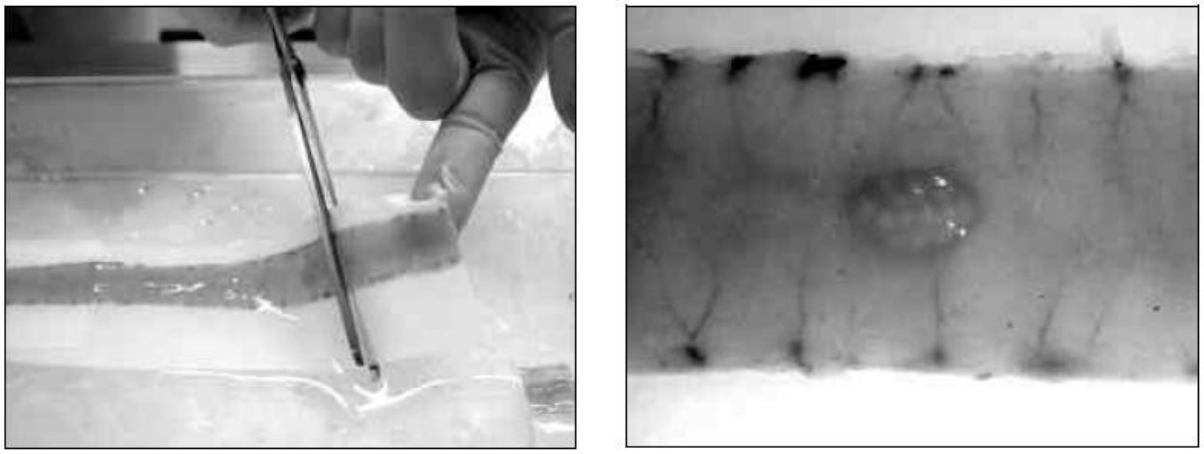

Slide 7 **Slide 8**

Figure 3.4: Photos demonstrating the cutting of the jejunum into pieces, avoiding segments containing Peyer's patches

The excised stripped tissue was mounted onto the pins of the preheated (37 ºC) half cells with the filter paper facing upwards and the mucosal side downwards (Figure 3.5: slides 9 & 10). The filter paper was used to limit handling and to prevent damage of the tissue. The filter paper was removed and the matching half-cells were clamped together with a metal ring (Figure 3.5: slides 11 & 12). Thereafter the assembled chambers were placed into the heating block which was preheated to 37 °C. Five millilitres fresh warmed (37 °C) Krebs-Ringer bicarbonate buffer were added to each chamber compartment. The buffer inside the half-cells was circulated by gas lift of 95% O_2 : 5% CO_2 with a flow rate of 15-20 ml/min. After the cells were placed in the heating block with their gas supply, it was left for 15 minutes to reach a state of equilibrium. The whole procedure from the incision was made in the abdomen till commencement of the transport studies, including the 15 minute adaption period, was performed within 45 minutes.

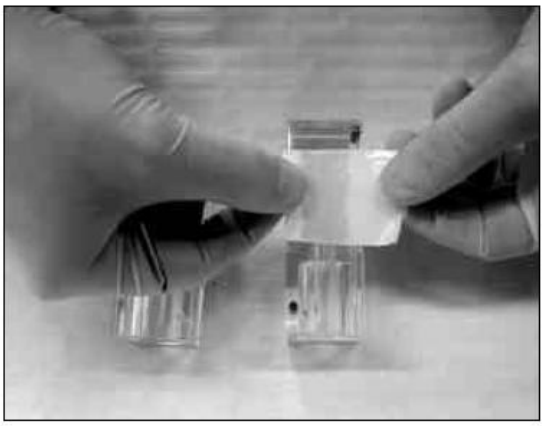

Slide 9

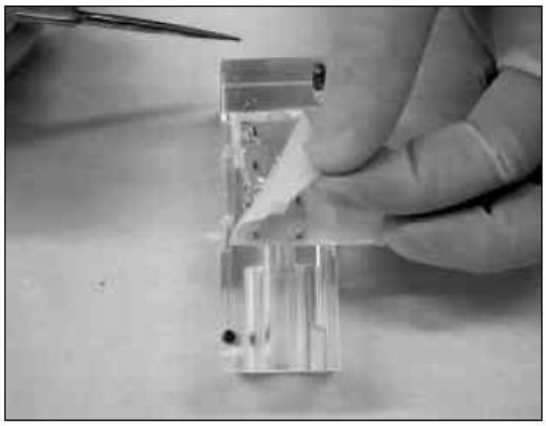

Slide 10

Slide 11

Slide 12

Figure 3.5: Photos demonstrating the mounting of the jejunum pieces onto the diffusion chamber half cells

3.4.2 Pig intestinal tissue preparation

Pig jejunum was collected from a local abattoir immediately after the pigs were slaughtered. A local veterinary surgeon was consulted to determine precisely which part of the small intestine should be used. Approximately 30% of the total length of the small intestine comprised of the duodenum, the following 60% is the jejunum and the last 10% the ileum. After collection of approximately 70 cm of jejunum from the pig gastrointestinal tract, it was roughly rinsed with ice cold Krebs-Ringer bicarbonate buffer and placed in a cooler box with ice cold Krebs-Ringer bicarbonate buffer and transported to the laboratory.

After arrival at the laboratory, the jejunum was thoroughly rinsed with ice cold Krebs-Ringer bicarbonate buffer and cut into shorter pieces with surgical scissors (Figure 3.6: slides 1 & 2).

During the preparation, the tissue samples were submerged in cold Krebs-Ringer bicarbonate buffer and all the procedures were done on ice.

Slide 1 **Slide 2**

Figure 3.6: Photos demonstrating the washing and cutting of the excised pig jejunum into shorter pieces

After the excised pig jejunum piece was cleaned, it was gently pulled onto a glass rod. The serosa and overlaying longitudinal and circular muscle layers were stripped off with blunt dissection (Figure 3.7: slides 3 to 6). The removal of the serosa was much easier from the excised pig jejunum pieces than in the excised rat jejunum pieces considering the fact that you had to cut through the serosa of the rat with the blunt side of a scalpel blade in order to remove it, while taking care not to damage the layers of the jejunum beneath the serosa.

Slide 3

Slide 4

Slide 5

Slide 6

Figure 3.7: Photos demonstrating removal of the serosal layer from the pig jejunum with blunt disection

A strip of heavy duty filter paper was moistened with the cold Krebs-Ringer bicarbonate buffer and placed underneath the glass rod that contained the excised pig jejunum piece. The jejunum was cut gently along the mesenteric border with a scalpel blade and washed off the glass rod onto the filter paper (Figure 3.8: slides 7 & 8). The jejunum and filter paper were cut together into lengths of approximately 2 cm (Figure 3.8: slide 9). These segments were kept moist with cold Krebs-Ringer bicarbonate buffer throughout the procedure. As with the excised rat jejunum pieces, segments containing Peyer's patches were avoided as a variation in transport rate might occur (Norris *et al.*, 1998:141).

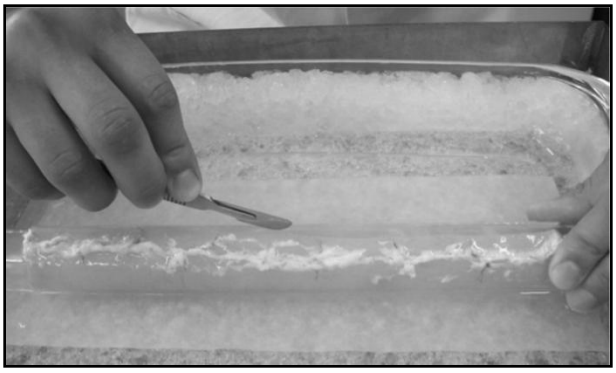

Slide 7

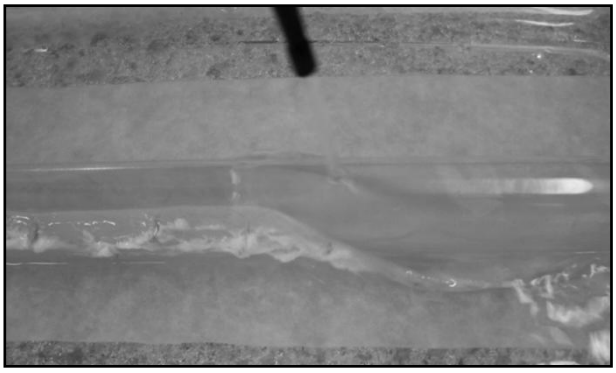

Slide 8

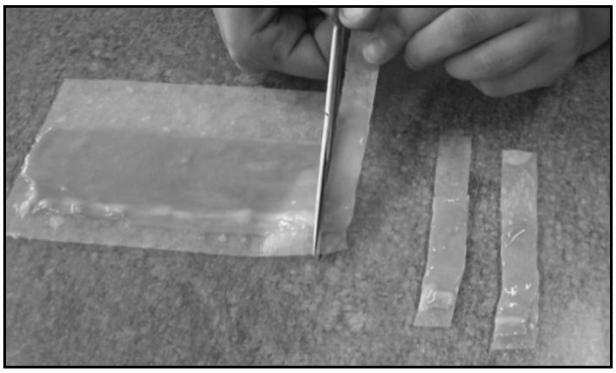

Slide 9

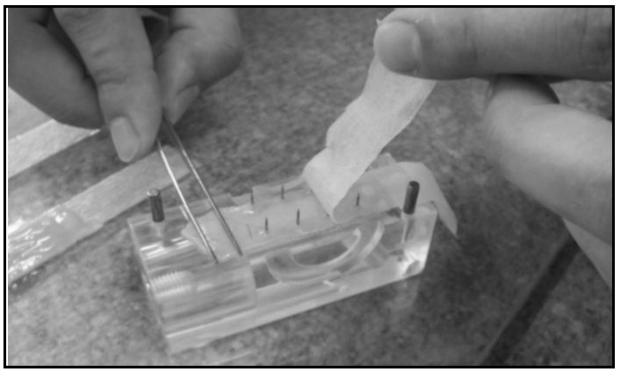

Slide 10

Figure 3.8: Photos demonstrating the cutting of the jejunum into pieces and mounting them onto the diffusion chamber half cells

The excised stripped tissue was mounted onto the pins of the pre-heated (37 °C) half-cells with the filter paper facing upwards and the mucosal side downwards (Figure 3.8: slide 10). The filter paper was used to limit handling and to prevent damage of the tissue. The filter paper was removed and the matching half-cells were clamped together with a metal ring. Thereafter the assembled chambers were placed into the heating block which was preheated to 37 °C. Five millilitres fresh warmed (37 °C) Krebs-Ringer bicarbonate buffer were added to each chamber compartment. The buffer inside the half-cells was circulated by gas lift of 95% O_2 : 5% CO_2 with a flow rate of 15-20 ml/min. After the cells were placed in the heating block with their gas supply, it was left for 15 minutes to reach a state of equilibrium (Figure 3.9: slide 11). The whole procedure from the collection of the jejunum till commencement of the transport studies, including the 15 minute adaption period, was performed within 60 minutes from collection of the tissue.

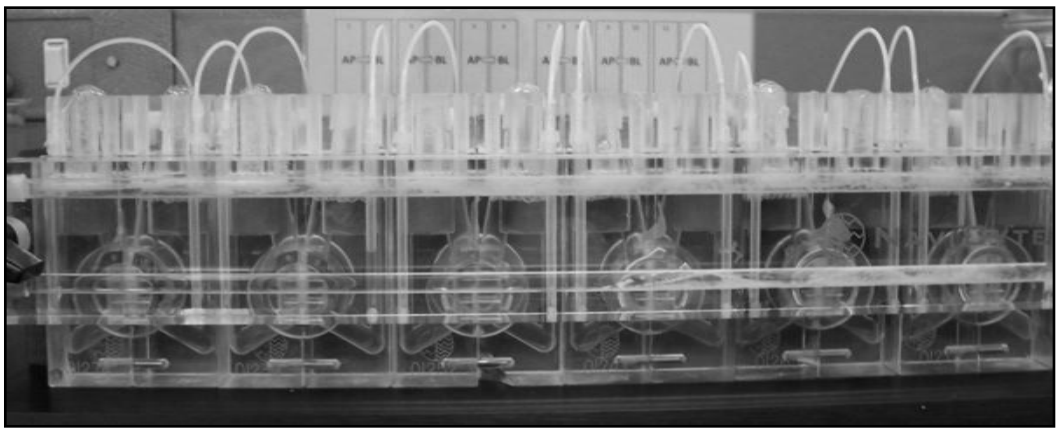

Slide 11

Figure 3.9: Diffusion apparatus with pig intestinal tissue mounted in between the side-by-side half cells

3.5 Transport studies

The transport of Rhodamine 123 was determined in the apical to basolateral (AP-BL) direction as well as in the basolateral to apical (BL-AP) direction across the jejunum segments. In the first three cell blocks of the diffusion apparatus, Rhodamine 123 movement was measured in the AP-BL direction and in the second three cell blocks the movement was measured in the BL-AP direction as presented schematically in Figure 3.10.

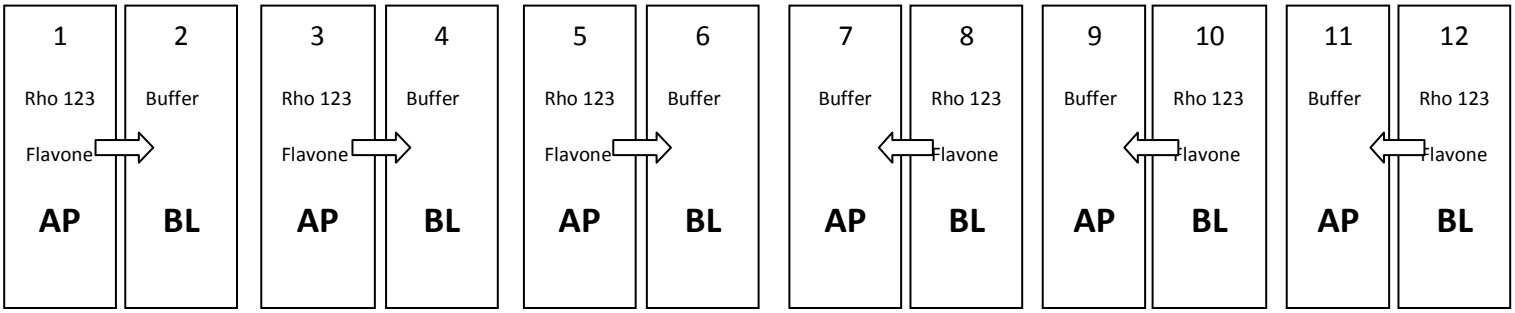

Figure 3.10: Schematic presentation of the setup for the Rhodamine 123 transport study for the different experimental groups

For the AP-BL study, 2 ml of the initial 5 ml Krebs-Ringer bicarbonate buffer withdrawn from the donor chambers (chambers 1, 3 and 5 in Figure 3.10, apical side) and a mixture of 2 ml Rhodamine 123 solution and 2 ml test compound solution were added to obtain a final volume

of 7 ml in each of these chambers. A volume of 2 ml of preheated Krebs-Ringer bicarbonate buffer was added to the acceptor chambers (chambers 2, 4 and 6 in Figure 3.10, basolateral side) to obtain a final volume of 7 ml in each of these chambers.

For the BL-AP study, 2 ml of the initial 5 ml Krebs-Ringer bicarbonate buffer was withdrawn from the donor chambers (chambers 8, 10 and 12 in Figure 3.10, basolateral side) and with a mixture of 2 ml Rhodamine 123 solution and 2 ml of test compound solution were added to reach a final volume of 7 ml in each of these chambers. A volume of 2 ml of preheated Krebs-Ringer bicarbonate buffer was added to the acceptor chambers (chambers 7, 9 and 11 in Figure 3.10, apical side) to obtain a final volume of 7 ml in each of these chambers.

Samples (200 μl) were withdrawn every 30 min from the six chambers (chambers 2, 4, 6, 7, 9 & 11 in Figure 3.10) over a total period of 120 min. Thereafter samples were placed in vials and frozen at -86 °C until analysed by means of a validated HPLC method (see Annexure A). Two hours are the optimum period over which *in vitro* transport experiments could be conducted using excised stripped intestinal tissue (Hattingh, 2002:63).

All the transport experiments with the flavones were done in triplicate to determine repeatability of the results. Two control groups were included in the experimental design, namely a positive and negative control. In the negative control group, the transport of Rhodamine 123 was determined and no modulator was added. In the positive control group, the transport of Rhodamine 123 was determined in the presence of Verapamil, which is known for its P-gp inhibitory effects. The control experiments were used to indicate that the effects of the modulators were caused by their modulation and not by chance interferences or external factors.

3.6 Data analysis and statistics

3.6.1 Apparent permeability (P_{app}) and efflux ratio (ER)

The apparent permeability is an index widely used as part of a general screening process to study drug absorption and is routinely obtained from *in vitro* and *ex vivo* experiments. It is defined as the initial flux of compound through the membrane, normalized by membrane surface area and donor concentration (Palumbo *et al.,* 2008:235) and is calculated by means of equation 3.1.

$$P_{app} = \frac{\mathrm{dQ}}{\mathrm{dt}} \mathrm{x} \frac{1}{\mathrm{A}.C_0.60} \quad 3.1$$

Where dQ/dt is the steady state change in concentration of the test compound with time on the receiver side, A the area and C_0 the concentration of the test compound at the donor side at t = 0 (Hayeshi *et al.,* 2006:72).

Efflux ratio (ER) values were determined from the resulting apparent permeability coefficient values using equation 3.2:

$$ER = \frac{P_{app}\ (BL-AP)}{P_{app}\ (AP-BL)} \quad 3.2$$

Where P_{app} (BL-AP) and P_{app} (AP-BL) display the apparent permeability in the secretory and absorptive directions, respectively.

3.6.2 Transepithelial flux (J)

Equation 3.3 was used for the calculation of the transepithelial flux (Hansen & Nilsen, 2009:88).

$$J = \frac{V(^{dC}/_{dt})}{A} \quad 3.3$$

Where *J* is the transepithelial flux, V the volume of the receiver chamber, dC the receiver chamber concentration, dt the transport time and A the membrane surface area.

The net flux was determined from the difference in flux in both directions by using equation 3.4 (Hansen & Nilsen, 2009:88).

$$J_{net} = J_{BL-AP} - J_{AP-BL} \quad 3.4$$

Where J(BL-AP) and J(AP-BL) display the flux in the secretory and absorptive directions, respectively.

3.6.3 Statistical analysis of results

The following statistical procedures were used on the transport results from the rat and the pig intestinal tissue datasets separately.

One-way analyses of variance (ANOVA) were done to determine if statistical significant differences exist between the mean efflux ratios (ER) of the test compounds and each of the positive and negative control groups in general. Levene's test was performed in each ANOVA's

case to assure equality of variances. In cases of unequalty of variances, Welch tests were performed. Normal probability plots on the residuals were done in each analysis to assure that the data were fairly normally distributed (Tabachnick & Fidell, 2001). Dunnett's tests were done to determine which of the test compounds' means differ statistically, significantly from the means of each of the standard compounds.

In order to test for interactions between the rat and pig tissue models' mean ER values, a two way analysis of variances was done for each of the test compounds separately. All these procedures mentioned above were also done on the net flux (J_{net}) values.

These procedures were done using Statistica (StatSoft, Inc. 2007). All tests were done on a 0.05 significant level. In case of p-values slightly higher than 0.05, interpretations were made on a 0.10 level.

Chapter 4

Results and discussion

4.1 Introduction

The potential modulating effect of four selected flavones on the transport of Rhodamine 123 was investigated using the Sweetana-Grass diffusion apparatus. Two control groups were included in the experiment design, namely a positive and negative control. In the negative control group, Rhodamine 123 was used alone and no modulator was added. In the positive control group, the transport of Rhodamine 123 was determined in the presence of Verapamil, which is known for its good P-gp inhibitory effects. The control experiments were used to indicate that the effects of the modulators were caused by their modulation and not by chance interferences or external factors.

Each experiment was done in triplicate to determine repeatability of the results. The transport of Rhodamine 123 was evaluated in both the apical to basolateral (AP-BL) and basolateral to apical (BL-AP) directions.

The relative transport of Rhodamine 123, the apparent permeability coefficient (P_{app}) values and flux (J) values in the AP-BL and BL-AP directions as well as the efflux ratio (ER) and net flux (J_{net}) were calculated. The concentration Rhodamine 123 present in the acceptor chamber was determined by means of a validated HPLC method (see Annexure A). The individual values of the cumulative transport of Rhodamine 123 in the absence and in the presence of selected flavonoids are presented in Annexure B. Statistical analysis was used to compare the results of the test groups with the control groups in order to indicate significant differences.

4.2 Transport of Rhodamine 123

Rhodamine 123 is a lipophilic cationic fluorescent dye that has often been used for studying the functional activity of P-gp as it is subjected to transport by this efflux active transporter (Balayssac *et al.*, 2005:321). The accumulation or retention of Rhodamine 123 in the presence or absence of P-gp modulators give important information regarding P-gp activity as well as the efficiency of modulators in reversing P-gp activity (Dodd, 2005:52).

4.2.1 Negative control (Rhodamine 123 alone)

The transport of Rhodamine 123 alone without any modulators was determined in the AP-BL direction for the first three cells and BL-AP direction for the last three cells of the Sweetana-Grass diffusion apparatus. The relative transport of Rhodamine 123 and the apparent permeability coefficient (P_{app}), flux (J), efflux ratio (ER) and net flux (J_{net}) values were calculated from the transport results obtained across both rat and pig intestinal tissues. These transport values obtained for Rhodamine 123 alone served as the negative control to which its transport in the presence of each modulator was compared.

4.2.1.1 Transport across excised rat intestinal tissue

4.2.1.1.1 Relative transport

The transport of Rhodamine 123 expressed as the percentage accumulated in the acceptor chamber over time relative to the initial concentration (10 µM) applied to the donor chamber, is presented in Table 4.1.

Table 4.1: Relative transport of Rhodamine 123 alone without modulators (negative control) in both directions across excised rat intestinal tissue

Group	Time (min)	AP - BL		BL - AP	
		Mean	SD	Mean	SD
Negative Control 1	**0**	0.00000	0.00	0.00000	0.00
	30	1.05135	0.18	0.90545	0.56
	60	0.96684	0.67	1.35432	1.55
	90	2.01295	0.09	2.31720	2.55
	120	2.69858	0.23	3.22072	3.72
Negative Control 2	**0**	0.00000	0.00	0.00000	0.00
	30	1.93204	0.07	2.02898	0.03
	60	2.08333	0.10	2.21652	0.04
	90	2.16639	0.22	2.58918	0.12
	120	2.49757	0.40	2.76193	0.27
Negative Control 3	**0**	0.00000	0.00	0.00000	0.00
	30	1.56902	0.01	1.71850	0.08
	60	1.63641	0.02	1.80541	0.04
	90	1.64693	0.09	1.84670	0.09
	120	1.79481	0.09	2.06769	0.09

4.2.1.1.2 Apparent permeability coefficient (P_{app}) and efflux ratio values

The apparent permeability coefficient (P_{app}) and the efflux ratio (ER) values for Rhodamine 123 alone (negative control) are given in Figure 4.1.

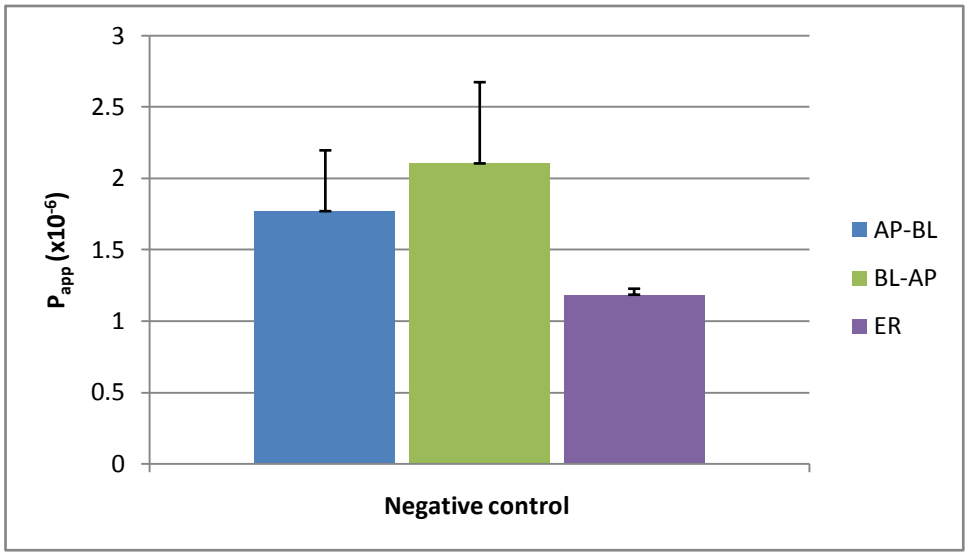

Figure 4.1: P_{app} and ER values of Rhodamine 123 alone without modulators (negative control) in both directions across excised rat intestinal tissue

4.2.1.1.3 Flux

The flux (J) and net flux (J_{net}), for Rhodamine 123 without modulators are given in Figure 4.2.

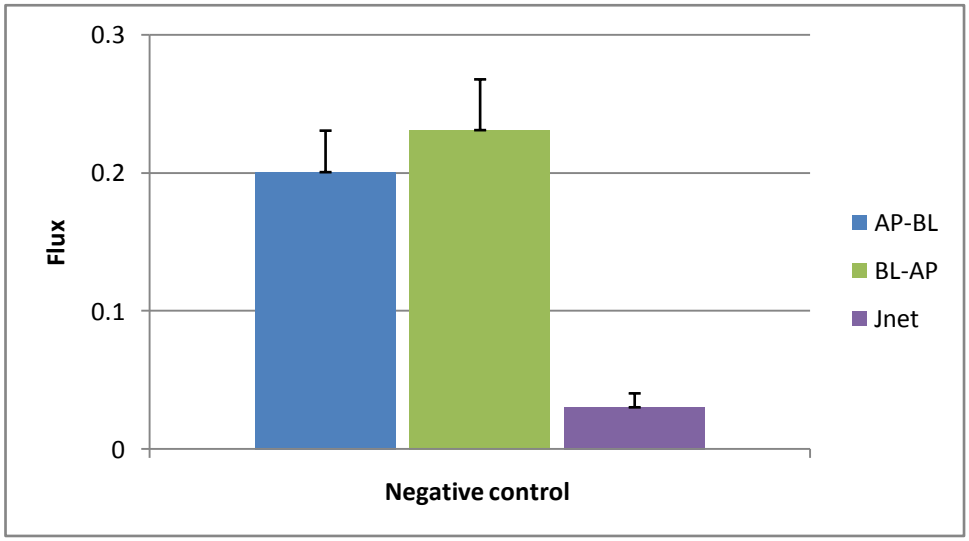

Figure 4.2: Flux and net flux values of Rhodamine 123 alone without modulators (negative control) in both directions across excised rat intestinal tissue

4.2.1.2 Transport across excised pig intestinal tissue

4.2.1.2.1 Relative transport

The transport of Rhodamine 123 expressed as the percentage accumulated in the acceptor chamber over time relative to the initial concentration (10 µM) applied to the donor chamber is presented in Table 4.4.

Table 4.2: Relative transport of Rhodamine 123 alone without modulators (negative control) in both directions across pig intestinal tissue

Group	Time (min)	AP - BL		BL - AP	
		Mean	SD	Mean	SD
Negative Control 1	**0**	0.00000	0.00	0.00000	0.00
	30	0.45443	0.58	0.65032	0.42
	60	0.47949	0.50	0.81370	0.75
	90	0.43181	0.40	0.77363	0.71
	120	0.51689	0.36	0.68598	0.56
Negative Control 2	**0**	0.00000	0.00	0.00000	0.00
	30	0.43415	0.24	0.67099	0.49
	60	0.43552	0.23	1.00384	0.75
	90	0.42000	0.22	0.90426	0.63
	120	0.44855	0.18	0.83481	0.55
Negative Control 3	**0**	0.00000	0.00	0.00000	0.00
	30	0.40620	0.26	0.65791	0.36
	60	0.53226	0.18	0.74757	0.55
	90	0.47887	0.09	0.74458	0.26
	120	0.58192	0.12	0.71966	0.33

4.2.1.2.2 Apparent permeability coefficient (P_{app}) and efflux ratio values

The apparent permeability coefficient (P_{app}) and the efflux ratio (ER) values for Rhodamine 123 alone (negative control) are given in Figure 4.3.

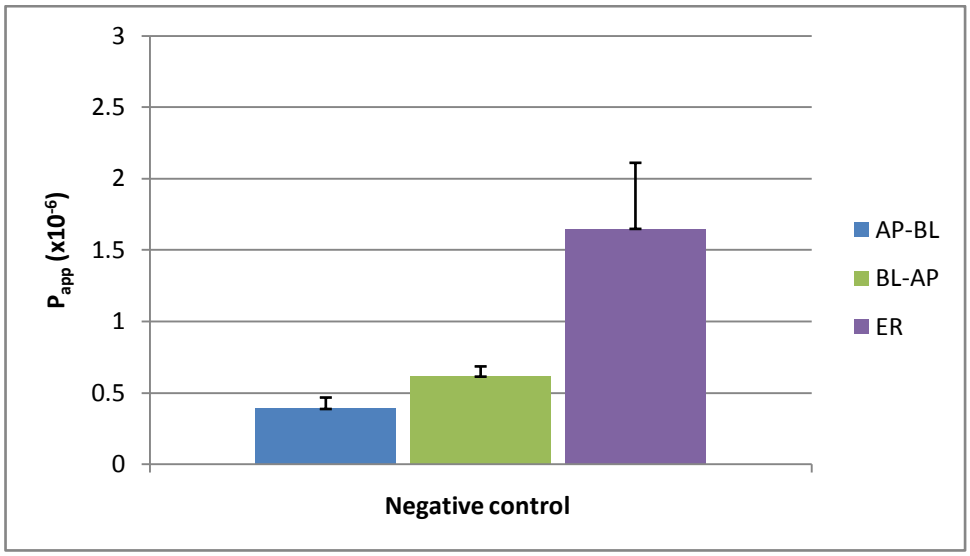

Figure 4.3: P_{app} and ER values of Rhodamine 123 alone without modulators (negative control) in both directions across excised pig intestinal tissue

4.2.1.2.3 Flux

The flux (J) as well as the net flux (J_{net}) values for Rhodamine 123 alone without modulators are given in Figure 4.4.

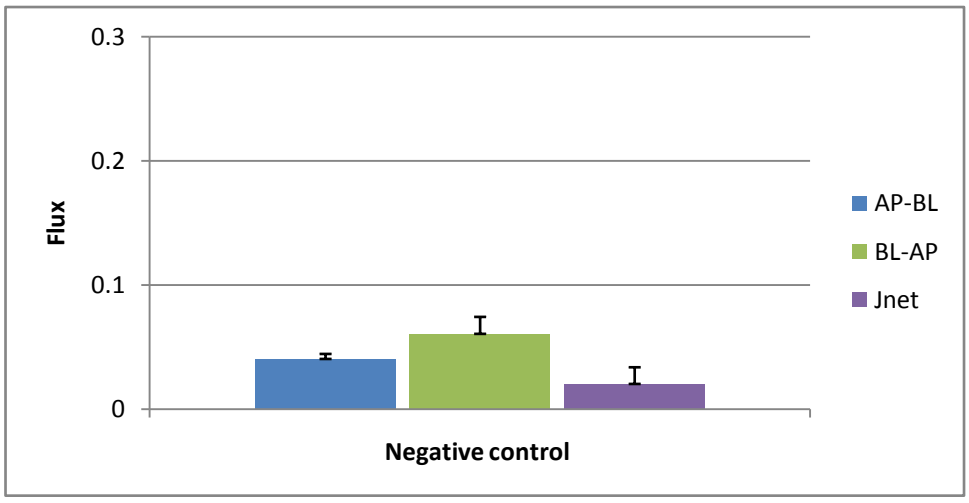

Figure 4.4: Flux and net flux values of Rhodamine 123 alone without modulators (negative control) in both directions across excised pig intestinal tissue

4.2.1.3 Discussion of results and conclusions

The use of Rhodamine 123 as a model compound for detecting the activity of the P-gp efflux pump *in vitro* has become a generally acknowledged technique in multi-drug resistance (MDR) research (Lorke *et al.*, 2001:651). According to Neyfakh (1988:168), Rhodamine 123 is classified as a typical P-gp substrate and is subjected to P-gp-dependent extrusion through the plasma membrane. It is clearly visible from the relative transport, apparent permeability coefficient (P_{app}) and flux values that the movement of the Rhodamine 123 is higher in the BL-AP (or secretory) direction compared to the movement in the AP-BL (or absorptive) direction for both the rat and pig excised intestinal tissue models. The results obtained in this study correspond well with results obtained from previous studies done by Van Huyssteen (2005:56) and Hattingh (2002:86) on rat jejunal segments due to the fact that the movement of Rhodamine 123 was also higher in the secretory direction than in the absorptive direction.

The results obtained in this negative control group (Rhodamine 123 alone without modulators) therefore confirm that Rhodamine 123 is a substrate for active efflux transporters and it is therefore a suitable model compound for purposes of investigating the effect of potential P-gp modulators such as flavones on its transport. Furthermore, the excised rat and pig intestinal tissues mounted in a Sweetana-Grass diffusion apparatus proved to be suitable *in vitro* transport models for these types of transport investigations by showing active efflux transport of Rhodamine 123.

4.2.2 Positive control (Rhodamine 123 in the presence of Verapamil)

The transport of Rhodamine 123 in the presence of 100 µM Verapamil was determined in the AP-BL direction for the first three cells and BL-AP direction for the last three cells of the Sweetana-Grass diffusion apparatus. The relative transport, apparent permeability coefficient (P_{app}), flux (J), efflux ratio (ER) and net flux (J_{net}) values were calculated from the transport results obtained across both the excised rat and pig intestinal tissues. Verapamil was used in the positive control group because it is a well-established P-gp inhibitor (Rautio *et al.*, 2006:789). The transport values obtained for Rhodamine 123 in the presence of Verapamil therefore could serve as the positive control to which the effect of each modulator or flavones investigated in this study can be compared.

4.2.2.1 Transport across excised rat intestinal tissue

4.2.2.1.1 Relative transport

The transport of Rhodamine 123 in the presence of Verapamil expressed as the percentage accumulated in the acceptor chamber relative to the initial concentration (10 µM) applied to the donor chamber is presented in Table 4.3.

Table 4.3: Relative transport of Rhodamine 123 in the presence of Verapamil (positive control) in both directions across rat intestinal tissue

Group	Time (min)	AP - BL		BL - AP	
		Mean	SD	Mean	SD
Positive Control 1	**0**	0.00000	0.00	0.00000	0.00
	30	2.31189	1.91	1.43313	1.10
	60	2.71792	2.02	1.90119	0.96
	90	2.78549	2.00	2.29714	0.88
	120	2.92924	1.98	2.54169	0.69
Positive Control 2	**0**	0.00000	0.00	0.00000	0.00
	30	0.59417	0.17	0.33185	0.14
	60	0.75658	0.19	0.41130	0.16
	90	0.90827	0.20	0.47516	0.18
	120	0.94299	0.22	0.59972	0.23
Positive Control 3	**0**	0.00000	0.00	0.00000	0.00
	30	0.98502	0.80	0.83012	0.69
	60	1.15769	0.82	1.02813	0.68
	90	1.22879	0.82	1.13128	0.58
	120	1.28406	0.79	1.20990	0.55

4.2.2.1.2 Apparent permeability coefficient (P_{app}) and efflux ratio values

The apparent permeability (P_{app}) and the efflux ratio (ER) values of Rhodamine 123 in the presence of Verapamil (positive control) are given in Figure 4.5.

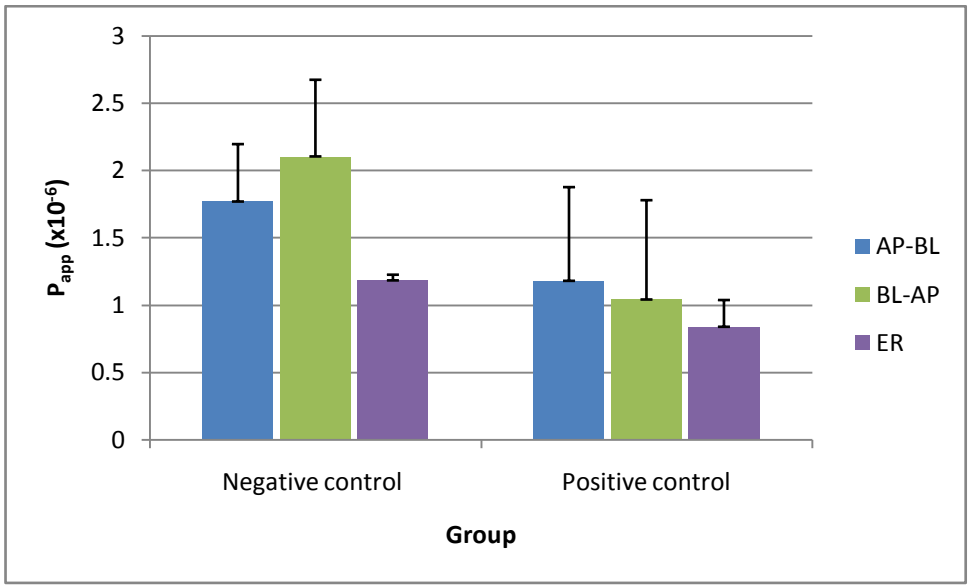

Figure 4.5: P_{app} and ER values of Rhodamine 123 in the presence of Verapamil (positive control) in both directions across excised rat intestinal tissue

4.2.2.1.3 Flux

The flux (J) as well as the net flux (J_{net}) values of Rhodamine 123 in the presence of Verapamil (positive control) are given in Figure 4.6.

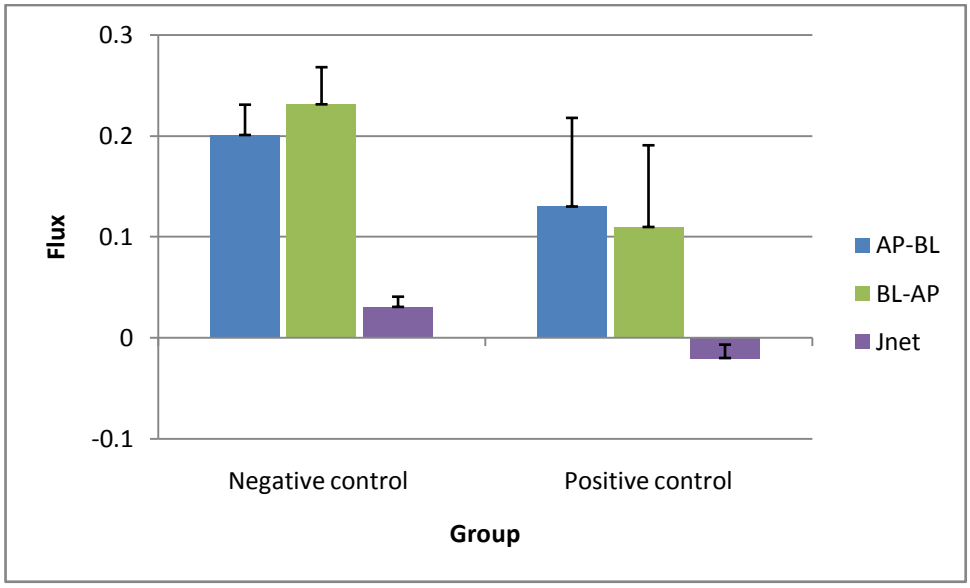

Figure 4.6: Flux and net flux values of Rhodamine 123 in the presence of Verapamil (positive control) in both directions across excised rat intestinal tissue

4.2.2.2 Transport across excised pig intestinal tissue

4.2.2.2.1 Relative transport

The transport of Rhodamine 123 in the presence of Verapamil expressed as the percentage accumulated in the acceptor chamber relative to the initial concentration (10 µM) applied to the donor chamber is presented in Table 4.4.

Table 4.4: Relative transport of Rhodamine 123 in the presence of Verapamil (positive control) in both directions across pig intestinal tissue

Group	Time (min)	AP - BL		BL - AP	
		Mean	SD	Mean	SD
Positive Control 1	**0**	0.00000	0.00	0.00000	0.00
	30	0.29266	0.09	0.18195	0.06
	60	0.35012	0.11	0.22348	0.07
	90	0.39942	0.15	0.23778	0.04
	120	0.70454	0.58	0.25758	0.03
Positive Control 2	**0**	0.00000	0.00	0.00000	0.00
	30	1.36533	0.75	1.02980	1.51
	60	1.57545	0.76	1.40296	1.43
	90	1.69274	0.74	1.62457	1.48
	120	1.84154	0.69	1.71751	1.28
Positive Control 3	**0**	0.00000	0.00	0.00000	0.00
	30	0.59652	0.24	0.44064	0.12
	60	0.69751	0.29	0.48817	0.11
	90	0.76883	0.32	0.53179	0.14
	120	0.77796	0.31	0.55072	0.14

4.2.2.2.2 Apparent permeability coefficient (P_{app}) and efflux ratio values

The apparent permeability coefficient (P_{app}) and the efflux ratio (ER) values for Rhodamine 123 in the presence of Verapamil (positive control) are given in Figure 4.7.

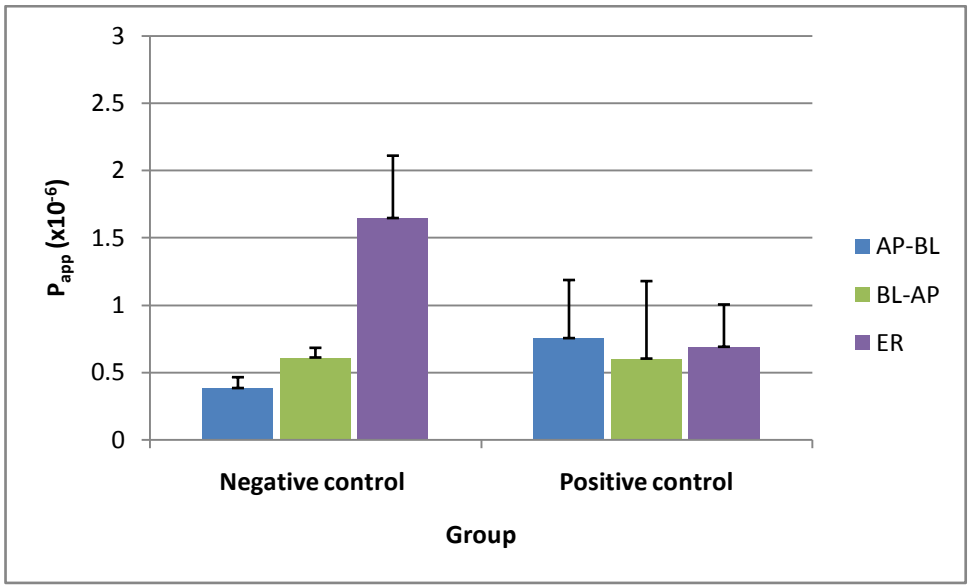

Figure 4.7: P_{app} and ER values of Rhodamine 123 in the presence of Verapamil (positive control) in both directions across excised pig intestinal tissue

4.2.2.2.3 Flux

The flux (J) as well as the net flux (J_{net}) values for Rhodamine 123 in the presence of Verapamil (positive control) are given in Figure 4.8.

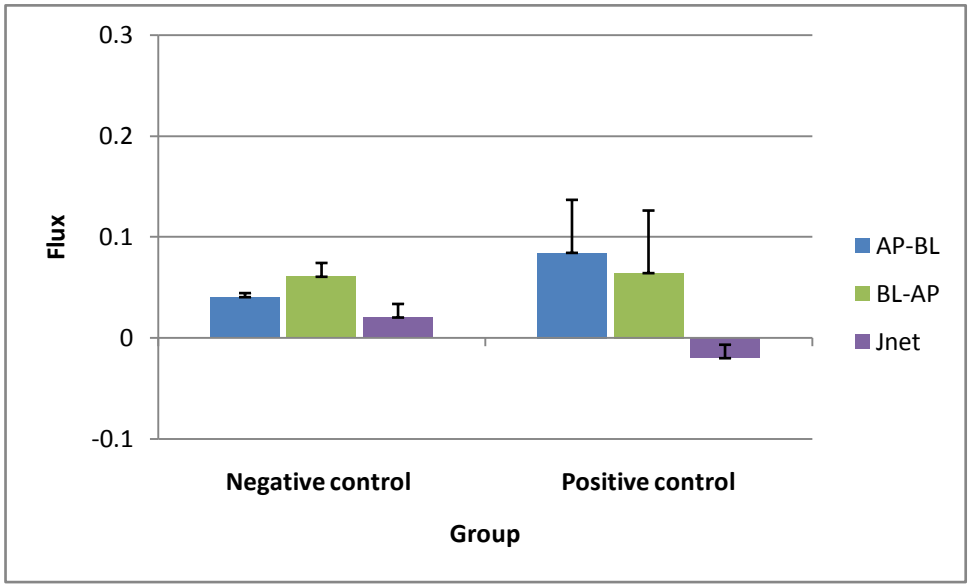

Figure 4.8: Flux and net flux values of Rhodamine 123 in the presence of Verapamil (positive control) in both directions across excised pig intestinal tissue

4.2.2.3 Discussion of results and conclusions

Verapamil is an example of a P-gp substrate that is well absorbed because absorptive permeation by passive diffusion is sufficient to overcome the negative contribution by active secretory transport (Aungst, 2000:437). From the transport results obtained in this study for Rhodamine 123 in the presence of Verapamil, it is noticeable that the transport of Rhodamine 123 in the BL-AP direction was statistically significant lower compared to that obtained for Rhodamine 123 alone. This is in line with the results obtained previously by Swart (2002:39) for *in vitro* Rhodamine 123 transport across rat jejunal segments. In fact, the net transport of Rhodamine 123 was changed from being in the BL-AP (or secretory) direction to being in the AP-BL (or absorptive) direction by the presence of Verapamil. This can clearly be seen from the results of the mean efflux ratio (ER) value of 0.83 across rat intestinal tissue and 0.69 across pig intestinal tissue compared to the ER values of the negative control (Rhodamine 123 alone) that were 1.18 across rat intestinal tissue and 1.65 across pig intestinal tissue. This was further demonstrated by the negative net flux results where the mean J_{net} values were -0.02 for both rat and pig intestinal tissue compared to the J_{net} values of the negative control that were 0.03 across rat intestinal tissue and 0.02 across pig intestinal tissue. Thus, for both the rat and pig intestinal tissue models the efflux of Rhodamine 123 was significantly decreased by the presence of Verapamil, a well known P-gp inhibitor. This confirms the ability of these excised tissue models to indicate the effects that compounds may have on P-gp related efflux of Rhodamine 123.

4.2.3 Morin

It has been found that certain flavonoids have the ability to modulate P-gp and thereby influence the transport of some co-administered compounds across intestinal epithelia (Chao *et al.*, 2002:219).

The effect of Morin on the *in vitro* transport of Rhodamine 123 across excised rat and pig jejunum was investigated in a Sweetana-Grass diffusion apparatus. The transport of Rhodamine 123 in the presence of 20 µM Morin was determined in two directions across both rat and pig intestinal segments and the relative transport, apparent permeability coefficient (P_{app}), flux (J), net flux (J_{net}) and efflux ratio (ER) values were calculated.

4.2.3.1 Transport across excised rat intestinal tissue

4.2.3.1.1 Relative transport

The transport of Rhodamine 123 in the presence of 20 µM Morin expressed as a percentage accumulated in the acceptor chamber relative to the initial concentration (10 µM) applied to the donor chamber is presented in Table 4.5.

Table 4.5: Relative transport of Rhodamine 123 in the presence of Morin in both directions across rat intestinal tissue

Group	Time (min)	AP - BL		BL - AP	
		Mean	SD	Mean	SD
Morin 1	**0**	0.00000	0.00	0.00000	0.00
	30	0.09019	0.02	0.08085	0.01
	60	0.10336	0.01	0.08800	0.01
	90	0.12320	0.03	0.11605	0.02
	120	0.15341	0.06	0.16105	0.05
Morin 2	**0**	0.00000	0.00	0.00000	0.00
	30	0.45940	0.66	0.21603	0.22
	60	0.51929	0.70	0.28743	0.18
	90	0.60971	0.77	0.36403	0.17
	120	0.73866	0.87	0.46151	0.13
Morin 3	**0**	0.00000	0.00	0.00000	0.00
	30	0.16455	0.23	0.16529	0.22
	60	0.22064	0.27	0.23407	0.22
	90	0.31807	0.30	0.29765	0.20
	120	0.49166	0.38	0.37755	0.19

4.2.3.1.2 Apparent permeability coefficient (P_{app}) and efflux ratio values

The apparent permeability coefficient (P_{app}) and the efflux ratio (ER) values of Rhodamine 123 in the presence of 20 µM Morin are given in Figure 4.9.

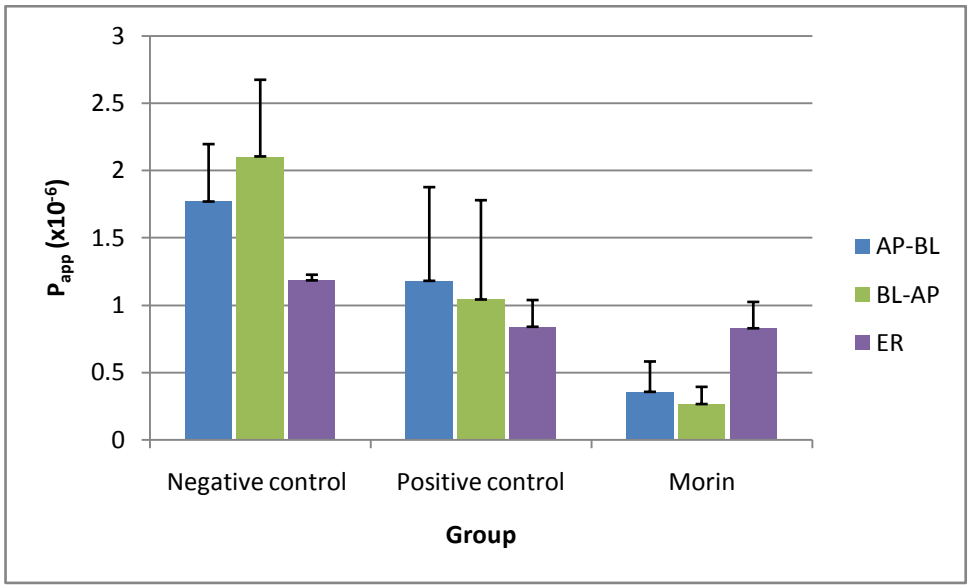

Figure 4.9: P_{app} and ER values of Rhodamine 123 in the presence of Morin in both directions across excised rat intestinal tissue

4.2.3.1.3 Flux

The flux (J) as well as the net flux (J_{net}) values of Rhodamine 123 in the presence of Morin are given in Figure 4.10.

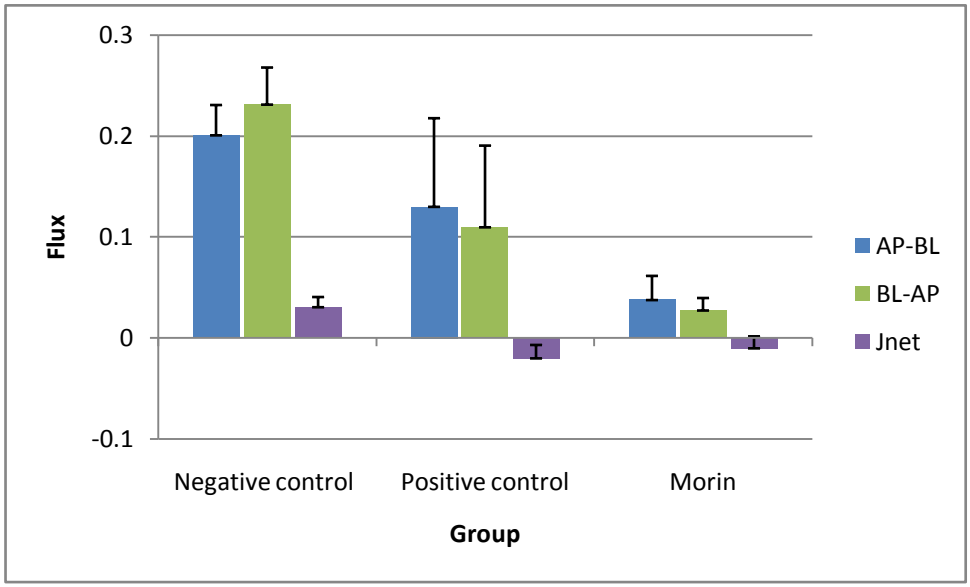

Figure 4.10: Flux and net flux values of Rhodamine 123 in the presence of Morin in both directions across excised rat intestinal tissue

4.2.3.2 Transport across excised pig intestinal tissue

4.2.3.2.1 Relative transport

The transport of Rhodamine 123 in the presence of 20 µM Morin expressed as a percentage accumulated in the acceptor chamber relative to the initial concentration (10 µM) applied to the donor chamber is presented in Table 4.6.

Table 4.6: Relative transport of Rhodamine 123 in the presence of Morin across excised pig intestinal tissue

Group	Time (min)	AP - BL		BL - AP	
		Mean	SD	Mean	SD
Morin 1	**0**	0.00000	0.00	0.00000	0.00
	30	0.08172	0.03	0.18774	0.15
	60	0.41808	0.31	0.20750	0.19
	90	0.84942	0.97	0.09067	0.02
	120	1.24812	1.45	0.08340	0.02
Morin 2	**0**	0.00000	0.00	0.00000	0.00
	30	0.19203	0.06	0.16340	0.03
	60	0.69675	0.70	0.16067	0.03
	90	0.64530	0.61	0.15615	0.02
	120	0.60911	0.58	0.16066	0.02
Morin 3	**0**	0.00000	0.00	0.00000	0.00
	30	0.41899	0.09	0.22744	0.03
	60	0.43513	0.12	0.23661	0.02
	90	0.37541	0.06	0.23670	0.02
	120	0.40100	0.06	0.24289	0.01

4.2.3.2.2 Apparent permeability coefficient (P_{app}) and efflux ratio values

The apparent permeability coefficient (P_{app}) and the efflux ratio (ER) values of Rhodamine 123 in the presence of 20 µM Morin are given in Figure 4.11.

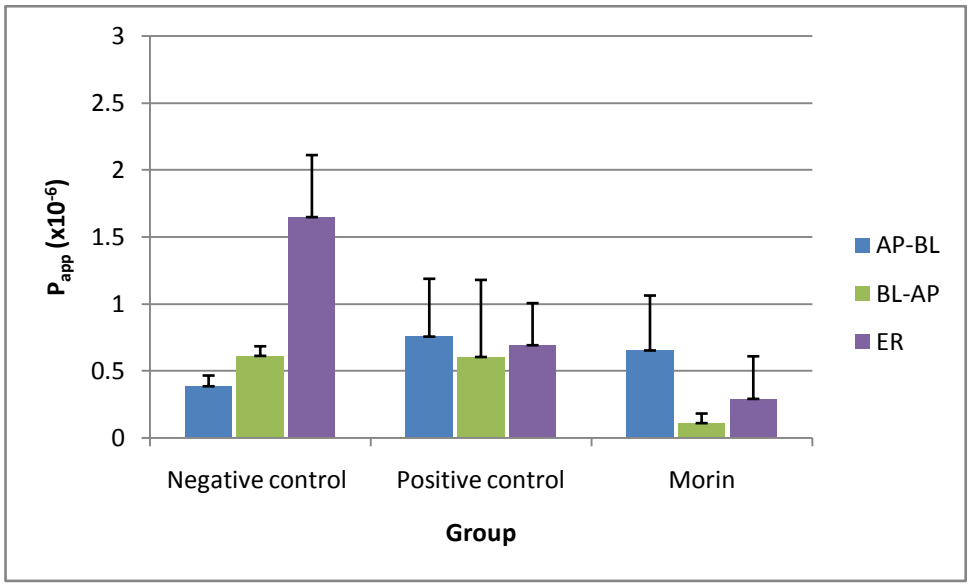

Figure 4.11: P_{app} and ER values of Rhodamine 123 in the presence of Morin in both directions across excised pig intestinal tissue

4.2.3.2.3 Flux

The flux (J) as well as the net flux (J_{net}) values of Rhodamine 123 in the presence of 20 µM Morin are given in Figure 4.12.

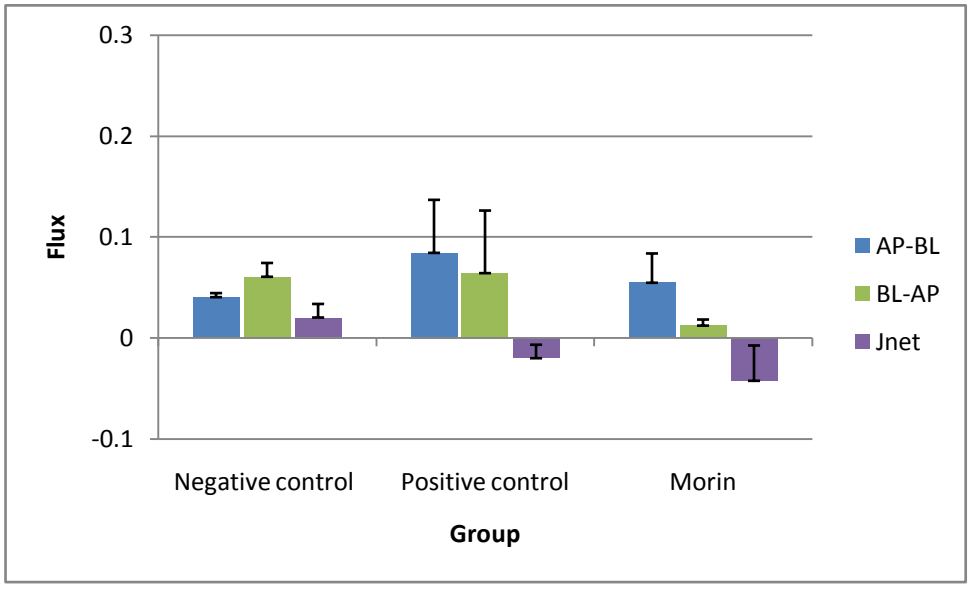

Figure 4.12: Flux and net flux values of Rhodamine 123 in the presence of Morin across excised pig intestinal tissue

4.2.3.3 Discussion of results and conclusions

The transport of Rhodamine 123 in the BA-AP direction was clearly decreased by Morin across both intestinal tissue models. The mean ER was 0.83 for the Rhodamine 123 transport across rat intestinal tissue and 0.29 across pig intestinal tissue, which are significantly ($p < 0.05$) lower compared to the ER values of the negative control of 1.18 across rat intestinal tissue and 1.65 across pig intestinal tissue and those of the positive control of 0.83 for rats and 0.69 for pigs. The mean J_{net} value was -0.01 for Rhodamine 123 transport across rat intestinal tissue and -0.04 across pig intestinal tissue compared to the J_{net} values of the negative control that were 0.03 for rat intestinal tissue and 0.02 for pig intestinal tissue, while the J_{net} values of the positive control were -0.02 across both rat and pig intestinal tissues. Thus, for both animal tissue models the ER and J_{net} values of Rhodamine 123 transport decreased significantly in the presence of Morin. The inhibitory effect by Morin on the P-gp related efflux of Rhodamine 123 across pig intestinal tissues has occurred to a larger extent than that obtained for Verapamil (positive control group); however, this difference was not statistically significant. These results correspond well with the findings obtained by Van Huyssteen (2005:63) who also found Morin to inhibit P-gp related efflux.

The implication of these transport results obtained for Morin is that the simultaneous intake of food or fruit that contain Morin and a drug by a patient will potentially increase the bioavailability of that drug. However, the clinical significance of such pharmacokinetic interaction between Morin and drugs that are substrates for P-gp should be determined by means of *in vivo* clinical trials before any conclusions in this regard can be made.

4.2.4 Galangin

The effect of Galangin on the *in vitro* transport of Rhodamine 123 in the presence of 20 µM Galangin was investigated across excised rat and pig jejunum in a Sweetana-Grass diffusion apparatus. The transport of Rhodamine 123 in two directions across both rat and pig intestinal segments in the presence of 20 µM Galangin was determined and the relative transport, apparent permeability coefficient (P_{app}), flux (J), efflux ratio (ER) and net flux (J_{net}) values were calculated.

4.2.4.1 Transport across excised rat intestinal tissue

4.2.4.1.1 Relative transport

The transport of Rhodamine 123 in the presence of 20 µM Galangin expressed as a percentage accumulated in the acceptor chamber relative to the initial concentration (10 µM) applied to the donor chamber is presented in Table 4.7.

Table 4.7: Relative transport of Rhodamine 123 in the presence of Galangin in both directions across rat intestinal tissue

Group	Time (min)	AP - BL		BL - AP	
		Mean	SD	Mean	SD
Galangin 1	**0**	0.00000	0.00	0.00000	0.00
	30	0.13257	0.13	0.09424	0.10
	60	0.26480	0.17	0.21901	0.14
	90	0.46718	0.20	0.36620	0.15
	120	0.72592	0.25	0.54147	0.16
Galangin 2	**0**	0.00000	0.00	0.00000	0.00
	30	0.29266	0.39	0.19056	0.13
	60	0.44939	0.39	0.31440	0.10
	90	0.71190	0.37	0.60042	0.10
	120	0.98843	0.31	0.85190	0.16
Galangin 3	**0**	0.00000	0.00	0.00000	0.00
	30	0.08073	0.05	0.05138	0.01
	60	0.11320	0.06	0.07913	0.01
	90	0.19419	0.06	0.13009	0.03
	120	0.27175	0.08	0.16806	0.05

4.2.4.1.2 Apparent permeability coefficient (P_{app}) and efflux ratio values

The P_{app} and ER values of Rhodamine 123 with 20 µM Galangin are given in Figure 4.13.

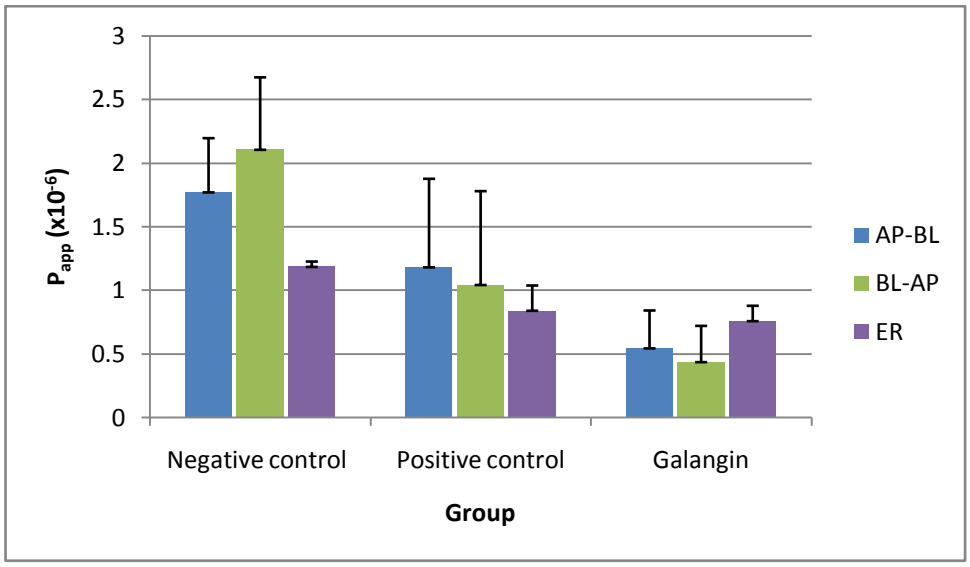

Figure 4.13: P_{app} and efflux ratio values of Rhodamine 123 in the presence of Galangin in both directions across excised rat intestinal tissue

4.2.4.1.3 Flux

The flux (J) as well as the net flux (J_{net}) values of Rhodamine 123 in the presence of 20 µM Galangin are given in Figure 4.14.

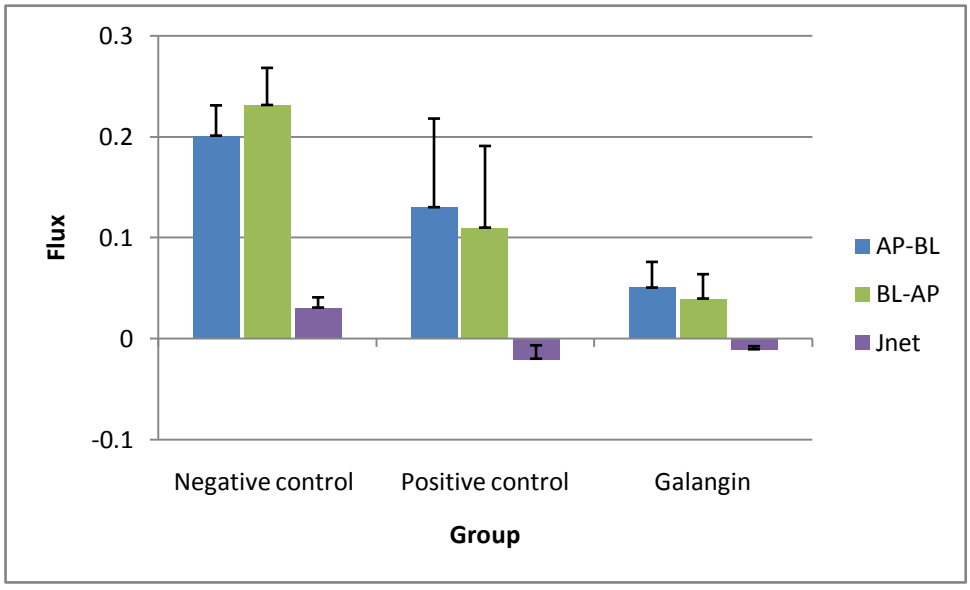

Figure 4.14: Flux and net flux values of Rhodamine 123 in the presence of Galangin in both directions across excised rat intestinal tissue

4.2.4.2 Transport across excised pig intestinal tissue

4.2.4.2.1 Relative transport

The transport of Rhodamine 123 in the presence of 20 µM Galangin expressed as a percentage accumulated in the acceptor chamber relative to the initial concentration (10 µM) applied to the donor chamber is presented in Table 4.8.

Table 4.8: Relative transport of Rhodamine 123 in the presence of Galangin across excised pig intestinal tissue

Group	Time (min)	AP - BL		BL - AP	
		Mean	SD	Mean	SD
Galangin 1	**0**	0.00000	0.00	0.00000	0.00
	30	1.07866	0.89	0.68643	0.98
	60	1.07707	0.91	0.68015	0.96
	90	1.10480	0.91	0.72147	0.87
	120	1.02728	0.89	0.67552	0.77
Galangin 2	**0**	0.00000	0.00	0.00000	0.00
	30	0.72197	0.58	0.40902	0.55
	60	0.71404	0.56	0.44760	0.52
	90	0.63580	0.51	0.37950	0.53
	120	0.62880	0.51	0.34156	0.47
Galangin 3	**0**	0.00000	0.00	0.00000	0.00
	30	0.45765	0.44	0.22179	0.08
	60	0.45058	0.43	0.24631	0.13
	90	0.45181	0.43	0.24492	0.14
	120	0.45263	0.46	0.24268	0.14

4.2.4.2.2 Apparent permeability coefficient (P_{app}) and efflux ratio values

The P_{app} and ER values of Rhodamine 123 with 20 µM Galangin are given in Figure 4.15.

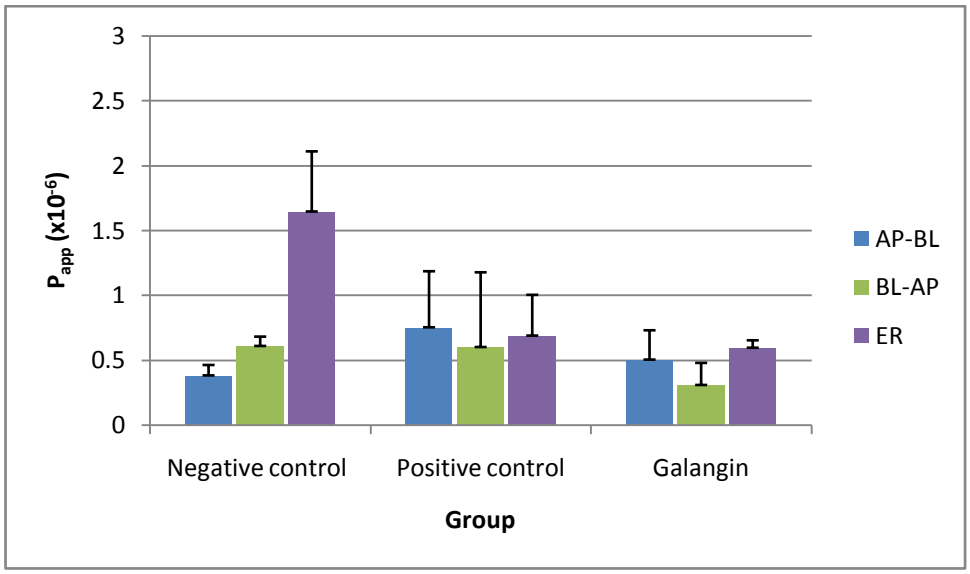

Figure 4.15: P_{app} and ER values of Rhodamine 123 in the presence of Morin in both directions across excised pig intestinal tissue

4.2.4.2.3 Flux

The flux (J) as well as the net flux (J_{net}) values of Rhodamine 123 in the presence of 20 µM Galangin are given in Figure 4.16.

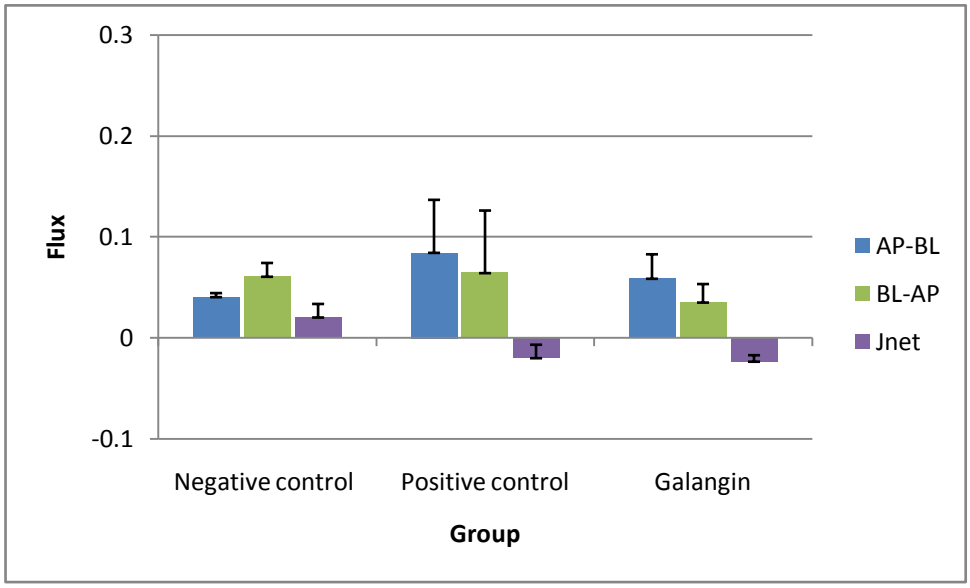

Figure 4.16: Flux and net flux values of Rhodamine 123 in the presence of Galangin in both directions across excised pig intestinal tissue

4.2.4.3 Discussion of results and conclusions

From the results obtained in this experimental group, it is clear that the transport of Rhodamine 123 in the BA-AP direction was decreased by the presence of Galangin. This corresponds with data obtained by Van Huyssteen (2005:66) and Bansal *et al.* (2009:54) as well as the findings obtained in another study done by Conseil *et al.* (1998:9835) that Galangin was able to modulate drug efflux in MDR cancer cells.

The mean ER values were 0.76 across rat intestinal tissue and 0.60 across pig intestinal tissue, which were statistically significantly lower ($p < 0.05$) than the ER values of the negative control of 1.18 across rat intestinal tissue and 1.65 across pig intestinal tissue. The mean J_{net} for Rhodamine 123 transport across rat intestinal tissue was -0.01 and across pig intestinal tissue it was -0.02 compared to the J_{net} values of the negative control of 0.03 across rat intestinal tissue and 0.02 across pig intestinal tissue. The negative net flux values indicate that Galangin decreased the BL-AP transport of Rhodamine 123 to such an extent that an overall influx in the absorptive direction (i.e. a higher transport in the AP-BL direction) was obtained.

Although the mean ER and J_{net} values across the rat as well as pig intestinal tissues were lower than those obtained for Verapamil (positive control group), they showed no statistical significant difference. It may be concluded that Galangin acts as an inhibitor of *in vitro* P-gp related efflux of Rhodamine 123 in a similar way as Verapamil. The implication of this is that when food or fruit containing Galangin is taken simultaneously with a drug that is a substrate for P-gp, it may increase the bioavailability of the drug. The clinical significance of this increased bioavailability by means of the pharmacokinetic interaction identified with the *in vitro* models in this study should be determined and confirmed by means of *in vivo* clinical trials.

4.2.5 6-Methoxyflavone

The effect of 6-Methoxyflavone on the *in vitro* transport of Rhodamine 123 in the presence of 20 µM 6-Methoxyflavone was investigated across excised rat and pig jejunum in a Sweetana-Grass diffusion apparatus. The transport of Rhodamine 123 in two directions across both rat and pig intestinal segments in the presence of 20 µM 6-Methoxyflavone was determined and the relative transport, apparent permeability coefficient (P_{app}), flux (J), efflux ratio (ER) and net flux (J_{net}) values were calculated.

4.2.5.1 Transport across excised rat intestinal tissue

4.2.5.1.1 Relative transport

The transport of Rhodamine 123 in the presence of 20 µM 6-Methoxyflavone expressed as a percentage accumulated in the acceptor chamber relative to the initial concentration (10 µM) applied to the donor chamber is presented in Table 4.9.

Table 4.9: Relative transport of Rhodamine 123 in the presence of 6-Methoxyflavone in both directions across rat intestinal tissue

Group	Time (min)	AP - BL		BL - AP	
		Mean	SD	Mean	SD
6-Methoxyflavone 1	**0**	0.00000	0.00	0.00000	0.00
	30	0.61661	0.12	0.35247	0.26
	60	0.64977	0.12	0.43714	0.30
	90	0.67557	0.12	0.50623	0.27
	120	0.71716	0.12	0.55685	0.25
6-Methoxyflavone 2	**0**	0.00000	0.00	0.00000	0.00
	30	0.22571	0.15	0.20723	0.14
	60	0.32445	0.16	0.35979	0.19
	90	0.48755	0.14	0.44474	0.19
	120	0.70867	0.20	0.51297	0.19
6-Methoxyflavone 3	**0**	0.00000	0.00	0.00000	0.00
	30	0.71825	0.91	0.41247	0.49
	60	0.78708	0.91	0.70717	0.44
	90	0.87567	0.87	0.83201	0.34
	120	0.99908	0.79	0.80550	0.45

4.2.5.1.2 Apparent permeability coefficient (P_{app}) and efflux ratio values

The apparent permeability coefficient (P_{app}) and the efflux ratio (ER) values of Rhodamine 123 in the presence of 20 µM 6-Methoxyflavone are given in Figure 4.17.

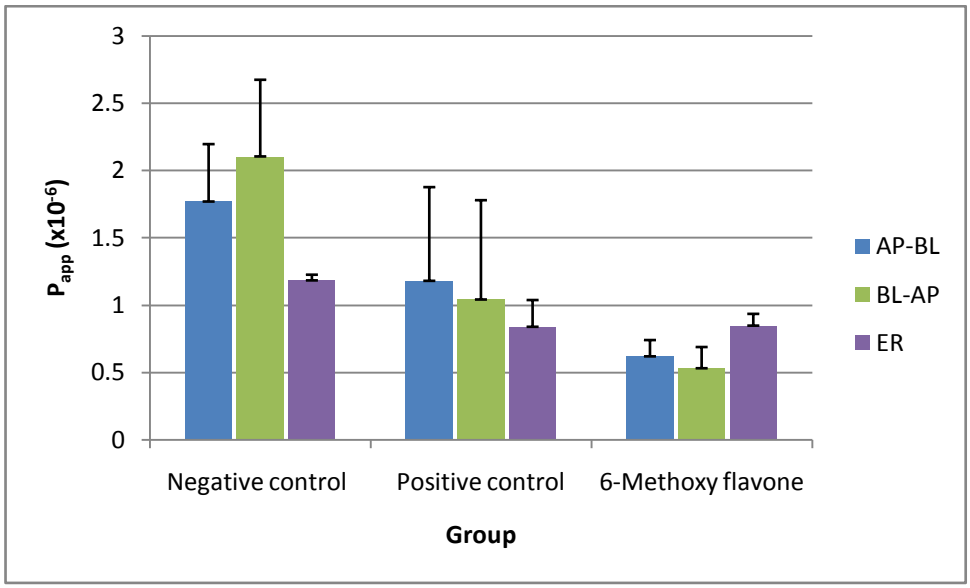

Figure 4.17: P_{app} and ER values of Rhodamine 123 in the presence of 6-Methoxyflavone in both directions across excised rat intestinal tissue

4.2.5.1.3 Flux

The flux (J) as well as the net flux (J_{net}) values of Rhodamine 123 in the presence of 6-Methoxyflavone are given in Figure 4.18.

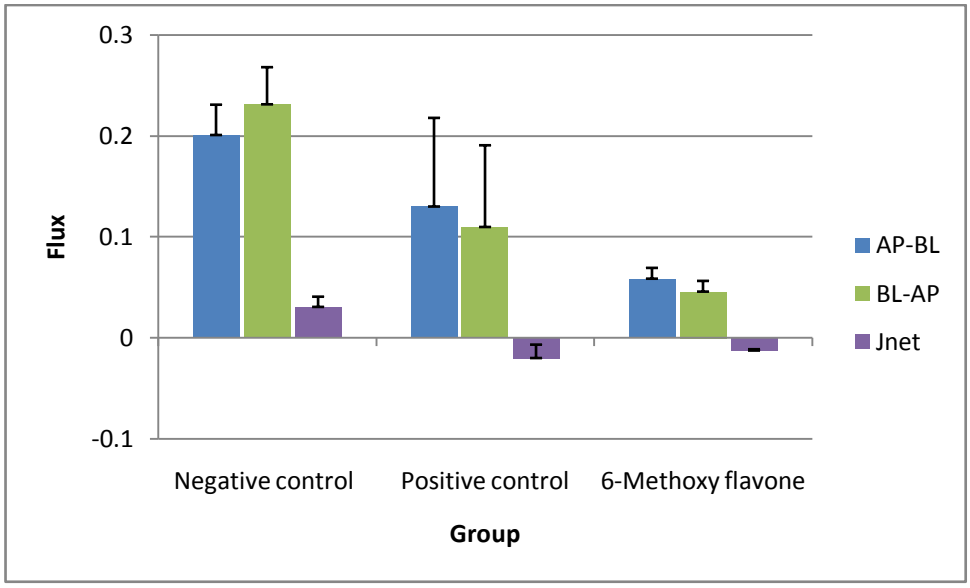

Figure 4.18: Flux and net flux values of Rhodamine 123 in the presence of 6-Methoxyflavone in both directions across excised rat intestinal tissue

4.2.5.2 Transport across excised pig intestinal tissue

4.2.5.2.1 Relative transport

The transport of Rhodamine 123 in the presence of 20 µM 6-Methoxyflavone expressed as a percentage accumulated in the acceptor chamber relative to the initial concentration (10 µM) applied to the donor chamber is presented in Table 4.10.

Table 4.10: Relative transport of Rhodamine 123 in the presence of 6-Methoxyflavone across excised pig intestinal tissue

Group	Time (min)	AP - BL		BL - AP	
		Mean	SD	Mean	SD
6-Methoxyflavone 1	**0**	0.00000	0.00	0.00000	0.00
	30	0.14458	0.11	0.06201	0.06
	60	0.12387	0.09	0.06414	0.07
	90	0.22639	0.11	0.05566	0.05
	120	0.10922	0.08	0.09070	0.04
6-Methoxyflavone 2	**0**	0.00000	0.00	0.00000	0.00
	30	0.21058	0.14	0.07151	0.01
	60	0.20875	0.14	0.07602	0.02
	90	0.21026	0.13	0.07689	0.02
	120	0.19897	0.11	0.07910	0.02
6-Methoxyflavone 3	**0**	0.00000	0.00	0.00000	0.00
	30	0.20418	0.13	0.16027	0.08
	60	0.22473	0.16	0.16945	0.08
	90	0.21699	0.17	0.18396	0.10
	120	0.21716	0.16	0.20122	0.09

4.2.5.2.2 Apparent permeability coefficient (P_{app}) and efflux ratio values

The apparent permeability coefficient (P_{app}) and the efflux ratio (ER) values of Rhodamine 123 in the presence of 20 µM 6-Methoxyflavone are given in Figure 4.19.

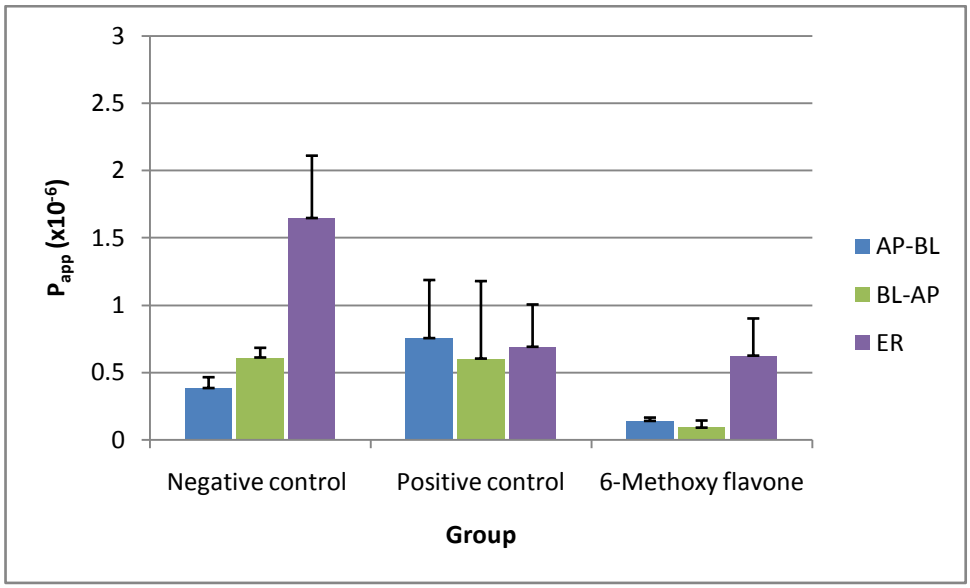

Figure 4.19: P_{app} and ER values of Rhodamine 123 in the presence of 6-Methoxyflavone in both directions across excised pig intestinal tissue

4.2.5.2.3 Flux

The flux (J) as well as the net flux (J_{net}) values of Rhodamine 123 in the presence of 20 µM 6-Methoxyflavone are given in Figure 4.20.

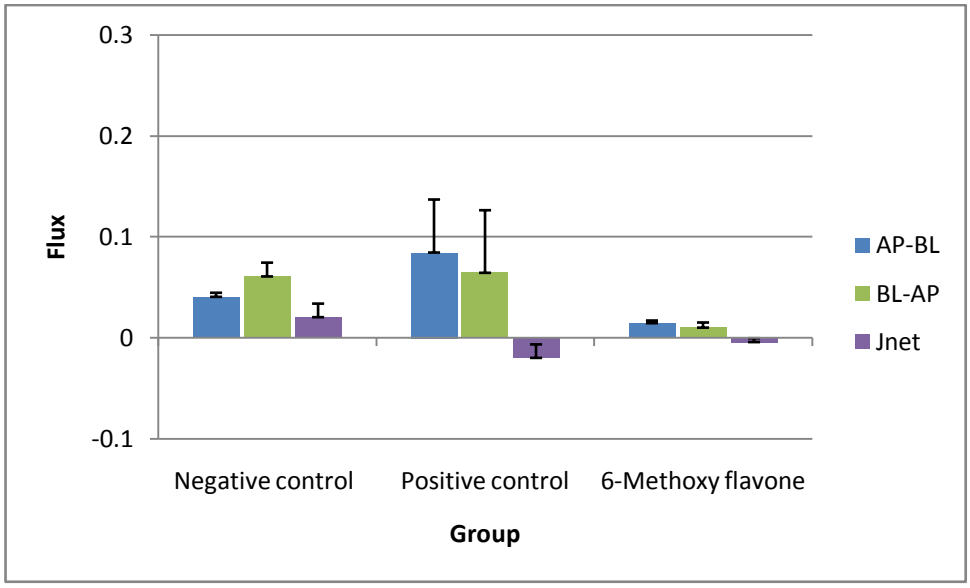

Figure 4.20: Flux and net flux values of Rhodamine 123 in the presence of 6-Methoxyflavone in both directions across excised pig intestinal tissue

4.2.5.3 Discussion of results and conclusions

Similar to the results obtained for Morin and Galangin, 6-Methoxyflavone also decreased the *in vitro* transport of Rhodamine 123 in the BA-AP direction in both animal intestinal tissue models used in this study. However, these results differ from the findings obtained by Dodd (2005:61) in an *in vitro* study across rat jejunal segments.

The mean ER value was 0.85 across rat intestinal tissue and 0.62 across pig intestinal tissue compared to the ER values of the negative control group of 1.18 across rat intestinal tissue and 1.65 across pig intestinal tissue, which were statistically significantly different. The ER value of the 6-Methoxyflavones group was not statistically significantly different from the ER value of the positive control group across rat intestinal tissue but, it was statistically significantly different from that of the positive control group across pig intestinal tissue. The mean J_{net} value for Rhodamine 123 transport in the presence of 6-Methoxyflavones was -0.01 across rat intestinal tissue and 0.00 across pig intestinal tissue compared to the J_{net} values of the negative control that were 0.03 across the rat intestinal tissue and 0.02 across pig intestinal tissue. Thus, in both animal models the ER and J_{net} values were decreased by 6-Methoxyflavone indicating a P-gp inhibiting effect and thereby increasing the transport of co-applied drugs that are substrates for P-gp in the absorptive direction. This may lead to an increase in the bioavailability of drugs that are administered simultaneously with food containing 6-Methoxyflavone, but its clinical significance should be determined by means of *in vivo* clinical trials.

4.2.6 7-Methoxyflavone

As mentioned before, it has been found that certain flavonoids have the ability to modulate P-gp and thereby influence the transport of co-administered compounds across intestinal epithelia that are substrates for P-gp (Chao *et al.*, 2002:219). The effect of 7-Methoxyflavone on the *in vitro* transport of Rhodamine 123 across excised rat and pig jejunum was investigated in a Sweetana-Grass diffusion apparatus. The bi-directional transport of Rhodamine 123 in the presence of 20 µM 7-Methoxyflavone was determined and the relative transport, apparent permeability coefficient (P_{app}), flux (J), net flux (J_{net}) and efflux ratio (ER) values were calculated in two directions across both rat and pig intestinal segments.

4.2.6.1 Transport across excised rat intestinal tissue

4.2.6.1.1 Relative transport

The transport of Rhodamine 123 in the presence of 20 µM 7-Methoxyflavone expressed as a percentage accumulated in the acceptor chamber relative to the initial concentration (10 µM) applied to the donor chamber is presented in Table 4.11.

Table 4.11: Relative transport of Rhodamine 123 in the presence of 7-Methoxyflavone in both directions across rat intestinal tissue

Group	Time (min)	AP - BL		BL - AP	
		Mean	SD	Mean	SD
7-Methoxyflavone 1	**0**	0.00000	0.00	0.00000	0.00
	30	0.21540	0.02	0.23043	0.11
	60	0.33721	0.04	0.36963	0.05
	90	0.42947	0.11	0.48417	0.09
	120	0.53156	0.14	0.63039	0.14
7-Methoxyflavone 2	**0**	0.00000	0.00	0.00000	0.00
	30	0.12504	0.01	0.18975	0.02
	60	0.21407	0.03	0.30413	0.05
	90	0.40047	0.15	0.44671	0.09
	120	0.55315	0.18	0.53530	0.07
7-Methoxyflavone 3	**0**	0.00000	0.00	0.00000	0.00
	30	0.29483	0.11	0.28655	0.14
	60	0.33966	0.12	0.31564	0.14
	90	0.38148	0.12	0.33996	0.13
	120	0.40549	0.14	0.37576	0.11

4.2.6.1.2 Apparent permeability coefficient (P_{app}) and efflux ratio values

The apparent permeability coefficient (P_{app}) and the efflux ratio (ER) values of Rhodamine 123 in the presence of 20 µM 7-Methoxyflavone are given in Figure 4.21.

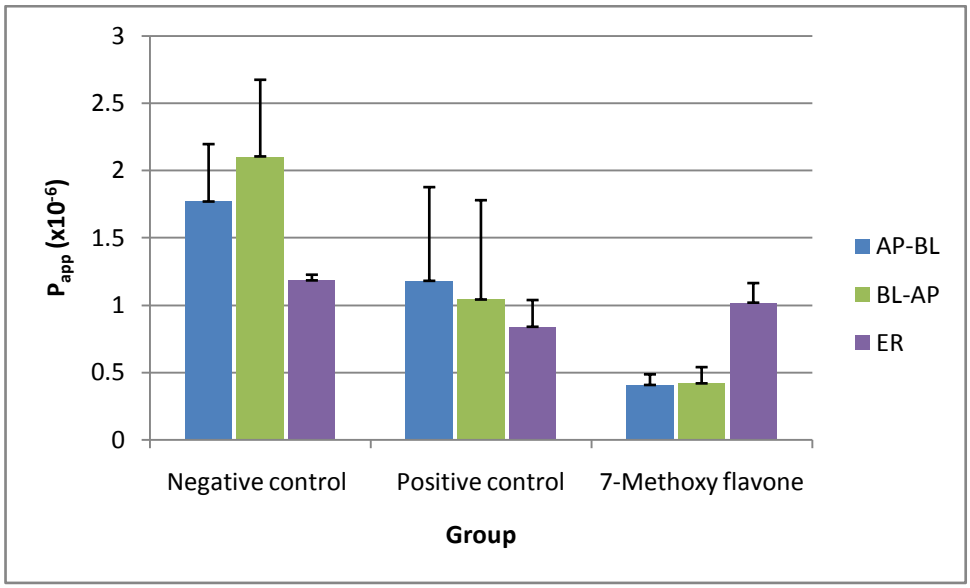

Figure 4.21: P_{app} and ER values of Rhodamine 123 in the presence of 7-Methoxyflavone in both directions across excised rat intestinal tissue

4.2.6.1.3 Flux

The flux (J) as well as the net flux (J_{net}), values of Rhodamine 123 in the presence of 7-Methoxyflavone are given in Figure 4.22.

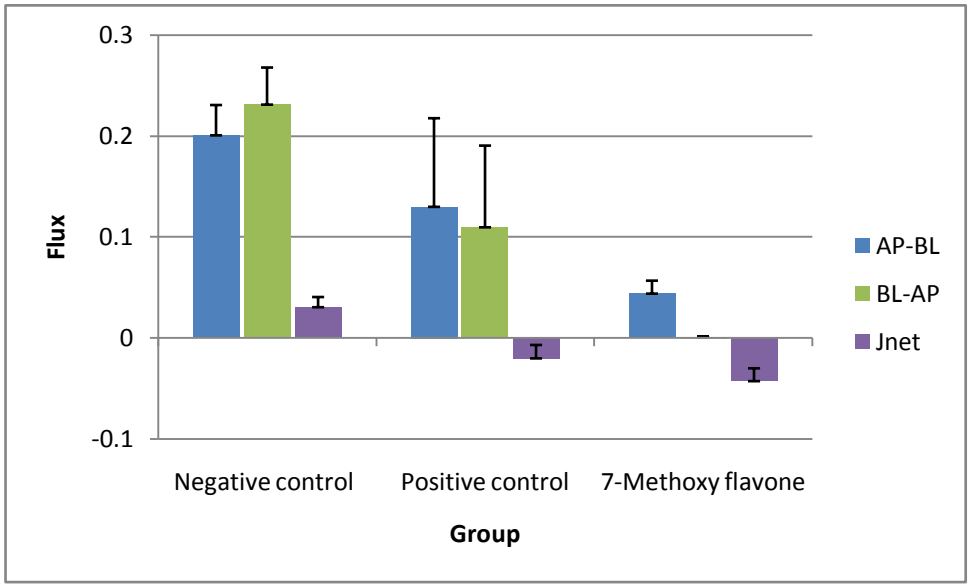

Figure 4.22: Flux and net flux values of Rhodamine 123 in the presence of 7-Methoxyflavone in both directions across excised rat intestinal tissue

4.2.6.2 Transport across excised pig intestinal tissue

4.2.6.2.1 Relative transport

The transport of Rhodamine 123 in the presence of 20 µM 7-Methoxyflavone expressed as a percentage accumulated in the acceptor chamber relative to the initial concentration (10 µM) applied to the donor chamber is presented in Table 4.12.

Table 4.12: Relative transport of Rhodamine 123 in the presence of 7-Methoxyflavone across excised pig intestinal tissue

Group	Time (min)	AP - BL		BL - AP	
		Mean	SD	Mean	SD
7-Methoxyflavone 1	**0**	0.00000	0.00	0.00000	0.00
	30	0.22205	0.11	0.14804	0.14
	60	0.24165	0.13	0.15981	0.15
	90	0.24479	0.13	0.15700	0.15
	120	0.24870	0.12	0.17007	0.15
7-Methoxyflavone 2	**0**	0.00000	0.00	0.00000	0.00
	30	0.24327	0.15	0.15429	0.03
	60	0.25308	0.15	0.15495	0.03
	90	0.29993	0.08	0.15631	0.03
	120	0.33720	0.06	0.15301	0.03
7-Methoxyflavone 3	**0**	0.00000	0.00	0.00000	0.00
	30	0.21544	0.11	0.33369	0.08
	60	0.23325	0.12	0.30842	0.06
	90	0.27107	0.16	0.32300	0.09
	120	0.26037	0.11	0.34099	0.12

4.2.5.2.2 Apparent permeability coefficient (P_{app}) and efflux ratio values

The apparent permeability coefficient (P_{app}) and the efflux ratio (ER) values of Rhodamine 123 in the presence of 20 µM 7-Methoxyflavone are given in Figure 4.23.

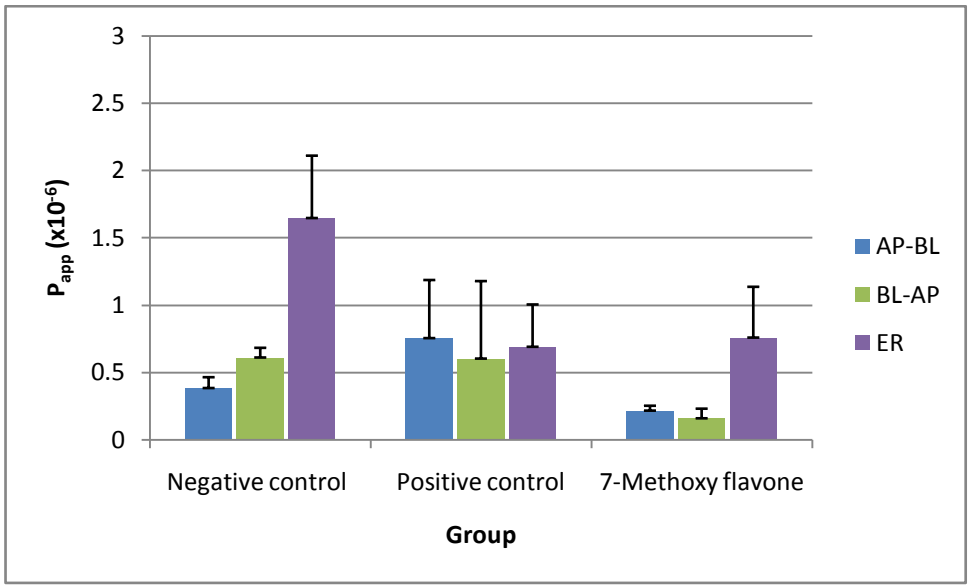

Figure 4.23: P_{app} and ER values of Rhodamine 123 in the presence of 7-Methoxyflavone in both directions across excised pig intestinal tissue

4.2.6.2.3 Flux

The flux (J) as well as the net flux (J_{net}) values of Rhodamine 123 in the presence of 20 µM 7-Methoxyflavone are given in Figure 4.24.

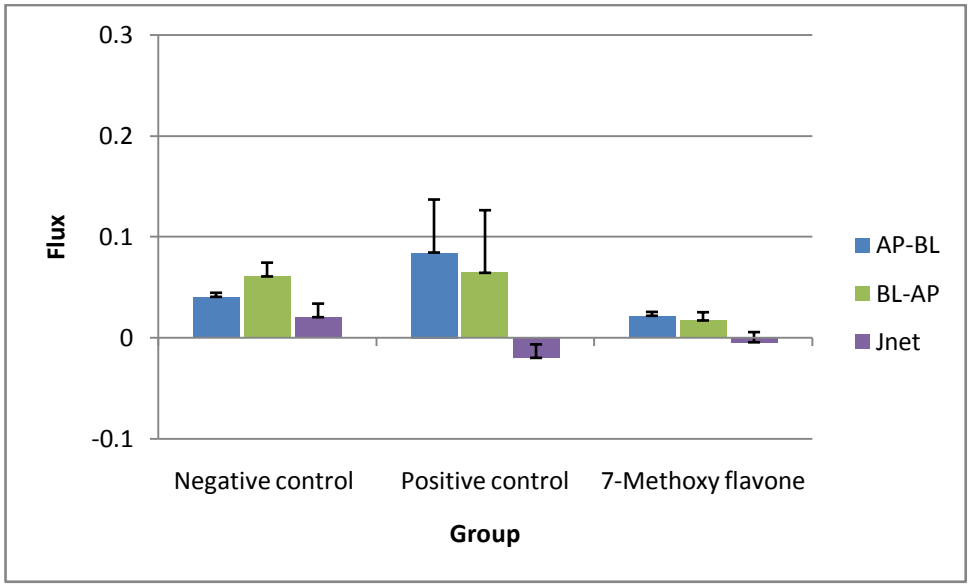

Figure 4.24: Flux and net flux values of Rhodamine 123 in the presence of 7-Methoxyflavone in both directions across excised pig intestinal tissue

4.2.6.3 Discussion of results and conclusions

From the results obtained, it can be observed that 7-Methoxyflavone was able to decrease the *in vitro* transport of Rhodamine 123 in the BL-AP direction and although it was statistically significant in some cases, this effect seemed to be lower as observed than that of other flavones investigated in this study. This corresponds with the findings obtained by Dodd (2005:63) in a transport study conducted across rat jejunal segments.

The mean ER value was 1.02 across rat intestinal tissue and 0.76 across pig intestinal tissue compared to the ER values of the negative control of 1.18 across rat intestinal tissue and 1.65 across pig intestinal tissue. The mean J_{net} values were -0.04 across rat intestinal tissue and 0.00 across pig intestinal tissue compared to the J_{net} values of the negative control that were 0.03 across rat intestinal tissue and 0.02 across pig intestinal tissue.

The mean ER value across pig intestinal tissue and the mean J_{net} value obtained for the rat intestinal tissue showed statistically significant differences ($p < 0.05$) from the values of negative control group (see Table 4.37 - 4.40). However, the mean ER value across rat intestinal tissue and the mean J_{net} value across pig intestinal tissue did not show statistically significant differences from those of the negative control group. Furthermore, the mean ER and J_{net} values calculated based on Rhodamine 123 transport across both rat and pig intestinal tissues, did not show statistically significant differences compared to the positive control group (excluding the mean J_{net} across rat intestinal tissue). Since mixed results were obtained for the effect of 7-Methoxyflavone on the transport of Rhodamine 123 in the two animal tissue models used and not all the results were statistically significantly different from the control groups, the findings are not conclusive in terms of its ability to inhibit P-gp.

4.2.7 Comparison and statistical analysis of transport results

4.2.7.1 Comparison of the transport results

The cumulative transport of Rhodamine 123 as a function of time in both directions across rat intestinal tissue for all the experimental and control groups is given in Figure 4.25 and that across pig intestinal tissue is given in Figure 4.26.

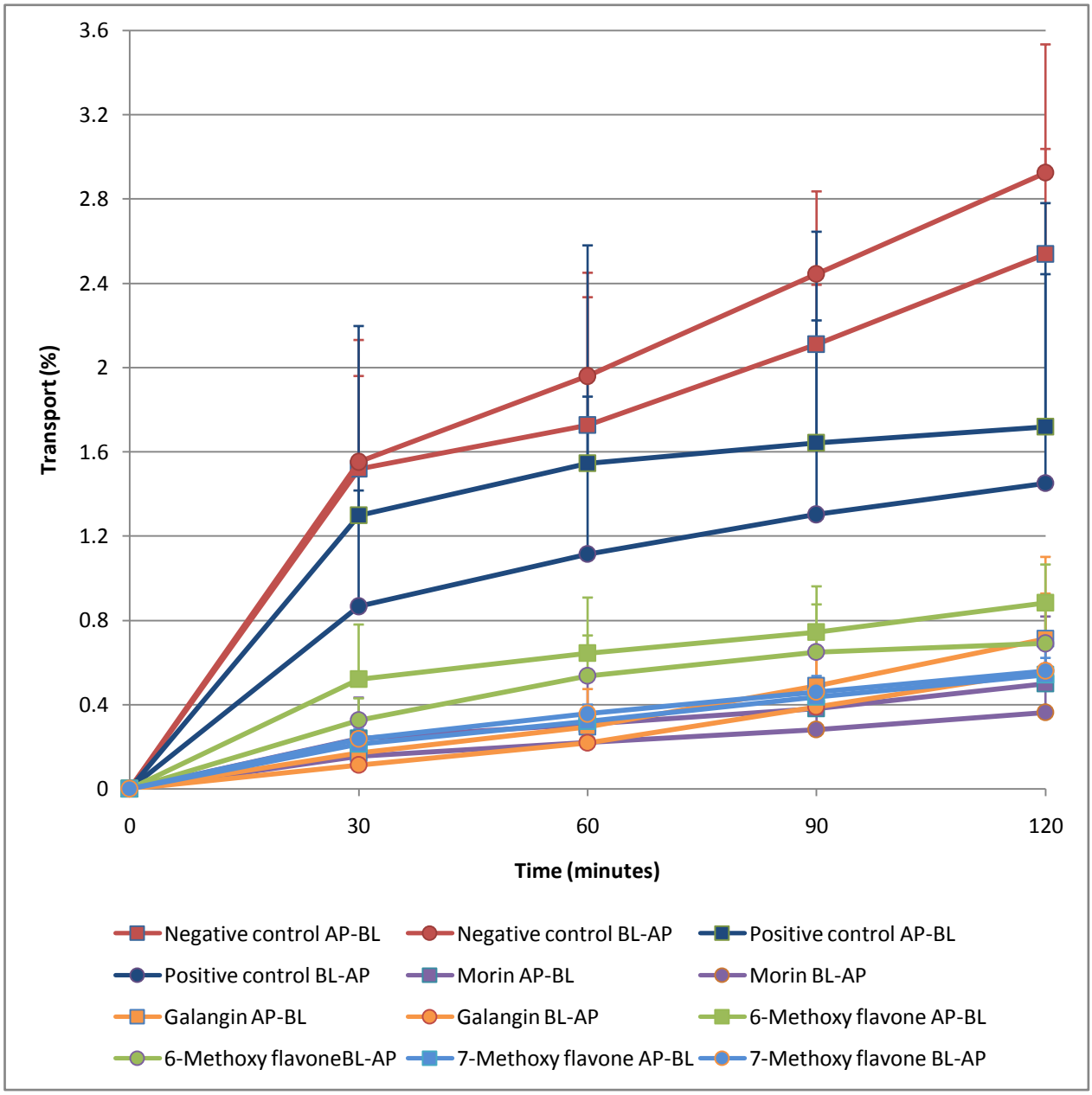

Figure 4.25: Bi-directional cumulative Rhodamine 123 transport as a function of time for all the groups across rat intestinal tissue

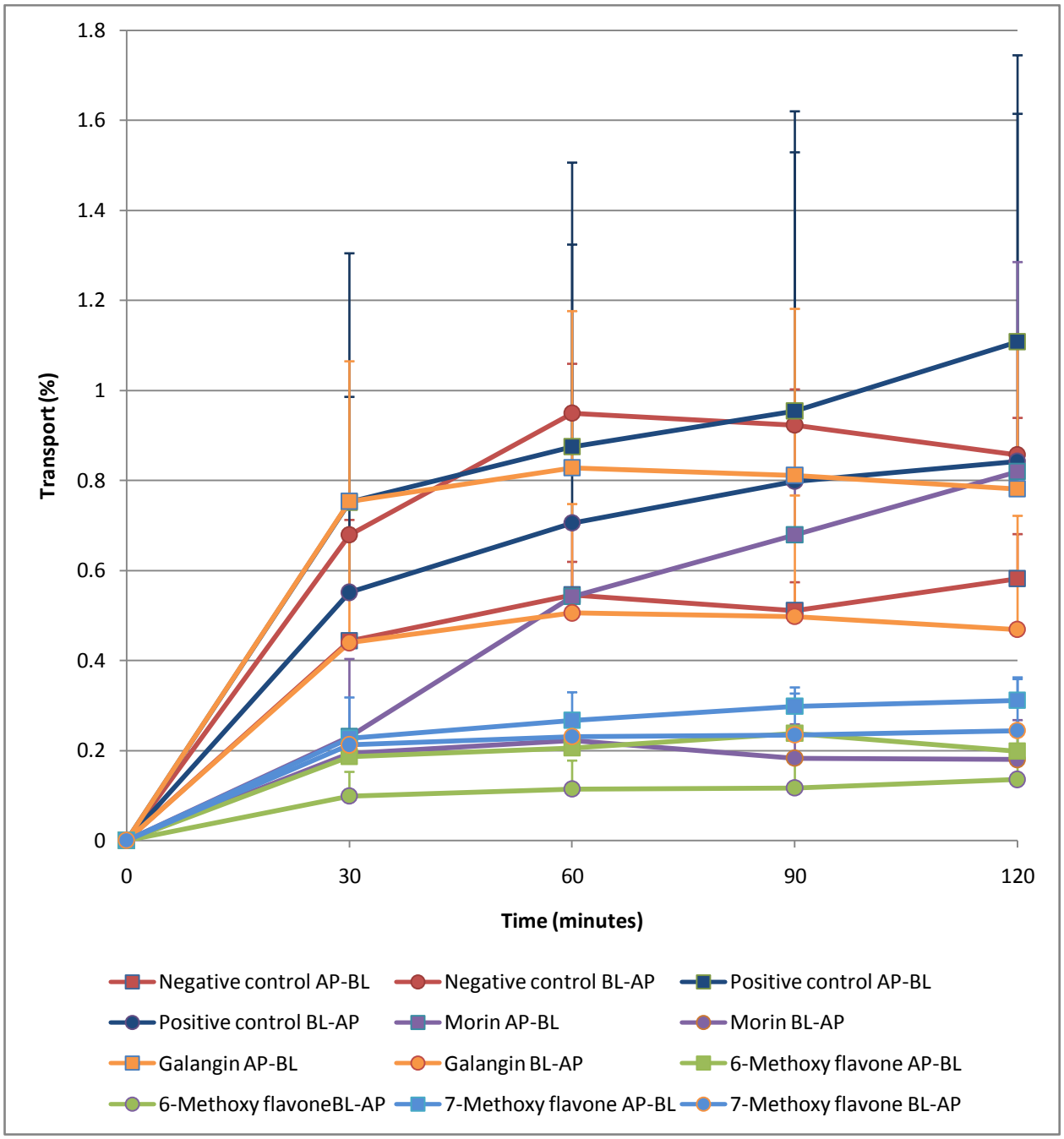

Figure 4.26: Bi-directional cumulative Rhodamine 123 transport as a function of time for all the groups across pig intestinal tissue

From Figures 4.25 and 4.26 it is clear that the four selected flavones each had an effect on Rhodamine 123 transport across both rat and pig intestinal tissues. These effects were statistically analysed by means of a one-way analysis of variance (ANOVA) and these findings are discussed in the following sections.

4.2.7.2 Efflux ratio (ER)

The p-values obtained when statistically comparing the mean ER values of Rhodamine 123 across both rat and pig intestinal tissues for the different experimental and control groups are given in Table 4.13, Table 4.14 and Figure 4.27.

Table 4.13: P-values for the ER values of Rhodamine 123 across rat intestinal tissue when comparing the different experimental groups with the control groups

Group	n	Mean ER	SD	p-value: Dunnett		
				ANOVA	Pos. Contr.	Neg. Contr.
Morin	3	0.83	0.20		1.00	0.02 *
Galangin	3	0.76	0.12		0.91	0.01*
6-Methoxyflavone	3	0.85	0.09		1.00	0.03*
7-Methoxyflavone	3	1.02	0.15		0.47	0.38
Positive control	3	0.84	0.20	0.39		
Negative control	3	1.18	0.04	0.01*		

* Statistically significantly different at 0.05 level

Table 4.14: P-values for the mean ER values of Rhodamine 123 across pig intestinal tissue when comparing the different experimental groups with the control groups

Group	n	Mean ER	SD	p-value: Dunnett		
				ANOVA	Pos. Contr.	Neg. Contr.
Morin	3	0.29	0.32		0.32	0.00 *
Galangin	3	0.60	0.06		0.98	0.01*
6-Methoxyflavone	3	0.62	0.28		1.00	0.01*
7-Methoxyflavone	3	0.76	0.67		0.99	0.02*
Positive control	3	0.69	0.31	0.39		
Negative control	3	1.65	0.46	0.01*		

* Statistically significantly different at 0.05 level

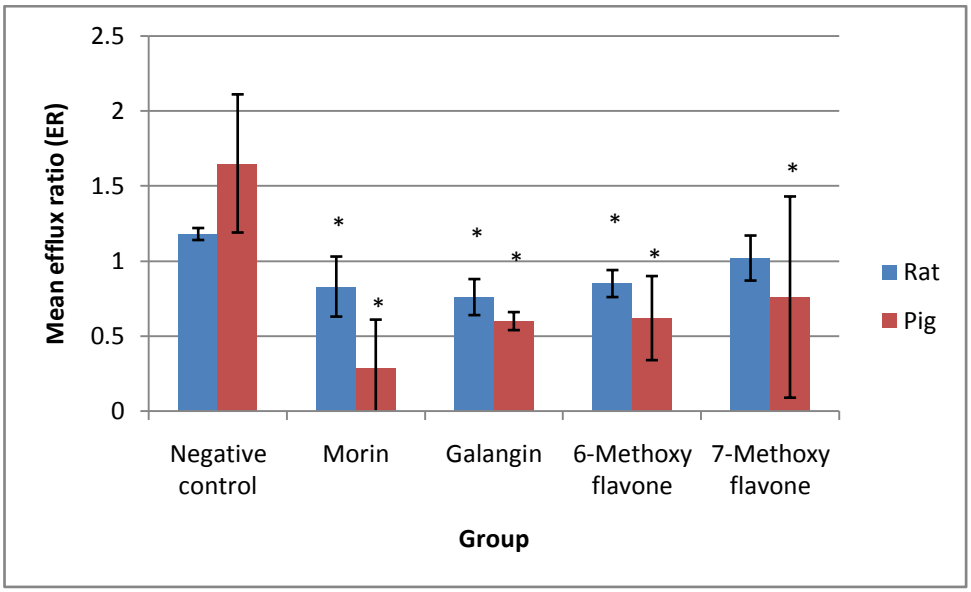

Figure 4.27: Mean ER values of the different experimental groups compared to the negative control group across both rat and pig intestinal tissues. An asterisk (*) indicates statistically significant difference of the experimental group with the negative control group

4.2.7.2.1 Discussion of statistical analysis of ER results

Based on the p-values of the ER for the transport studies across rat intestinal tissue, statistical significant differences exist between three experimental groups namely Morin ($p < 0.05$), Galangin ($p < 0.05$) as well as 6-Methoxyflavone ($p < 0.05$) and the negative control group. The only test substance that did not differ statistically significantly from the negative control group in the rat intestinal tissue model was 7-Methoxyflavone ($p = 0.38$). Based on the p-values of the ER for the transport studies across pig intestinal tissue, statistical significant differences existed between all four experimental groups namely Morin ($p < 0.05$), Galangin ($p < 0.05$), 6-Methoxyflavone ($p < 0.05$) as well as 7-Methoxyflavone ($p < 0.05$), and the negative control group ($p < 0.05$).

With regards to the ER values, none of the test groups for both the rat and pig intestinal tissue models showed any statistical significant difference with the positive control group (Verapamil). In summary, it is clear that Morin, Galangin and 6-Methoxyflavone have a significant inhibitory effect on the Rhodamine 123 efflux (probably P-gp related) in both the rat and pig intestinal tissue models. These three compounds when taken simultaneously with drugs that are substrates for P-gp efflux in concentrations tested in this study may therefore influence the bioavailability of the drugs, but this needs to be confirmed by means of *in vivo* experiments. On

the other hand, 7-Methoxyflavone showed a significant effect on the efflux of Rhodamine 123 in the pig intestinal tissue model but not in the rat intestinal tissue model. Based on the discrepancy of the results obtained in the different models used in this study, it can therefore not be conclusively stated that 7-Methoxyflavone is definitely an inhibitor of P-gp. Further studies are needed to reach a conclusion in this regard.

4.2.7.3 Net flux

The p-values of the mean net flux values for rats and pigs are given in Table 4.15, Table 4.16 and Figure 4.28.

Table 4.15: P-values for the mean net flux (J_{net}) values of Rhodamine 123 across rat intestinal tissue when comparing the different experimental groups with the control groups

Group	n	Mean J_{net}	SD	p-value: Dunnett		
				ANOVA	Pos. Contr.	Neg. Contr.
Morin	3	-0.01	0.01		0.57	0.00 *
Galangin	3	-0.01	0.00		0.62	0.00*
6-Methoxyflavone	3	-0.01	0.00		0.77	0.00*
7-Methoxyflavone	3	-0.04	0.01		0.06•	0.00*
Positive control	3	-0.02	0.01	0.01*		
Negative control	3	0.03	0.01	0.00*		

* Statistically significantly different at 0.05 level, • Statistically significantly different at 0.10 level

Table 4.16: P-values for the mean net flux (J_{net}) values of Rhodamine 123 across pig intestinal tissue when comparing the different experimental groups with the control groups

Group	Pig						
	n	Mean J_{net}	SD	p-value		p-value: Dunnett	
				ANOVA	Welch	Pos. Contr.	Neg. Contr.
Morin	3	-0.04	0.03			0.39	0.00 *
Galangin	3	-0.02	0.01			1.00	0.04*
6-Methoxyflavone	3	-0.00	0.00			0.66	0.31
7-Methoxyflavone	3	-0.00	0.01			0.67	0.31
Positive control	3	-0.02	0.01		0.08		
Negative control	3	0.02	0.01		0.04*		

* Statistically significantly different at 0.05 level

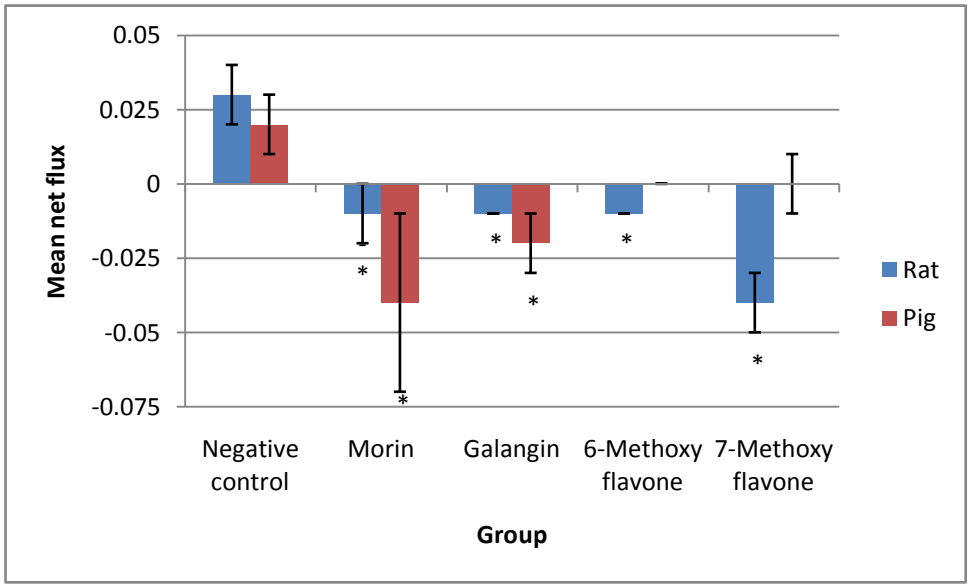

Figure 4.28: Mean net flux (J_{net}) values of the different experimental groups compared to the negative control group across both rat and pig intestinal tissues

4.2.7.3.1 Discussion of the statistical analysis of flux results

Based on the p-values of the J_{net} for the Rhodamine 123 transport studies across rat intestinal tissue it is evident that Morin ($p < 0.05$), Galangin ($p < 0.05$), 6-Methoxyflavone ($p < 0.05$) and 7-Methoxyflavone ($p < 0.05$) were statistically significantly different from the J_{net} for the negative control group. Based on the p-values of the J_{net} for the transport studies across pig intestinal tissue it is clear that only Morin ($p < 0.05$) and Galangin ($p < 0.05$) were statistically significantly different from the negative control group ($p < 0.05$). The substances that did not have a significant effect on the J_{net} values of Rhodamine 123 transport across pig intestinal tissue as compared to that obtained in the negative control group were 6-Methoxyflavone ($p = 0.31$) and 7-Methoxyflavone ($p = 0.31$).

Based on the J_{net} values of the test compounds compared to the J_{net} values of the negative control group, Morin and Galangin showed significant P-gp inhibitory effects in both the rat and pig intestinal tissue models, while 6-Methoxyflavone and 7-Methoxyflavone only showed significant efflux inhibitory effects across rat intestinal tissue. In summary, the net flux results are therefore not conclusive in terms of the P-gp inhibitory effects of 6-Methoxyflavones and 7-Methoxyflavones since they could not significantly influence Rhodamine 123 across both animal tissue models used in this study.

4.3 Statistical comparison of the rat and pig intestinal tissue models

4.3.1 Efflux Ratio (ER)

A comparison of the mean ER based on Rhodamine 123 transport obtained in the two different animal tissue models including the negative and positive control groups and the experimental groups is given in Figure 4.29 and Figure 4.30.

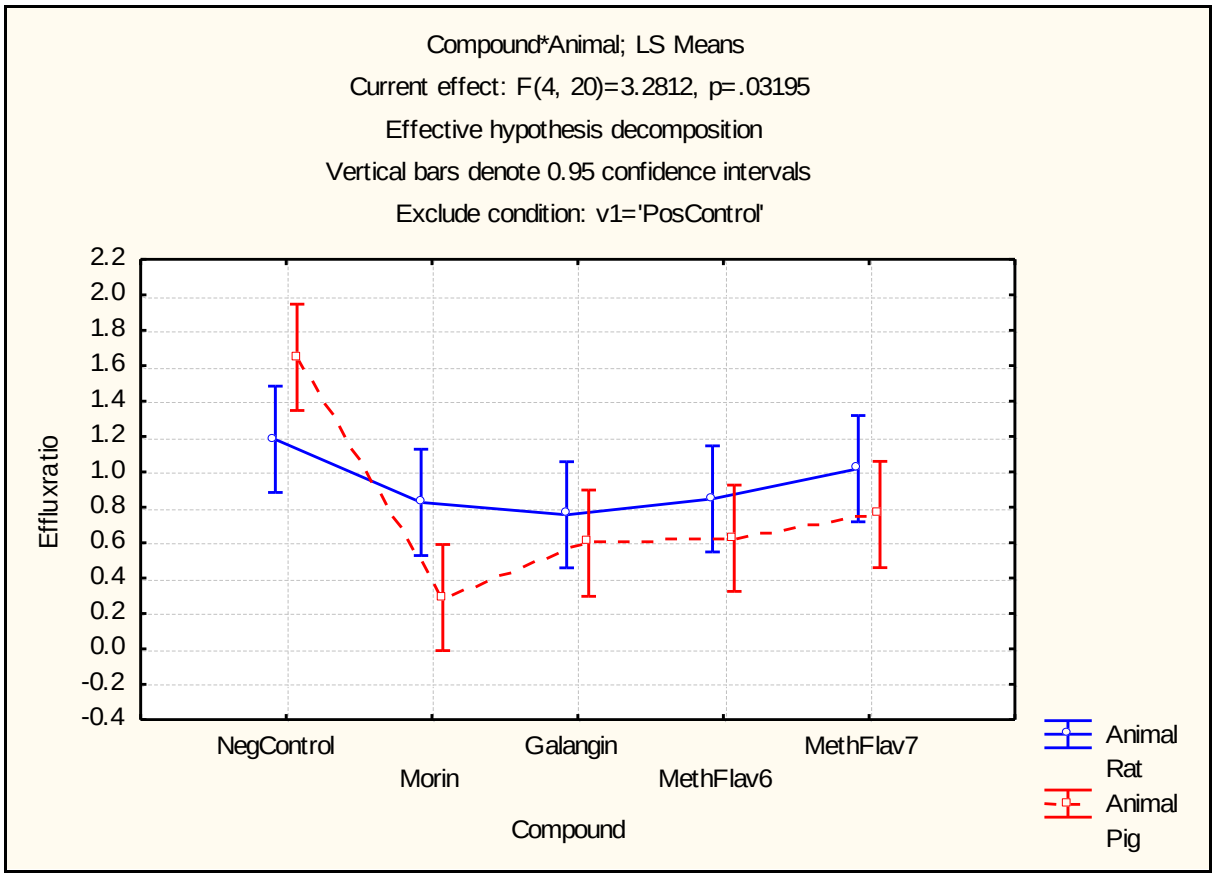

Figure 4.29: Comparison of the ER values of the rat intestinal tissue model to the pig intestinal tissue model including the negative control group

According to the plot presented in Figure 4.27 where the ER values of the rat and pig intestinal tissue models are compared for all the experimental groups and the negative control group, the crossing of the two lines on the graph indicates differences between the two animal tissue models. This can be confirmed by the p-value of a two-way analysis of variance (ANOVA) of 0.03 that this difference is statistically significant. Therefore, the rat intestinal tissue model and the pig intestinal tissue model with regard to the ER of the different test compounds and the negative control group do not correspond.

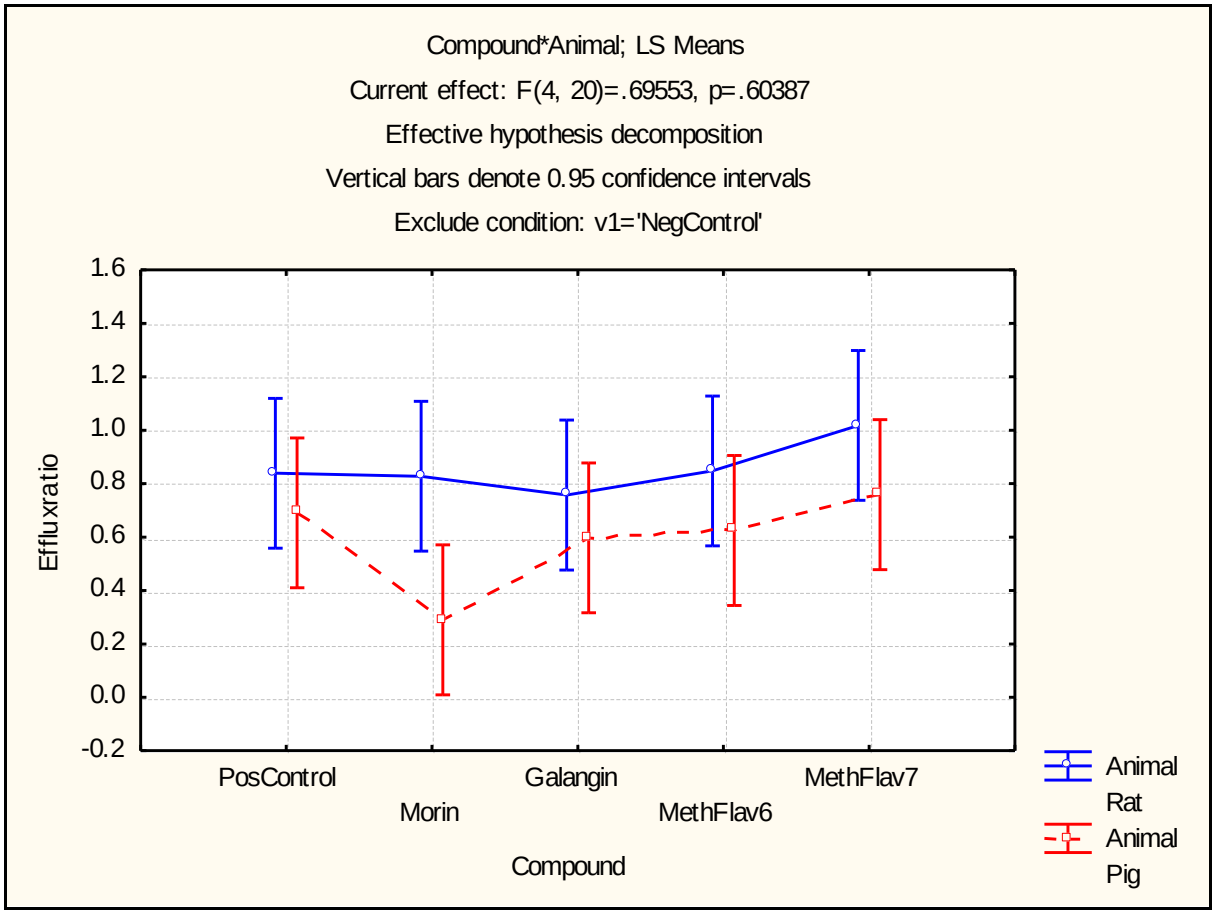

Figure 4.30: Comparison of the ER values of the rat intestinal tissue model and the pig intestinal tissue model including the positive control group

According to the plot presented in Figure 4.28 where the ER values of the rat intestinal tissue and pig intestinal tissue models were compared for the different experimental groups and the positive control group, the trend of both models with regard to the compounds is similar. The only substance that slightly deviated was Morin, but confirmed by the two-way analysis of variance (ANOVA) p-value of 0.60, this deviation was not statistically significant.

The rat intestinal tissue model and pig intestinal tissue model with regard to the ER based on Rhodamine 123 transport in the presence of different compounds and the positive control therefore corresponds.

4.3.2 Net flux (J_{net})

A comparison of the mean J_{net} based on Rhodamine 123 transport obtained in the negative and positive control groups and the experimental groups are given in Figure 4.31 and Figure 4.32.

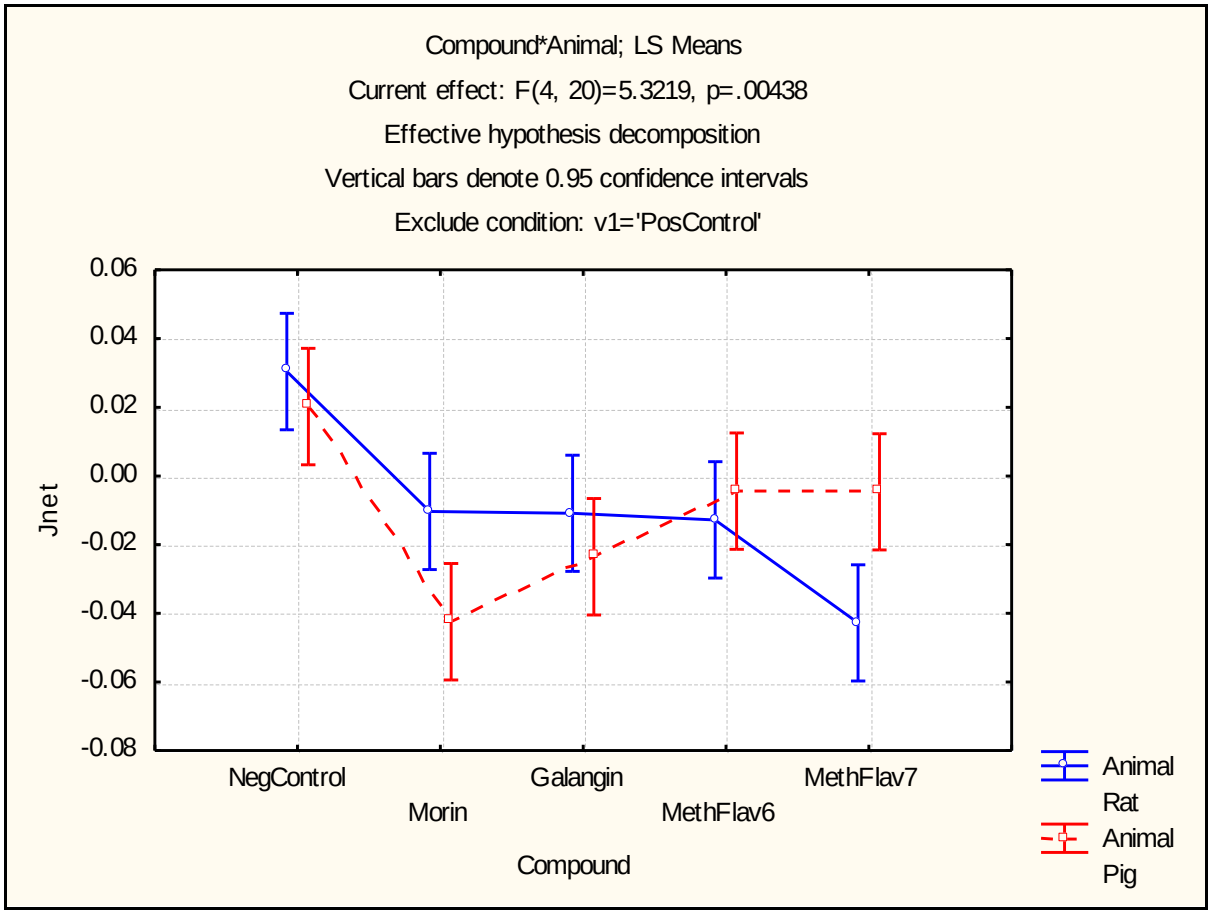

Figure 4.31: Comparison of the J_{net} values of the rat intestinal tissue model to the pig intestinal tissue model including the negative control group

According to the plot presented in Figure 4.29 where the J_{net} values of the rat and pig intestinal tissue models were compared for the different experimental groups and the negative control group, the crossing of the two lines on the graph indicates differences between the two animal tissue models. This can be confirmed by the p-value of a two-way analysis of variance (ANOVA) of 0.004 that this difference is statistically significant.

The rat intestinal tissue model and pig intestinal tissue model with regard to the J_{net} of the different test compounds and the negative control group do not correspond.

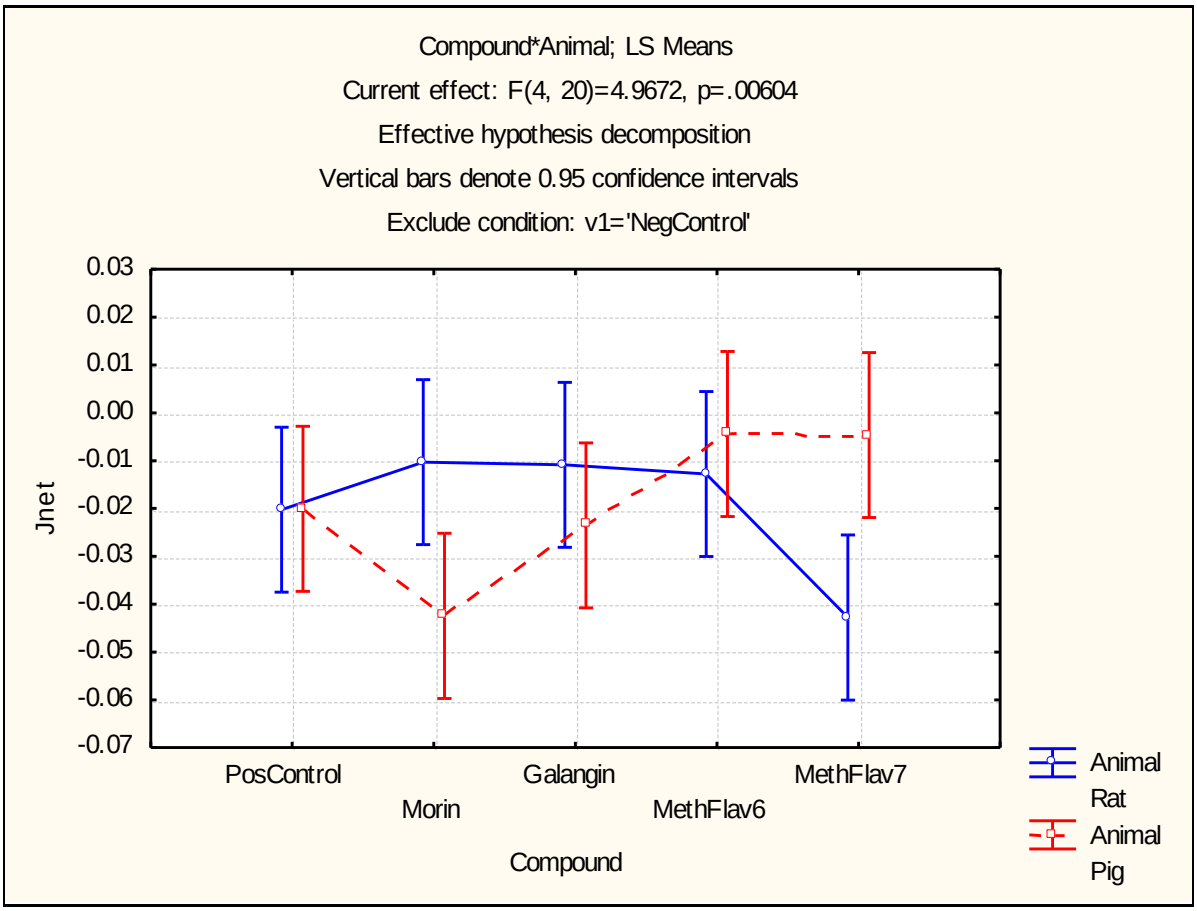

Figure 4.32: Comparison of the J_{net} values of the rat intestinal tissue model to the pig intestinal tissue model including the positive control group

According to the plot presented in Figure 4.30 where the J_{net} values of the rat and pig intestinal tissue models were compared to the positive control, the crossing of the two lines on the graph indicates differences between the two animal tissue models. This can be confirmed by the p-value of a two-way analysis of variance (ANOVA) of 0.006 that this difference is statistically significant.

The rat intestinal tissue model and pig intestinal tissue model with regard to the J_{net} of the different test compounds and the positive control group do not correspond.

Chapter 5

Final conclusions and future recommendations

5.1 Introduction

Transport of drug substances across the intestinal membrane is a complex and dynamic process (Balimane *et al.*, 2000:301). Transporters present in the intestinal membrane are responsible for two important permeation mechanisms, namely active uptake and efflux (Kerns & Di, 2008:103). There are counter uptake efflux proteins that expel specific drugs after they have been absorbed. One of the key counter efflux transporter proteins of importance in this study, is P-gp (Aulton, 2007:283). This efflux pump plays a major role in altering the pharmacokinetics of a wide variety of drugs as it limits the permeability and thus affecting their peroral absorption and bioavailability (Varma *et al., 2006:*367). It has become clear that flavonoids are important modulators or substrates of intestinal transport proteins, including P-gp (Brand *et al.*, 2006:515; Bansal *et al.*, 2009:68).

Many flavonoids have been shown to interact with P-gp mediated efflux in *in vitro* studies (Bansal *et al.*, 2009:68). The effects of flavonoids are found to be comparable with those of well-known P-gp inhibitors Verapamil and Cyclosporin (Bansal *et al.*, 2009:46). Many natural products of plant origin contain flavonoids, which are sometimes taken in conjunction with allopathic medicines. This may alter the bioavailability of drugs and may become clinically significant, especially in the case of drugs with narrow therapeutic indices.

Numerous *in vitro* methods have been used to study drug absorption across the intestinal membrane. Because of the multivariate processes involved in drug absorption from the intestine, it is often difficult to only use one *in vitro* model to accurately predict permeability characteristics (Balimane *et al.*, 2000:301).

The purpose of this study was to determine the effect of four selected hydroxy- and methoxy-flavonoids on the *in vitro* transport of Rhodamine 123, a known P-gp substrate, across stripped excised rat and pig intestinal tissue using the Sweetana-Grass diffusion chamber to determine whether the results obtained in the two different animal tissue models corresponded to each other with regards to possible P-gp inhibition.

The relative transport of Rhodamine 123, apparent permeability coefficient (P_{app}) values and transepithelial flux (J) values in the AP-BL and BL-AP directions as well as the efflux ratio (ER) and net flux (J_{net}) were calculated in order to interpret the transport results.

5.2 Results and conclusions

Rhodamine 123 alone (negative control group) was transported to a higher extent in the BL-AP direction in both the rat and pig intestinal tissue models than in the AP-BL direction indicating active efflux of this model compound as expected. This efflux was significantly inhibited by Verapamil (positive control group), which confirmed suitability of the excised intestinal tissues to measure the effect of flavonones on P-gp related efflux of Rhodamine 123. Both the ER and J_{net} values of Rhodamine 123 transport decreased significantly in the presence of Morin. Furthermore, the inhibitory effect exhibited by Morin on the P-gp related efflux of Rhodamine 123 across excised pig intestinal tissue has occurred to a larger extent than that obtained for Verapamil. However, it was not statistically significant differences from the effect of Verapamil. These results correspond well with previous findings obtained by Van Huyssteen (2005:63) who also found Morin to inhibit P-gp related efflux.

The transport of Rhodamine 123 in the BL-AP direction was further decreased by Galangin. This result corresponds with data obtained by Van Huyssteen (2005:66) and Bansal *et al.* (2009:54) as well as the findings obtained in another study done by Conseil *et al.* (1998:9835) which indicates that Galangin was able to modulate drug efflux in MDR cancer cells. The negative net flux values obtained indicate that Galangin decreased the BL-AP transport of Rhodamine 123 to such an extent that an overall influx in the absorptive direction (i.e. a higher transport in the AP-BL direction) was obtained. Although the mean ER and J_{net} values across the rat as well as pig intestinal tissues were lower than those obtained for Verapamil, they showed no statistical significant difference. It may be concluded from the results obatained in both the rat and pig intestinal tissue models that Galangin acts as an inhibitor of *in vitro* P-gp related efflux of Rhodamine 123 in a similar way as that of Verapamil.

Similar to results obtained with Morin and Galangin, 6-Methoxyflavone also increased the *in vitro* transport of Rhodamine 123 in the AP-BL direction in both animal intestinal tissue models due to inhibition of BL-AP transport or efflux of Rhodamine 123. In both animal models, the ER and J_{net} values were decreased by 6-Methoxyflavone indicating a P-gp inhibiting effect and thereby increasing the transport of co-applied drugs that are substrates for P-gp in the absorptive direction. Although the ER value of the 6-Methoxyflavone group did not have a

statistically significant difference from the ER value of the positive control group across rat intestinal tissue, it had a statistically significant difference from that of the positive control group across pig intestinal tissue indicating a significantly higher inhibition of Rhodamine 123 efflux compared to that obtained by Verapamil.

7-Methoxyflavone was also able to decrease the *in vitro* transport of Rhodamine 123 in the BL-AP direction, albeit not statistically significant compared to the positive control group. The mean ER and J_{net} values calculated based on Rhodamine 123 transport across both rat and pig intestinal tissues did not show a statistically significant difference compared to the positive control group (excluding the mean J_{net} across rat intestinal tissue). Since mixed results were obtained for the effect of 7-Methoxyflavone on the transport of Rhodamine 123 in the two animal tissue models used and not all the results were statistically significantly different from the control groups, the findings are not conclusive in terms of its ability to inhibit P-gp.

In summary, it is evident that Morin, Galangin and 6-Methoxyflavone have a significant inhibitory effect on the Rhodamine 123 efflux (probably P-gp related) in both the rat and pig intestinal tissue models. On the other hand, 7-Methoxyflavone showed a significant effect on the efflux of Rhodamine 123 in the pig intestinal tissue model but not in the rat intestinal tissue model. Based on the discrepancy of the results obtained in the different models used in this study, it cannot be conclusively stated that 7-Methoxyflavone is definitely an inhibitor of P-gp. Further studies are needed to reach a conclusion in this regard. As previously mentioned, it has been found that certain flavonoids have the ability to modulate P-gp and thereby influence the transport of co-administered compounds across intestinal epithelia that are substrates for P-gp (Chao *et al.,* 2002:219). The implication of this is that when natural products, food or fruit containing Morin, Galangin and 6-Methoxyflavone are taken simultaneously with a drug that is a substrate of P-gp in concentrations tested in this study, it may increase the bioavailability of the drug with potential toxic effects. However, the clinical significance of the P-gp related efflux inhibition of these flavones needs to be confirmed by means of *in vivo* experiments in humans before final conclusions regarding their effects on drug bioavailability can be made.

With regard to the different animal tissue models used, the following observations were made. Based on ER, the transport of Rhodamine 123 in the presence of different compounds and the positive control did correspond in the two models, but not with regard to the negative control. Based on the J_{net}, the transport of Rhodamine 123 in the presence of the different compounds in both controls did not correspond. Therefore it can be concluded that data obtained from the rat

intestinal tissue model cannot be compared and extrapolated to data obtained from the pig intestinal tissue model. The significance of this difference between the two models has been confirmed by means of a two-way analysis of variance (ANOVA). It is therefore not possible to make any conclusions about pharmacokinetic interactions of the tested phytochemicals on drug transport based on one *in vitro* model only.

5.3 Recommendations for future studies

It is recommended that *in vivo* absorption studies be conducted with the flavones in animals and in humans to verify clinical significance of their effects on drug bioavailability. Correlation of *in vitro* findings obtained in tests with different animal tissues can then also be correlated with *in vivo* results, which will establish the possibility to identify the most suitable *in vitro* model for future investigations. It is further recommended that these flavones are not only tested in their pure isolated forms but also in crude extracts from plant materials in order to mimic the real life situation more realistically. Since many P-gp substrates/inhibitors are substrates for cytochrome P450 enzymes, it is suggested that these compounds be tested for their potential to inhibit these enzymes. This will reveal another potential mechanism of pharmacokinetic interactions with drugs. It is of importance for patient safety to identify and quantify pharmacokinetic interactions between phytochemicals and drugs that are taken simultaneously by patients on a regular basis.

Annexures

Annexure A

A.1 Validation of HPLC method

The purpose of a validating process is to demonstrate that the analytical procedure is adequate for the intended use. A number of parameters were determined to validate the analytical procedure namely specificity, linearity, accuracy and precision.

A.1.1 HPLC analysis of Rhodamine 123

The analysis of Rhodamine 123 was done with an Agilent high pressure liquid chromatograph (HPLC). An analytical method for Rhodamine 123 was adapted from the method used by Hatting (2002:65). The apparatus and conditions are summarized in Table A.1.

Table A.1: HPLC system and conditions

Hardware and analytical conditions	Specifics
Software	ChemStation for LC, Rev. A. 10.01 [1635], Agilent Technologies
HPLC pump	Agilent 1100 Series, G1310A Isopump, Serial # DE14904334
HPLC fluorescence detector	RF-551 Spectrofluorometric detector
Detection wavelengths	Excitation: 485 nm; Emission: 546 nm
HPLC autosampler	Agilent 1100 Series, G1313A ALS, Serial # DE14918029
HPLC column	Luna C18, 250 x 4.6 mm
Sample volume injected	20 µl
Flow rate	1 ml/min
Mobile phase	Acetonitrile: 1% CH_3COOH in H_2O, 40 : 60
Room temperature	23°C

A.1.2 Chemicals used

The substances used in the mobile phase, acetonitrile and acetic acid of HPLC grade were obtained from Sigma-Aldrich, South Africa. Distilled water degassed for HPLC was also used.

A.1.3 Method validation

A.1.3.1 Specificity

Specificity is the ability to accurately test for a substance in the presence of other components. To accomplish this all components that might have been present were analysed separately by HPLC. Not one of these substances interfered with the peak of Rhodamine 123.

A.1.3.2 Linearity

The linearity of an analytical procedure is its ability (within a given range) to obtain test results, which are directly proportional to the concentration (amount) of an analyte in the sample (ICH guidelines, 1996).

Table A.2: Linearity data for Rhodamine 123

Concentration (ng/ml)	Mean Peak Area (n=6)	Standard Deviation
2.3	1241.5	112.7
4.7	2840.1	175.9
11.7	5185.2	237.3
23.4	10918.9	301.6
46.7	24220.4	361.6
116.8	54024.8	424.6

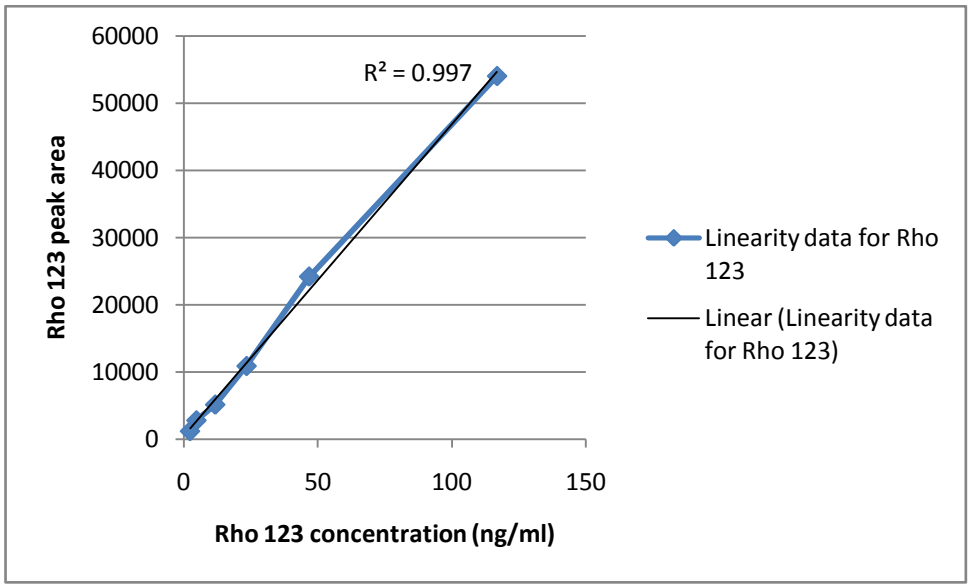

Figure A.3: Rhodamine 123 standard curve

A.1.3.3 Accuracy

The accuracy of an analytical procedure expresses the closeness of agreement between the value which is accepted as theoretical and the experimental value (ICH guidelines, 1996).

Table A.3: Accuracy data for Rhodamine 123

Concentration (ng/ml)	Mean Rho 123 area (n=6)	Concentration determined (ng/ml)	Percentage recovery (%)
11.7	5185.2	11.11	94.96
46.7	24220.4	51.91	111.16
116.8	54024.8	115.78	99.13
Average recovery			101.75
Standard deviation			8.41
Relative standard deviation (%)			8.27

A relative standard deviation of 8.27% was found, which is below the accepted maximum of 15% (Shah *et al.*, 1992:590).

A.1.3.4 Precision

The precision of an analytical procedure expresses the closeness of agreement between a series of measurements obtained from multiple sampling of the same homogeneous sample (ICH guidelines, 1996). Precision can be divided into two categories namely intra-day and inter-day precision.

- **Intra-day precision**

The intra-day precision was done by analysing 6 replicates of three different Rhodamine 123 concentrations on the same day.

Table A.4: Intra-day precision data for Rhodamine 123

Samples	Area counts of 9.5 ng/ml	Area counts of 18.9 ng/ml	Area counts of 71.0 ng/ml
1	1.32971	4.0643	5.05326
2	1.32545	3.268	5.07998
3	1.30786	4.03755	4.63147
4	1.31193	3.95589	4.66397
5	1.32428	4.06681	4.35244
6	1.3654	4.26506	5.0352
Average	1.327438	3.942935	4.802733
Standard deviation	0.020416	0.345976	0.298348
Relative Standard Deviation (%)	1.537974	8.774574	6.212047

The results show an average relative standard deviation of 5.51% which is below the accepted maximum of 15% (Shah *et al.*, 1992:590).

- **Inter-day precision**

The inter-day precision was done by analysing 2 replicates of three different Rhodamine 123 concentrations on three consecutive days.

Table A.5: Inter-day precision data for Rhodamine 123

Day	**Mean area of 6 ng/ml**	**Mean area of 12 ng/ml**	**Mean area of 24 ng/ml**
1	1.13956	1.4917	1.73253
2	1.1327	1.5418	1.69772
3	1.13637	1.51786	1.72356
Average	1.136207	1.51712	1.717935
Standard deviation	0.00343	0.025058	0.018073
Relative Standard Deviation (%)	0.30188	1.65168	1.05202

The results show an average relative standard deviation of 1% which is below the accepted maximum of 15% (Shah *et al.*, 1992:590).

A.1.3.5 System repeatability

A sample was injected six times to test for repeatability of the peak area and the retention time.

Table A.6: System repeatability data for Rhodamine 123

	Peak area	**Retention time (min)**
1	40694.3	4.378
2	39268.0	4.376
3	40375.5	4.369
4	39558.9	4.375
5	40668.1	4.366
6	42650.6	4.382
Average	40535.9	4.374
Standard deviation	1191.835	0.006
Relative standard deviation (%)	2.94	0.14

The results indicated a relative standard deviation of 12.94% and 0.14% respectively for peak area and retention time which is below the accepted maximum of 15% (Shah *et al.*, 1992:590).

A.1.3.6 Discussion

The results obtained through this validation process proved that the HPLC-fluorometric method is accurate for the analysis of the experimental samples.

Annexure B

Table B.1: Peak areas of the negative control with rat intestinal tissue

Experiment	Time	AP-BL			BL-AP			AP-BL		BL-AP	
	(min)	Cell 1	Cell 2	Cell 3	Cell 1	Cell 2	Cell 3	Mean	SD	Mean	SD
Negative	**30**	3345.5	2643.6	2404.3	2317.9	958.6	3952.1	2797.8	489.2	2409.5	1498.9
Control 1	**60**	3672.9	503.9	3541.9	8298.3	1901.1	612.8	2572.9	1793.0	3604.1	4116.0
Rat	**90**	5526.6	5071.0	5472.7	13896.4	3346.3	1256.6	5356.8	248.9	6166.4	6775.4
	120	7247.4	6544.3	7752.3	19859.0	4531.0	1322.5	7181.3	606.7	8570.8	9906.6
Negative	**30**	31073.4	33329.8	31926.8	33384.7	34370.5	33408.1	32110.0	1139.3	33721.1	562.5
Control 2	**60**	33548.4	36597.3	33727.4	37350.0	36054.0	37110.0	34624.4	1711.0	36838.0	689.5
Rat	**90**	34292.8	40256.1	33465.5	45209.2	41173.3	42712.0	36004.8	3704.9	43031.5	2036.8
	120	39432.8	49030.6	36063.3	51048.7	43189.4	43469.6	41508.9	6728.3	45902.6	4458.9
Negative	**30**	32982.4	32676.5	32634.4	37672.5	34126.6	35859.0	32764.4	189.9	35886.0	1773.1
Control 3	**60**	34550.3	33839.3	34125.6	38402.0	36851.9	37848.9	34171.7	357.7	37700.9	785.6
Rat	**90**	36488.1	33425.0	33260.9	37861.8	37096.2	40731.0	34391.3	1817.7	38563.0	1916.2
	120	39673.6	36509.7	36255.4	41453.6	45323.5	42756.1	37479.6	1904.3	43177.7	1969.1

Table B.2: P_{app} values and the efflux ratio of the negative control with rat intestinal tissue

P_{app} : Negative Control					
Rat	**AP-BL ($x10^{-6}$)**	**BL-AP ($x10^{-6}$)**	**Efflux Ratio**	**Mean**	**SD**
1	2.151588332	2.651323747	1.23226349	1.18	0.04
2	1.846731868	2.146186519	1.162153833		
3	1.309544089	1.514583668	1.156573254		

Table B.3: Flux and net flux of the negative control with rat intestinal tissue

Flux (J) : Negative Control					
Rat	**AP-BL**	**BL-AP**	**Net Flux**	**Mean**	**SD**
1	0.221024568	0.26309756	0.042072992	0.03	0.01
2	0.214694161	0.239049753	0.024355592		
3	0.166118275	0.190916881	0.024798606		

Table B.4: Peak areas of the negative control with pig intestinal tissue

Experiment	Time	AP-BL			BL-AP			AP-BL		BL-AP	
	(min)	Cell 1	Cell 2	Cell 3	Cell 1	Cell 2	Cell 3	Mean	SD	Mean	SD
Negative	**30**	1880.0	1134.6	14091.1	2901.0	8073.4	13504.9	5701.9	7274.8	8159.8	5302.5
Control 1	**60**	2760.8	2027.2	13260.8	3222.1	6449.4	20957.7	6016.3	6284.7	10209.7	9446.8
Pig	**90**	2884.3	2150.6	11219.3	3017.3	6204.7	19899.0	5418.1	5037.4	9707.0	8969.3
	120	4510.3	3300.1	11646.2	3105.3	6179.7	16536.7	6485.5	4510.0	8607.2	7037.1
Negative	**30**	6844.0	1979.4	7509.9	1329.4	11864.1	12050.2	5444.4	3019.2	8414.6	6136.6
Control 2	**60**	6551.0	2160.7	7673.4	2074.2	20105.6	15586.3	5461.7	2913.3	12588.7	9382.0
Pig	**90**	6470.6	2121.4	7209.1	2324.2	17125.8	14569.6	5267.0	2749.1	11339.9	7911.7
	120	6930.9	3019.4	6925.0	2561.5	13911.0	14934.2	5625.1	2256.6	10468.9	6867.1
Negative	**30**	2389.4	1629.7	1377.1	10060.5	3731.0	16398.3	1798.7	526.9	10063.3	6333.7
Control 3	**60**	1932.6	2276.5	5309.2	10666.2	5697.6	19822.6	3172.8	1858.2	12062.1	7165.2
Pig	**90**	2138.3	2753.2	2178.8	2319.0	6938.3	21321.1	2356.8	343.9	10192.8	9910.3
	120	2177.4	3442.9	2415.3	13668.3	7791.3	21165.8	2678.5	672.6	14208.5	6703.6

Table B.5: P_{app} values and the efflux ratio of the negative control for pigs

P_{app} : Negative Control					
Pig	**AP-BL ($x10^{-6}$)**	**BL-AP ($x10^{-6}$)**	**Efflux Ratio**	**Mean**	**SD**
1	0.36050575	0.545644022	1.513551512	1.65	0.46
2	0.318235327	0.687953428	2.161775797		
3	0.473654071	0.598997735	1.26463124		

Table B.6: Flux and net flux of the negative control for pigs

Flux (J) : Negative Control					
Pig	**AP-BL**	**BL-AP**	**Net Flux**	**Mean**	**SD**
1	0.0363829	0.049673594	0.013290694	0.02	0.01
2	0.040205232	0.075896038	0.035690805		
3	0.044468333	0.056139823	0.01167149		

Table B.7: Peak areas of the positive control with rat intestinal tissue

Experiment	Time	AP-BL			BL-AP			AP-BL		BL-AP	
	(min)	Cell 1	Cell 2	Cell 3	Cell 1	Cell 2	Cell 3	Mean	SD	Mean	SD
Positive	**30**	82906.0	78437.3	2630.5	4214.8	44331.6	53100.7	54657.9	45112.5	33882.4	26064.3
Control 1	**60**	83930.6	88067.4	3205.3	15876.4	48576.9	59500.5	58401.1	47845.7	41317.9	22699.9
Rat	**90**	84556.3	89163.1	5073.7	29318.1	49296.7	71031.9	59597.7	47275.3	49882.2	20863.1
	120	86954.0	92775.8	8874.4	41624.6	49730.8	72884.0	62868.1	46850.4	54746.5	16222.1
Positive	**30**	8869.7	16043.0	14219.5	4839.9	6389.2	10626.9	13044.1	3728.3	7285.3	2995.8
Control 2	**60**	10691.7	18915.3	16028.5	5263.8	7321.4	12161.3	15211.8	4172.2	8248.9	3541.0
Rat	**90**	13173.6	21069.7	20685.9	6626.8	8114.0	13902.0	18309.7	4452.2	9547.6	3843.6
	120	15725.5	24221.1	16273.7	9144.6	9351.2	17933.0	18740.1	4754.6	12143.0	5015.4
Positive	**30**	33296.9	27445.1	1636.0	16452.1	3589.9	32526.7	20792.7	16846.2	17522.9	14498.1
Control 3	**60**	34350.3	30012.0	2267.3	17417.5	6738.5	35320.0	22209.9	17406.5	19825.3	14442.1
Rat	**90**	35291.7	31661.5	3723.1	20516.2	10076.9	34674.5	23558.8	17273.8	21755.9	12345.6
	120	35478.9	32802.8	5460.9	20723.4	13017.7	35885.1	24580.9	16612.3	23208.7	11634.5

Table B.8: P_{app} values and the efflux ratio of the positive control in rats

P_{app} : Positive Control					
Rat	**AP-BL ($x10^{-6}$)**	**BL-AP ($x10^{-6}$)**	**Efflux Ratio**	**Mean**	**SD**
1	1.976308283	1.856237046	0.939244683	0.83	0.20
2	0.686666241	0.419085107	0.610318495		
3	0.877615674	0.849238382	0.967665469		

Table B.9: Flux and net flux of the positive control for rats

Flux (J) : Positive Control					
Rat	**AP-BL**	**BL-AP**	**Net Flux**	**Mean**	**SD**
1	0.230389847	0.1999083	-0.030481547	-0.02	0.01
2	0.068870108	0.043799814	-0.025070293		
3	0.090171912	0.084964513	-0.005207399		

Table B.10: Peak areas of the positive control with pig intestinal tissue

Experiment	Time	AP-BL			BL-AP			AP-BL		BL-AP	
	(min)	Cell 1	Cell 2	Cell 3	Cell 1	Cell 2	Cell 3	Mean	SD	Mean	SD
Positive	**30**	9755.8	5013.8	7743.9	5125.3	5867.2	3004.7	7504.5	2380.0	4665.8	1485.6
Control 1	**60**	11174.6	5309.7	8037.2	5179.2	6931.5	3581.7	8173.8	2934.9	5230.8	1675.5
Pig	**90**	12341.5	5093.4	10664.2	5679.3	6572.7	4358.6	9366.4	3794.3	5536.9	1113.9
	120	12098.8	5261.4	33827.6	5850.4	6759.1	5426.0	17062.6	14916.0	6011.8	681.1
Positive	**30**	44646.5	12880.2	47505.2	6094.3	70959.0	2167.0	35010.6	19218.7	26406.8	38633.3
Control 2	**60**	46928.6	14171.5	48842.4	22354.6	73977.4	3106.2	36647.5	19488.3	33146.1	36647.3
Pig	**90**	48822.1	17510.2	52106.8	29595.9	79513.9	5210.5	39479.7	19096.9	38106.8	37875.8
	120	52515.0	22562.8	53897.6	36893.1	74285.3	8697.4	42991.8	17705.5	39958.6	32901.2
Positive	**30**	11848.3	8622.3	18863.0	9183.2	12537.6	7333.9	13111.2	5235.9	9684.9	2637.9
Control 3	**60**	11499.8	9188.0	21090.5	9245.5	12303.6	7526.8	13926.1	6311.3	9692.0	2419.5
Pig	**90**	10940.7	10004.5	21668.3	9665.3	12759.2	7032.6	14204.5	6480.8	9819.0	2866.4
	120	10355.7	10882.6	21491.3	10338.3	12788.6	7197.6	14243.2	6282.6	10108.2	2802.6

Table B.11: P_{app} values and the efflux ratio of the positive control for pigs

P_{app} : Positive Control					
Pig	**AP-BL ($x10^{-6}$)**	**BL-AP ($x10^{-6}$)**	**Efflux Ratio**	**Mean**	**SD**
1	0.473107331	0.178211715	0.376683478	0.69	0.31
2	1.251712342	1.257739388	1.004815041		
3	0.539397688	0.372220181	0.690066327		

Table B.12: Flux and net flux of the positive control for pigs

Flux (J) : Positive Control					
Pig	**AP-BL**	**BL-AP**	**Net Flux**	**Mean**	**SD**
1	0.055413021	0.020259197	-0.035153823	-0.02	0.01
2	0.144840126	0.13508541	-0.009754716		
3	0.052446738	0.037127345	-0.015319393		

Table B.13: Peak areas of Morin with rat intestinal tissue

Experiment	Time	AP-BL			BL-AP			AP-BL		BL-AP	
	(min)	Cell 1	Cell 2	Cell 3	Cell 1	Cell 2	Cell 3	Mean	SD	Mean	SD
Morin 1	**30**	1961.6	1630.7	1333.0	1622.0	1411.9	1381.2	1641.7	314.4	1471.7	131.1
Rat	**60**	2164.7	1650.0	1829.6	1632.1	1491.2	1682.6	1881.4	261.2	1602.0	99.2
	90	2249.1	1722.6	2756.5	2251.7	1631.8	2454.0	2242.7	517.0	2112.5	428.4
	120	2573.4	1884.3	3920.0	2558.4	2174.2	4062.7	2792.6	1035.4	2931.7	998.1
Morin 2	**30**	26798.6	1179.0	2280.6	1642.4	2273.0	10313.3	10086.1	14484.0	4742.9	4834.4
Rat	**60**	29011.9	1705.2	3485.4	2878.9	5499.4	10553.1	11400.9	15277.6	6310.4	3900.9
	90	32900.3	2189.3	5068.2	4174.1	8254.7	11547.6	13385.9	16961.2	7992.1	3693.8
	120	38073.6	3343.0	7234.5	7034.8	10457.2	12905.2	16217.0	19028.1	10132.4	2948.7
Morin 3	**30**	16359.5	872.7	1394.5	1284.7	15667.4	1758.0	6208.9	8794.6	6236.7	8170.6
Rat	**60**	20217.2	2110.5	2647.8	2963.0	18194.0	5339.0	8325.2	10302.3	8832.0	8194.3
	90	25068.1	5624.5	5311.8	5818.1	19953.3	7922.0	12001.5	11317.1	11231.1	7626.5
	120	35208.5	11382.3	9063.6	8251.4	22029.5	12456.1	18551.5	14471.9	14245.7	7061.2

Table B.14: P_{app} values and the efflux ratio in the presence of Morin for rats

P_{app} : Morin					
Rat	**AP-BL ($x10^{-6}$)**	**BL-AP ($x10^{-6}$)**	**Efflux Ratio**	**Mean**	**SD**
1	0.117759941	0.12222322	1.037901507	0.83	0.20
2	0.566138907	0.368235376	0.650432909		
3	0.383472379	0.30472085	0.794635719		

Table B.15: Flux and net flux in the presence of Morin for rats

Flux (J) : Morin					
Rat	**AP-BL**	**BL-AP**	**Net Flux**	**Mean**	**SD**
1	0.013103958	0.013644979	0.000541021	-0.01	0.01
2	0.060976293	0.037960475	-0.023015818		
3	0.038396974	0.029902963	-0.008494011		

Table B.16: Peak areas of Morin with pig intestinal tissue

Experiment	Time	AP-BL			BL-AP			AP-BL		BL-AP	
	(min)	Cell 1	Cell 2	Cell 3	Cell 1	Cell 2	Cell 3	Mean	SD	Mean	SD
Morin 1	**30**	2222.6	4004.6	2264.6	12530.5	4712.4	2264.9	2830.6	1016.9	6502.6	5361.8
Pig	**60**	26973.3	8033.7	8434.5	14571.4	4123.8	2865.7	14480.5	10820.9	7186.9	6426.0
	90	68080.6	9100.2	11081.2	3300.8	3617.8	2503.1	29420.7	33495.1	3140.5	574.4
	120	100239.0	24686.6	4764.5	3063.7	3464.4	2137.5	43230.0	50366.0	2888.5	680.6
Morin 2	**30**	6095.0	4292.2	3158.3	4719.5	3213.0	3594.0	4515.1	1481.0	3842.2	783.3
Pig	**60**	11155.3	34887.2	3106.2	4496.4	3233.0	3604.0	16382.9	16522.8	3777.8	649.4
	90	11303.0	30985.2	3231.1	4308.4	3278.5	3427.9	15173.1	14276.1	3671.6	556.5
	120	10022.5	29613.1	3330.7	4180.0	3473.0	3679.6	14322.1	13658.6	3777.5	363.5
Morin 3	**30**	10667.4	10488.7	15168.3	5939.2	6276.7	7502.0	12108.1	2651.7	6572.6	822.4
Pig	**60**	10650.4	10623.9	16449.5	6741.3	6198.9	7572.9	12574.6	3355.8	6837.7	692.1
	90	10257.9	9463.4	12824.6	6915.0	6291.0	7314.2	10848.6	1756.7	6840.1	515.7
	120	9993.1	11486.1	13285.2	6875.8	6805.4	7376.2	11588.1	1648.4	7019.1	311.2

Table B.17: P_{app} values and the efflux ratio in the presence of Morin for pigs

.	P_{app} : Morin				
Pig	**AP-BL ($x10^{-6}$)**	**BL-AP ($x10^{-6}$)**	**Efflux Ratio**	**Mean**	**SD**
1	1.089499987	0.034764654	0.031908816	0.29	0.32
2	0.588148228	0.113837072	0.19355167		
3	0.276365856	0.178248066	0.644971376		

Table B.18: Flux and net flux in the presence of Morin for pigs

Flux (J) : Morin					
Pig	**AP-BL**	**BL-AP**	**Net Flux**	**Mean**	**SD**
1	0.086515449	0.006015485	-0.080499964	-0.04	0.03
2	0.047629582	0.012456847	-0.035172734		
3	0.029745128	0.018084277	-0.011660851		

Table B.19: Peak areas of Galangin with rat intestinal tissue

Experiment	Time	AP-BL			BL-AP			AP-BL		BL-AP	
	(min)	Cell 1	Cell 2	Cell 3	Cell 1	Cell 2	Cell 3	Mean	SD	Mean	SD
Galangin 1	**30**	1691.8	9394.5	1924.7	1313.5	1116.5	6818.7	4337.0	4381.5	3082.9	3236.8
Rat	**60**	4384.8	14802.8	6801.4	4117.0	4993.5	12384.0	8663.0	5452.8	7164.8	4541.1
	90	9124.7	21887.8	14838.2	8360.8	10054.2	17525.7	15283.6	6393.2	11980.2	4876.6
	120	15126.8	31256.3	24861.6	13880.9	15408.8	23852.6	23748.2	8122.2	17714.1	5370.7
Galangin 2	**30**	1321.8	16952.6	1695.5	2233.2	3091.1	7678.3	6656.6	8918.5	4334.2	2927.7
Rat	**60**	5870.7	20306.8	4486.4	5316.1	6467.4	9670.0	10221.3	8761.7	7151.1	2256.0
	90	13686.5	25565.5	9324.8	11165.9	14562.0	15242.0	16192.3	8405.3	13656.6	2183.7
	120	20804.7	30109.0	16531.8	15671.2	23111.4	19346.8	22481.8	6942.2	19376.5	3720.2
Galangin 3	**30**	1356.5	2881.0	981.0	1309.4	1116.6	895.4	1739.5	1006.2	1107.1	207.2
Rat	**60**	2367.9	3696.0	1253.9	1599.5	1640.5	1875.2	2439.2	1222.6	1705.1	148.8
	90	4638.4	5200.9	2713.2	2362.7	2463.3	3583.2	4184.2	1304.6	2803.0	677.5
	120	6615.9	7165.2	3785.2	3071.5	3041.4	4750.8	5855.4	1813.8	3621.2	978.4

Table B.20: P_{app} values and the efflux ratio in the presence of Galangin for rats

P_{app} : Galangin					
Rat	**AP-BL ($x10^{-6}$)**	**BL-AP ($x10^{-6}$)**	**Efflux Ratio**	**Mean**	**SD**
1	0.597667487	0.4546967	0.760785403	0.76	0.12
2	0.810486659	0.710367138	0.876469872		
3	0.221813027	0.140817071	0.634845811		

Table B.21: Flux and net flux in the presence of Galangin for rats

Flux (J) : Galangin					
Rat	**AP-BL**	**BL-AP**	**Net Flux**	**Mean**	**SD**
1	0.056672228	0.042411254	-0.014260973	-0.01	0.00
2	0.071777862	0.061768382	-0.01000948		
3	0.022187941	0.013803121	-0.00838482		

Table B.22: Peak areas of Galangin with pig intestinal tissue

Experiment	Time	AP-BL			BL-AP			AP-BL		BL-AP	
	(min)	Cell 1	Cell 2	Cell 3	Cell 1	Cell 2	Cell 3	Mean	SD	Mean	SD
Galangin 1	**30**	47182.5	2928.7	32054.4	46202.0	2922.8	3163.3	27388.5	22492.9	17429.4	24918.1
Pig	**60**	48587.8	2800.8	30655.7	45439.2	3246.6	3124.1	27348.1	23072.0	17270.0	24395.4
	90	49024.8	3162.9	31968.9	43824.3	3410.9	7721.6	28052.2	23180.4	18318.9	22193.2
	120	48433.3	3237.8	26580.4	39399.5	3404.6	8652.5	26083.8	22601.8	17152.2	19444.6
Galangin 2	**30**	31595.2	31355.5	1687.4	2240.7	31241.3	3138.0	21546.0	17198.5	12206.7	16490.6
Pig	**60**	30828.5	31128.7	1970.6	5782.4	31298.1	2993.1	21309.3	16748.4	13357.8	15599.2
	90	26661.7	28908.1	1353.7	1451.2	29639.7	2885.6	18974.5	15301.3	11325.5	15876.8
	120	26206.6	28812.2	1277.9	1290.6	26525.0	2764.6	18765.6	15200.7	10193.4	14162.8
Galangin 3	**30**	9551.9	28656.5	3083.7	5855.3	4876.1	9280.3	13764.1	13296.5	6670.6	2312.5
Pig	**60**	9758.5	27822.9	3073.1	5963.3	4416.1	11844.0	13551.5	12803.5	7407.8	3919.0
	90	9454.6	28222.3	3088.3	5780.7	4034.8	12282.7	13588.4	13067.0	7366.1	4346.5
	120	9041.4	29129.3	2668.7	5861.1	3965.3	12069.8	13613.2	13810.0	7298.7	4239.2

Table B.23: P_{app} values and the efflux ratio in the presence of Galangin for pigs

P_{app} : Galangin					
Pig	**AP-BL ($x10^{-6}$)**	**BL-AP ($x10^{-6}$)**	**Efflux Ratio**	**Mean**	**SD**
1	0.759310731	0.503601303	0.663234802	0.60	0.06
2	0.432016549	0.244343214	0.565587625		
3	0.326003556	0.183320335	0.562326181		

Table B.24: Flux and net flux in the presence of Galangin for pigs

Flux (J) : Galangin					
Pig	**AP-BL**	**BL-AP**	**Net Flux**	**Mean**	**SD**
1	0.083670798	0.054980888	-0.02868991	-0.02	0.01
2	0.056771716	0.031136113	-0.025635603		
3	0.035185189	0.018884847	-0.016300342		

Table B.25: Peak areas of 6-Methoxyflavone with rat intestinal tissue

Experiment	Time	AP-BL			BL-AP			AP-BL		BL-AP	
	(min)	Cell 1	Cell 2	Cell 3	Cell 1	Cell 2	Cell 3	Mean	SD	Mean	SD
6-Methoxy	**30**	11692.8	16703.7	12928.5	12601.2	9540.4	1480.9	13775.0	2610.5	7874.2	5744.3
flavone 1	**60**	12198.4	17551.1	13797.4	16019.0	10518.2	2759.7	14515.6	2747.7	9765.6	6661.6
Rat	**90**	13193.6	18208.6	13873.8	17639.8	10731.6	5555.5	15092.0	2720.4	11309.0	6062.8
	120	14328.4	19003.7	14731.3	18365.6	11634.6	7319.8	16021.1	2590.8	12440.0	5566.8
6-Methoxy	**30**	9558.0	7975.3	1621.0	5516.0	9850.4	2220.0	6384.8	4200.7	5862.1	3827.0
flavone 2	**60**	13308.0	9797.1	4429.0	7622.9	16494.2	6416.3	9178.0	4471.7	10177.8	5503.3
Rat	**90**	18384.3	12347.8	10642.8	9167.8	18920.8	9653.3	13791.6	4067.7	12580.6	5496.1
	120	26575.8	16818.4	16746.4	10837.7	20587.8	12107.2	20046.9	5654.3	14510.9	5300.9
6-Methoxy	**30**	1602.9	32368.9	5713.2	1858.1	2905.0	18026.6	13228.3	16703.1	7596.6	9047.8
flavone 3	**60**	3156.1	33691.3	6641.0	14619.4	4332.9	20120.4	14496.1	16714.6	13024.2	8013.7
Rat	**90**	6580.7	34639.6	7162.3	17104.2	8438.3	20428.0	16127.5	16034.5	15323.5	6190.0
	120	10459.5	35133.4	9608.7	17580.9	5615.2	21309.6	18400.5	14497.3	14835.2	8199.5

Table B.26: P_{app} values and the efflux ratio in the presence of 6-Methoxyflavone for rats

P_{app} : 6-Methoxyflavone					
Rat	**AP-BL ($x10^{-6}$)**	**BL-AP ($x10^{-6}$)**	**Efflux Ratio**	**Mean**	**SD**
1	0.532974922	0.444061585	0.833175383	0.85	0.09
2	0.567548337	0.436111693	0.768413304		
3	0.757662862	0.71304519	0.941111445		

Table B.27: Flux and net flux in the presence of 6-Methoxyflavone for rats

Flux (J) : 6-Methoxyflavone					
Rat	**AP-BL**	**BL-AP**	**Net Flux**	**Mean**	**SD**
1	0.051008729	0.03948002	-0.011528709	-0.01	0.00
2	0.053434491	0.039369402	-0.01406509		
3	0.07060761	0.057798926	-0.012808684		

Table B.28: Peak areas of 6-Methoxyflavone with pig intestinal tissue

Experiment	Time	AP-BL			BL-AP			AP-BL		BL-AP	
	(min)	Cell 1	Cell 2	Cell 3	Cell 1	Cell 2	Cell 3	Mean	SD	Mean	SD
6-Methoxy	**30**	10521.6	1204.8	7894.0	1014.2	6043.9	1356.8	6540.1	4803.7	2805.0	2810.2
flavone 1	**60**	8563.3	1148.4	7098.1	952.7	6435.9	1315.4	5603.2	3926.9	2901.3	3066.4
Pig	**90**	8657.8	15593.1	6471.4	945.2	5213.2	1395.5	10240.8	4762.4	2517.9	2345.0
	120	7614.0	965.5	6242.0	3665.3	6221.5	2421.0	4940.5	3510.1	4102.6	1937.7
6-Methoxy	**30**	2402.7	6028.8	11369.5	1724.6	2504.9	2494.8	6600.3	4510.6	2241.4	447.6
flavone 2	**60**	2343.0	6273.2	11013.5	2459.9	2815.9	1872.3	6543.2	4341.5	2382.7	476.5
Pig	**90**	2607.7	6528.0	10635.2	1831.4	2739.7	2658.8	6590.3	4014.1	2410.0	502.6
	120	2724.8	6128.1	9857.2	2257.7	3083.8	2096.2	6236.7	3567.4	2479.3	529.7
6-Methoxy	**30**	10148.2	3900.0	3292.9	3027.8	7087.9	3496.4	5780.4	3794.8	4537.3	2221.2
flavone 3	**60**	11604.2	4299.5	3183.0	2944.8	7220.9	4226.0	6362.2	4573.9	4797.2	2194.6
Pig	**90**	11747.5	3547.1	3134.3	2942.5	8384.4	4296.7	6142.9	4858.1	5207.8	2833.1
	120	11362.6	3798.7	3281.8	3769.5	8749.2	4570.7	6147.7	4523.6	5696.5	2673.9

Table B.29: P_{app} values and the efflux ratio in the presence of 6-Methoxyflavone for pigs

P_{app} : 6-Methoxyflavone					
Pig	**AP-BL ($x10^{-6}$)**	**BL-AP ($x10^{-6}$)**	**Efflux Ratio**	**Mean**	**SD**
1	0.11299289	0.060500421	0.53543564	0.62	0.28
2	0.145147091	0.058736765	0.404670633		
3	0.161577238	0.150964928	0.934320514		

Table B.30: Flux and net flux in the presence of 6-Methoxyflavone for pigs

Flux (J) : 6-Methoxyflavone					
Pig	**AP-BL**	**BL-AP**	**Net Flux**	**Mean**	**SD**
1	0.011622744	0.008416873	-0.003205871	0.00	0.00
2	0.014310287	0.005642383	-0.008667905		
3	0.016882204	0.015514392	-0.001367813		

Table B.31: Peak areas of 7-Methoxyflavone with rat intestinal tissue

Experiment	Time	AP-BL			BL-AP			AP-BL		BL-AP	
	(min)	Cell 1	Cell 2	Cell 3	Cell 1	Cell 2	Cell 3	Mean	SD	Mean	SD
7-Methoxy	**30**	4493.5	4044.2	4842.1	6784.0	2303.7	5226.0	4459.9	400.0	4771.3	2274.5
flavone 1	**60**	6838.2	6143.7	7964.5	6977.9	7221.8	8760.7	6982.1	918.9	7653.4	966.6
Rat	**90**	8724.4	6711.1	11241.5	8103.5	11712.6	10259.0	8892.4	2269.9	10025.0	1815.9
	120	9099.9	9546.7	14372.2	10201.5	15815.5	13140.7	11006.3	2923.5	13052.6	2808.0
7-Methoxy	**30**	5203.5	4625.1	4573.3	7851.8	7713.0	6290.4	4800.6	349.8	7285.1	864.2
flavone 2	**60**	9348.2	8570.7	6738.0	9629.1	13649.9	11750.3	8219.0	1340.2	11676.4	2011.4
Rat	**90**	21400.9	15221.1	9503.5	14003.6	20802.7	16645.1	15375.2	5950.2	17150.5	3427.6
	120	28524.1	20224.5	14963.4	19920.5	23611.6	18123.3	21237.3	6836.9	20551.8	2798.1
7-Methoxy	**30**	7147.4	3450.8	7412.6	6881.1	2679.1	7944.7	6003.6	2214.8	5835.0	2784.3
flavone 3	**60**	8446.0	4206.0	8097.4	7145.6	3379.6	8757.3	6916.5	2353.8	6427.5	2759.8
Rat	**90**	9589.4	4971.7	8743.4	7855.9	3941.2	8971.1	7768.1	2458.5	6922.7	2641.6
	120	10548.5	5170.2	9052.3	7999.8	5187.5	9767.7	8257.0	2775.9	7651.6	2309.8

Table B.32: P_{app} values and the efflux ratio in the presence of 7-Methoxyflavone for rats

P_{app} : 7-Methoxyflavone					
Rat	**AP-BL ($x10^{-6}$)**	**BL-AP ($x10^{-6}$)**	**Efflux Ratio**	**Mean**	**SD**
1	0.438623048	0.517437655	1.179686424	1.02	0.15
2	0.465195963	0.454389192	0.976769421		
3	0.317029217	0.284521132	0.897460287		

Table B.33: Flux and net flux in the presence of 7-Methoxyflavone for rats

Flux (J) : 7-Methoxyflavone					
Rat	**AP-BL**	**BL-AP**	**Net Flux**	**Mean**	**SD**
1	0.055577682	0.00113568	-0.054442002	-0.04	0.01
2	0.045866519	0.001172031	-0.044694488		
3	0.030103341	0.000877671	-0.029225671		

Table B.34: Peak areas of 7-Methoxyflavone with pig intestinal tissue

Experiment	Time	AP-BL			BL-AP			AP-BL		BL-AP	
	(min)	Cell 1	Cell 2	Cell 3	Cell 1	Cell 2	Cell 3	Mean	SD	Mean	SD
7-Methoxy	**30**	10822.7	3219.5	8898.7	3270.1	1500.1	10524.0	7647.0	3953.1	5098.1	4781.6
flavone 1	**60**	12259.2	3422.8	9284.1	3608.0	1525.3	11377.1	8322.1	4496.1	5503.5	5192.2
Pig	**90**	3517.3	12074.9	9698.4	3404.9	1421.0	11394.8	8430.2	4417.5	5406.9	5279.7
	120	11846.1	3976.1	9871.9	4242.9	1623.9	11703.8	8564.7	4094.6	5856.9	5230.2
7-Methoxy	**30**	3401.1	8532.3	13591.2	6513.9	4799.1	4875.3	8508.2	5095.1	5396.1	968.8
flavone 2	**60**	3727.7	8393.0	14433.0	6473.0	4812.6	4972.2	8851.2	5367.4	5419.3	916.0
Pig	**90**	8910.4	8661.4	13897.2	6644.1	4630.7	5125.1	10489.7	2953.6	5466.6	1049.2
	120	11449.4	9885.5	14045.2	6302.9	4493.8	5257.7	11793.4	2101.1	5351.5	908.2
7-Methoxy	**30**	7017.5	8544.8	2735.9	7046.7	9703.9	11591.0	6099.4	3011.3	9447.2	2283.0
flavone 3	**60**	7736.0	9314.1	2760.4	6679.7	10182.5	9332.6	6603.5	3420.5	8731.6	1827.1
Pig	**90**	8016.9	11918.1	3087.5	6306.7	11044.2	10082.6	7674.2	4425.3	9144.5	2504.2
	120	8968.4	9419.5	3726.1	5815.4	11870.3	11275.2	7371.3	3164.9	9653.6	3337.3

Table B.35: P_{app} values and the efflux ratio in the presence of 7-Methoxyflavone for pigs

P_{app} : 7-Methoxyflavone					
Pig	**AP-BL ($x10^{-6}$)**	**BL-AP ($x10^{-6}$)**	**Efflux Ratio**	**Mean**	**SD**
1	0.186794245	0.124804562	0.668139226	0.76	0.38
2	0.256694855	0.111779027	0.435454879		
3	0.205818095	0.241429207	1.173022257		

Table B.36: Flux and net flux in the presence of 7-Methoxyflavone for pigs

Flux (J) : 7-Methoxyflavone					
Pig	**AP-BL**	**BL-AP**	**Net flux**	**Mean**	**SD**
1	0.018534426	0.01259944	-0.005934985	-0.00	0.01
2	0.025936624	0.011921323	-0.014015302		
3	0.020323808	0.02637577	0.006051963		

Annexure C

NORTH-WEST UNIVERSITY
YUNIBESITI YA BOKONE-BOPHIRIMA
NOORDWES-UNIVERSITEIT

Private Bag X6001, Potchefstroom
South Africa 2520

Tel: (018) 299-4900
Faks: (018) 299-4910
Web: http://www.nwu.ac.za

Dr. MM Malan

Ethics Committee
Tel +27 18 299 4850
Fax +27 18 293 5329
Email Ethics@nwu.ac.za

2009-06-22

ETHICS APPROVAL OF PROJECT

The North-West University Ethics Committee (NWU-EC) hereby approves your project as indicated below. This implies that the NWU-EC grants its permission that, provided the special conditions specified below are met and pending any other authorisation that may be necessary, the project may be initiated, using the ethics number below.

Project title : Comparison of the Sweetana-Grass and Caco-2 Cell models as methods to study the in vitro efflux of Rhodamine 123

Ethics number: N W U - 0 0 1 8 - 0 9 - A 5
(Institution – Project Number – Year – Status)

Status: S = Submission; R = Re-Submission; P = Provisional Authorisation; A = Authorisation

Approval date: 13 May 2008 **Expiry date:** 12 May 2014

Special conditions of the approval (if any): None

General conditions:

While this ethics approval is subject to all declarations, undertakings and agreements incorporated and signed in the application form, please note the following:

- *The project leader (principle investigator) must report in the prescribed format to the NWU-EC:*
  - *annually (or as otherwise requested) on the progress of the project,*
  - *without any delay in case of any adverse event (or any matter that interrupts sound ethical principles) during the course of the project.*
- *The approval applies strictly to the protocol as stipulated in the application form. Would any changes to the protocol be deemed necessary during the course of the project, the project leader must apply for approval of these changes at the NWU-EC. Would there be deviated from the project protocol without the necessary approval of such changes, the ethics approval is immediately and automatically forfeited.*
- *The date of approval indicates the first date that the project may be started. Would the project have to continue after the expiry date, a new application must be made to the NWU-EC and new approval received before or on the expiry date.*
- *In the interest of ethical responsibility the NWU-EC retains the right to:*
  - *request access to any information or data at any time during the course or after completion of the project;*
  - *withdraw or postpone approval if:*
    - *any unethical principles or practices of the project are revealed or suspected,*
    - *it becomes apparent that any relevant information was withheld from the NWU-EC or that information has been false or misrepresented,*
    - *the required annual report and reporting of adverse events was not done timely and accurately,*
    - *new institutional rules, national legislation or international conventions deem it necessary.*

The Ethics Committee would like to remain at your service as scientist and researcher, and wishes you well with your project. Please do not hesitate to contact the Ethics Committee for any further enquiries or requests for assistance.

Yours sincerely

Prof MMJ Lowes
(chair NWU Ethics Committee)

Prof J Du Plessis
(Chairman: NWU Ethics Committee:Unit for Drug Research and Development))

Certificate of Analysis

SIGMA-ALDRICH

Product Name	Rhodamine 123
Product Number	R8004
Product Brand	SIGMA
CAS Number	62669-70-9
Molecular Formula	$C_{21}H_{17}ClN_2O_3$
Molecular Weight	380.82

TEST	**LOT 127K3752 RESULTS**
APPEARANCE	BROWN POWDER WITH A RED CAST
SOLUBILITY	CLEAR RED-ORANGE
IR SPECTRUM	CONFORMS
WATER BY KARL FISCHER	9.4%
CARBON *	64.7%
NITROGEN *	7.1%
RECOMMENDED RETEST	FEBRUARY 2011
QC RELEASE DATE	DECEMBER 2007

Rodney Burbach

Rodney Burbach, Manager
Quality Control
St. Louis, Missouri USA

Certificate of Analysis

SIGMA-ALDRICH

Product Name	Morin hydrate, powder
Product Number	M4008
Product Brand	SIGMA
CAS Number	654055-01-3
Molecular Formula	$C_{15}H_{10}O_7 \cdot xH_2O$
Molecular Weight	302.24 (anhydrous basis)

TEST	LOT 117k2574 RESULTS
APPEARANCE	YELLOW BROWN POWDER
SOLUBILITY	DARK BROWN SOLUTION AT 250MG PLUS 5 ML OF METHANOL
WATER BY KARL FISCHER	6%
UV-VIS SPECTRUM	E1% = 369 AT LAMBDA MAX 359 NM IN METHANOL
PURITY BY HPLC	87%
QC RELEASE DATE	NOVEMBER 2007
PRODUCT CROSS REFERENCE INFORMATION	REPLACEMENT FOR ALDRICH #M87630

Rodney Burbach, Manager
Quality Control
St. Louis, Missouri USA

Certificate of Analysis

SIGMA-ALDRICH

Product Name	Galangin
Product Number	282200
Product Brand	SIGMA
CAS Number	548-83-4
Molecular Formula	$C_{15}H_{10}O_5$
Molecular Weight	270.24

TEST	SPECIFICATION	LOT 08420hh RESULTS
APPEARANCE	YELLOW POWDER	YELLOW POWDER
INFRARED SPECTRUM		CONFORMS TO STRUCTURE.
HIGH PRESSURE LIQUID CHROMATOGRAPHY	TYPICALLY 95+%	99.9 %
PRODUCT CROSS		REPLACES PRODUCT NUMBER 48291
REFERENCE INFORMATION		
QUALITY CONTROL		JUNE 2007
ACCEPTANCE DATE		

Barbara Rajzer, Supervisor
Quality Control
Milwaukee, Wisconsin USA

Certificate of Analysis

SIGMA-ALDRICH

Product Name	6-Methoxyflavone, 99%
Product Number	419737
Product Brand	ALDRICH
CAS Number	26964-24-9
Molecular Formula	$C_{16}H_{12}O_3$
Molecular Weight	252.26

TEST	**LOT 05906ae RESULTS**
APPEARANCE	LIGHT YELLOW
INFRARED SPECTRUM	CONFORMS TO STRUCTURE.
ELEMENTAL ANALYSIS	CARBON 76.14%
GAS LIQUID CHROMATOGRAPHY	99.9%
QC RELEASE DATE	JANUARY 2006

Barbara Rajzer, Supervisor
Quality Control
Milwaukee, Wisconsin USA

Certificate of Analysis

SIGMA-ALDRICH

Product Name	7-Methoxyflavone, 99%
Product Number	419745
Product Brand	ALDRICH
CAS Number	22395-22-8
Molecular Formula	$C_{16}H_{12}O_3$
Molecular Weight	252.26

TEST	**LOT 10102dc RESULTS**
APPEARANCE	OFF WHITE POWDER
MELTING POINT	109.8-111.8 DEGREES CELSIUS
INFRARED SPECTRUM	CONFORMS TO STRUCTURE AND STANDARD
ELEMENTAL ANALYSIS	CARBON 76.05%
GAS LIQUID CHROMATOGRAPHY	99.9 %
QUALITY CONTROL ACCEPTANCE DATE	APRIL 2004

Barbara Rajzer, Supervisor
Quality Control
Milwaukee, Wisconsin USA

References

AMBUDKAR, S.V., KIM, I. & SAUNA Z.E. 2006. The power of the pump: mechanisms of action of P-glycoprotein (ABCB1). *European journal of pharmaceutical sciences,* 27:392-400.

ARTURSSON, P., UNGELL, A. & LÖFROTH, J. 1993. Selective paracellular permeability in two models of intestinal absorption: cultured monolayers of human intestinal epithelial cells and rat intestinal segments. *Pharmaceutical research,* 10(8):1123-1129.

AULTON, M.E., ed. 2007. Pharmaceutics: The design and manufacture of medicines. 3rd ed. s.l.: Elsevier. 717p.

AUNGST, B.J., 2000. Intestinal permeation enhancers. *Journal of pharmaceutical sciences,* 89:429-442, Jan.

BALAYSSAC, D., AUTHIER, N., CAYRE, A. & COUDORE, F. 2005. Does inhibition of P-glycoprotein lead to drug-drug interactions? *Toxicology letters,* 156:319-329, Jan.

BALIMANE, P.V. & CHONG, S. 2005. Cell culture-based models for intestinal permeability: a critique. *Drug discovery today,* 10(5):335-343, Mar.

BALIMANE, P.V., CHONG, S. & MORRISON, R.A. 2000. Current methodologies used for evaluation of intestinal permeability and absorption. *Journal of pharmacological and toxicological methods,* 44:301-312, Sep.

BALIMANE, P.V., HAN, Y. & CHONG, S. 2006. Current industrial practices of assessing permeability and P-glycoprotein interaction. *The American association of pharmaceutical sciences,* 8(1):1-13, Jan.

BANSAL, T., JAGGI, M., KHAR, R.K. & TALEGAONKAR, S. 2009. Emerging significance of flavonoids as P-glycoprotein inhibitors in cancer chemotherapy. *Journal of pharmacy & pharmaceutical sciences,* 12(1):46-78, Mar.

BERGGREN, S. 2006. Drug transport and metabolism in rat and human intestine. Uppsala: Uppsala University. (Dissertation – Ph.D.) 53 p.

BOHETS, H., ANNAERT, P., MANNENS, G., VAN BEIJSTERVELDT, L., ANCIAUX, K., VERBOVEN, P., MEULDERMANS, W. & LAVRIJSEN, K. 2001. Strategies for absorption screening in drug discovery and development. *Current topics in medicinal chemistry,* 1:367-383.

BRAND, W., SCHUTTE, M.E., WILLIAMSON, G., VAN ZANDEN, J.J., CNUBBEN, N.H.P., GROTEN, J.P., VAN BLADEREN, P.J. & RIETJENS, I.M.C.M. 2006. Flavonoid-mediated inhibition of intestinal ABC transporters may affect the oral bioavailability of drugs, food-borne toxic compounds and bioactive ingredients. *Biomedicine and pharmacotherapy,* 60:508-519, Sep.

CARVALHO, F.C., BRUSCHI, M.L., EVANGELISTA, R.C. & GREMIAO, M.P.D. 2010. Mucoadhesive drug delivery systems. *Brazilian journal of pharmaceutical sciences,* 46(1):1-17, Jan.

CHAN, L.M.S., LOWES, S. & HIRST, B.H. 2004. The ABCs of drug transport in intestine and liver: efflux proteins limiting drug absorption and bioavailability. *European journal of pharmaceutical sciences,* 21:25-51.

CHAO, P.L., HSIU, S. & HOU, Y. 2002. Flavonoids in herbs: biological fates and potential interactions with xenobiotics. *Journal of food and drug analysis,* 10(4):219-228, Dec.

CHOI, C. 2005. ABC transporters as multidrug resistance mechanisms and the development of chemosensitizers for their reversal. *Cancer cell international,* 5(30):1-13, Oct.

CHOI, C., KIM, J. & KIM S. 2004. Reversal of P-glycoprotein-mediated MDR by 5,7,3',4',5'-pentamethoxyflavone and SAR. *Biomedical and biophysical research communications,* 350:672-679, Jun.

CONSEIL, G., BAUBICHON-CORTAY, H., DAYAN, G., JAULT, J., BARRON, D. & DI PIETRO, A. 1998. Flavonoids: a class of modulators with bifunctional interactions at vicinal ATP- and steroid-binding sites on mouse P-glycoprotein. *National academy of sciences,* 95:9831-9836, Aug.

CSÁKY, T.Z., *ed.* 1984. Intestinal permeation and permeability: an overview. p.51-60. (*In* Csáky, T.Z., ed. Pharmacology of intestinal permeation. Vol.1. Berlin: Springer.)

D'SOUZA, B. 2008. Everted gut sac technique: an ex vivo screening method for new drugs. *http://faculty.mercer.edu/strom_jg/pha897/abstracts/dsouza.pdf* Date of access: 22 Sep. 2010

DAUGHERTY, A.L. & MRSNY, R.J. 1999. Transcellular uptake mechanisms of the intestinal epithelial barrier: part one. *Pharmaceutical science and technology today,* 2(4):144-151, Apr.

DEFERME, S., ANNAERT, P. & AUGUSTIJNS, P. 2008. *In vitro* screening models to assess intestinal drug absorption and metabolism. *Biotechnology: pharmaceutical aspects,* 7(2):182-215.

DESESSO, J.M. & JACOBSON, C.F. 2001. Anatomical and physiological parameters affecting gastrointestinal absorption in humans and rats. *Food and chemical toxicology*, 39(3):209-228, Mar.

DESESSO, J.M. & JACOBSON, C.F. 2008. Anatomical and physiological parameters affecting gastrointestinal absorption in humans and rats. *Food and chemical toxicology,* 39:209-228, Sep.

DESESSO, J.M. & WILLIAMS, A.L. 2008. Contrasting the gastrointestinal tract of mammals: factors that influence absorption. *Annual reports in medicinal chemistry,* 43:353-371.

DODD, S.A. 2005. The effect of selected methoxy flavonoids on the *in vitro* efflux transport of Rhodamine 123 using rat jejunum. Potchefstroom: NWU. (Dissertation – M.Sc.) 88p.

EVANS, A.M. 2000. Influence of dietary components on the gastrointestinal metabolism and transport of drugs. *Therapeutic drug monitoring,* 22:131-136.

GRASS, G.M. & SWEETANA, S.A. 1988. *In vitro* measurement of gastrointestinal tissue permeability using a new diffusion cell. *Pharmaceutical research,* 5(6):372-376, Jan.

HANSEN, T.S. & NILSEN, O.G. 2009. *Echinacea purpurea* and P-glycoprotein drug transport in caco-2 cells. *Phytotherapy research,* 23:86-91.

HATTINGH, O.N. 2002. Validation of the Sweetana-Grass diffusion cell technique as a model for studying drug transport. Potchefstroom: PU vir CHO. (Dissertation – M.Sc.) 118p.

HAYESHI, R., MASIMIREMBWA C., MUKANGANYAMA, S. & UNGELL, A.B. 2006. The potential inhibitory effect of antiparasitic drugs and natural products on P-glycoprotein mediated efflux. *European journal of pharmaceutical sciences,* 29:70-81, Jun.

HIDALGO I.J. 2001. Assessing the absorption of new pharmaceuticals. *Current topics in medicinal chemistry,* 1(5):385-401.

HIGGINS, C.F. 2001 ABC transporters: physiology, structure and mechanism – an overview. *Research in microbiology,* 152:205-210, Feb.

HOCHMAN, J.H., YAMAZAKI, M., OHE, T. & LIN, J.H. 2002. Evaluation of drug interactions with P-glycoprotein in drug discovery: *in vitro* assessment of the potential for drug-drug interactions with P-glycoprotein. *Current drug metabolism,* 3(3):257-273.

HUNTER, J. & HIRST, B.H. 1997. Intestinal secretions of drugs: The role of P-glycoprotein and related drug efflux systems in limiting oral drug absorption. *Advanced drug delivery reviews,* 25:129-157.

INGERSOLL, RE. 2005. Herbaceuticals: an overview for counsellors. *Journal of Counseling and Development,* 83:434-43.

INTERNATIONAL CONFERENCE ON HARMONISATION OF TECHNICAL REQUIREMENTS FOR REGISTRATION OF PHARMACEUTICALS FOR HUMAN USE (ICH). 1996. Validation of analytical procedures: methodology. ICH Steering Committee. 9p.

JULIANO, R.L. & LING, V. 1976. A surface glycoprotein modulating drug permeability in Chinese hamster ovary cell mutants. *Biochimica et biophysica acta (BBA) – biomembranes,* 455(1):152-162, Nov.

KERNS, E.H. & DI, L. 2008. Drug-like properties: concepts, structure design and methods. s.l.: Academic press. 526p.

LE FERREC, E., CHESNE, C., ARTUSSON, P., BRAYDEN, D., FABRE, G., GIRES, P., GUILLOU, F., ROUSSET, M., RUBAS, W. & SCARINO, M. 2001. *In vitro* models of the intestinal barrier: The report and recommendations of ECVAM workshop 46. *Alternatives to laboratory animals,* 29:649-668.

LORKE, D.E., KRÜGER, M., BUCHERT, R., BOHUSLAVIZKI, K.H., CLAUSEN, M. & SCHUMACHER, U. 2001. *In vitro* and *in vivo* tracer characteristics of an established multi-drug resistant human colon cancer cell line. *The journal of nuclear medicine,* 42(4):646-654, Apr.

NEYFAKH, A.A. 1988. Use of fluorescent dyes as molecular probes for the study of multidrug resistance. *Experimental cell research,* 174:168-176.

NORRIS, D.A., PURI, N. & SINKO, P.J. 1998. The effect of physical barriers and properties on the oral absorption of particulates. *Advanced drug delivery reviews,* 34:135-154, Jul.

PALUMBO, P., PICCHINI, U., BECK, B., VAN GELDER, J., DELBAR, N. & DEGAETANO, A. 2008. A general approach to the apparent permeability index. *Journal of pharmacokinetics and pharmacodynamics,* 35:235-248, Mar.

PANG, K.S. 2003. Modeling of intestinal drug absorption: roles of transporters and metabolic enzymes (for the Gillette review series). *Drug metabolism and disposition,* 31(12):1507-1519, Jul.

PELKONEN, O., BOOBIS, A.R. & GUNDERT-REMY, U. 2001. *In vitro* prediction of gastrointestinal absorption and bioavailability: an experts' meeting report. *European journal of clinical pharmacology,* 57(9):621-629, Nov.

RAUTIO, J., HUMPHREYS, J.E., WEBSTER, L.O., BALAKRISHNAN, A., KEOGH, J.P., KUNTA, J.R., SERABJIT-SINGH, C.J. & POLLI, J.W. 2006. *In vitro* P-glycoprotein inhibition assays for assessment of clinical drug interaction potential of new drug candidates: a recommendation for probe substrates. *Drug metabolism and disposition,* 34(5):786-792.

SCALA, S., AKHMED, N., RAO, U.S., PAULL, K., LAN, L., DICKSTEIN, B., LEE, J.S., ELGEMEIE, G.H., STEIN, W.D. & BATES, S.E. 1997. P-glycoprotein substrates and antagonists cluster into two distinct groups. *Molecular pharmacology,* 51:1024-1033.

SHAH, V.P., MIDHA, K.K., DIGHE, S., McGILVERAY, I.J., SKELLY, J.P., YACOBI, A., LAYLOFF, T., VISWANATHAN, C.T., COOK, C.E., McDOWALL, R.D., PITTMAN, K.A. & SPECTOR, S. 1992. Analytical methods validation: bioavailability, bioequivalence and pharmacokinetic studies. *Pharmaceutical research,* 9:588-592.

SHAPIRO, A.B. & LING, V. 1998. The mechanism of ATP-dependent multidrug transport by P-glycoprotein. *Acta physiologica scandinavica,* 163:227-234.

SHARGEL, L. & YU, A.B.C. 1999. Applied biopharmaceutics and pharmacokinetics. 4th ed. Norwalk, Conn.: Appleton & Lange. 768p.

SHAROM, F.J. 2006. Shedding light on drug transport: structure and function of the P-glycoprotein multidrug transporter (ABCB1). *Biochemistry and cell biology,* 84(6):979-992, Dec.

SHAROM, F.J. 2008. ABC multidrug transporters: structure, function and role in chemoresistance. *Pharmacogenomics,* 9(1):105-127.

STATSOFT, INC. (2007). Statistica (data analysis software system), version 8.0. www.statsoft.com.

SWART, K. 2002. An investigation to determine the effect of selected compounds on the transport of Rhodamine 123 across rat jejunum. Potchefstroom: PU vir CHO. (Dissertation – M.Sc.) 84p.

SWEETANA, S.A. & GRASS, G.M. 1993. Apparatus for *in vitro* determination of substances across membranes, biological tissues, or cell cultures. Patent: US 5,183,760. 9 p.

TABACHNICK, B.G. & FIDELL, L.S. 2001. *Using Multivariate Statistics*, 4th Ed., Allyn & Bacon, Boston. 966 p.

TARIRAI, C., VILJOEN, A.M. & HAMMAN, J.H. 2010. Herb-drug pharmacokinetic interactions reviewed. *Expert Opinion in Drug Metabolism and Toxicity*, 6(12):1-24.

VAN HUYSSTEEN, S. 2005. The effect of selected hydroxy flavonoids on the *in vitro* efflux transport of Rhodamine 123 using rat jejunum. Potchefstroom: NWU. (Dissertation – M.Sc.) 103p.

VARMA, M.V.S., ASHOKRAJ, Y., DEY, C.S. & PANCHAGNULA, R. 2003. P-glycoprotein inhibitors and their screening: a perspective from bioavailability enhancement. *Pharmacological research,* 48:347-359, Apr.

VARMA, M.V.S., PERUMAL, O.P. & PANCHAGNULA, R. 2006. Functional role of P-glycoprotein in limiting peroral drug absorption: optimizing drug delivery. *Current opinion in chemical biology,* 10:367-373, Jun.

YAMASHITA, S., FURUBAYASHI, T., KATAOKA, M., SAKANE, T., SEZAKI, H. & TOKUDA, H. 2000. Optimized conditions for prediction of intestinal drug permeability using Caco-2 cells. *European journal of pharmaceutical sciences,* 10:195-204, Jan.